UCRL-ID-104557
PATC-IR 89-03

FUSELAGE MODEL CRASH TESTS

August 14, 1989

Billy W. Davis, Carl E. Walter, C. K. Chou

Prepared for
U.S. Nuclear Regulatory Commission

DISCLAIMER

This work was supported by the United States Nuclear Regulatory Commission under a Memorandum of Understanding with the United States Department of Energy.

PATC-IR 89-03

FUSELAGE MODEL CRASH TESTS

August 14, 1989

Billy W. Davis, Carl E. Walter, C. K. Chou

Prepared for
U.S. Nuclear Regulatory Commission

ABSTRACT

A series of model "crash" tests have been conducted for the purpose of understanding the mechanisms which produced the catastrophic shattering and fragmentation associated with the crash of PSA Flight 1771. Public Law 100-203 defines conditions under which air transportation of plutonium from a foreign nation to a foreign nation through United States airspace may be permitted. Section 5062 of that Law specifies that proof of survivability of the packaging, with no leakage of plutonium, shall be provided for a "worst-case" accident, and that the proof of survivability shall be demonstrated by, among other requirements, an aircraft crash test which replicates the worst-case accident. The U.S. Nuclear Regulatory Commission (NRC) has specified that the conditions associated with the crash of PSA Flight 1771 represent the "worst-case". The accident occurred near Paso Robles on December 7, 1987. Shattering and fragmentation of every physical aspect of the aircraft, including its contents, characterized the crash conditions. A short-term, yet intense effort has been applied toward understanding the phenomena which produced global shattering/fragmentation. Ten tests were conducted, using a 2.5-in. diameter gas gun, in an effort to reproduce the PSA Flight 1771 shattering conditions in model fuselages. Five phenomenological shatter-producing candidates emerged; they were 1) high-strain rate, 2) high-deformation rate, 3) air pressure buildup inside the fuselage on impact, 4) "shrapnel" from fragmenting rigid/semi-rigid mass internal to the fuselage, and 5) eruption of deformable mass internal to the fuselage. The tests demonstrated that superposition of either of the latter three "shatter-producing" candidates upon the first two (high-strain rate and high-deformation rate), would produce catastrophic shattering.

TABLE OF CONTENTS

TABLE OF CONTENTS
(continued)

ACKNOWLEDGMENTS

Several staff members of the Nuclear Systems Safety Program and the technical support group of the Mechanical Engineering's Nuclear Test Engineering Division, as well as staff and technical support personnel of the Nuclear Chemistry Department, have contributed to this effort. The contributors are gratefully acknowledged:

Greg Bianchini
Dennis Chakedis
Jim Caywood
J. C. Chen
Mark Eli
Larry Fischer
Bill Gourdin
Gerald Goudreau
Lisa Hensel
Charles Herget
Garry Holman
Bob Ramos
Jim Van Sant
Gilbert Vayer
Bennie Walker
Stuart Weinland
Monika Witte

Bob Ramos, Nuclear Test Engineering Division, served as Senior Mechanical Technologist. The high-speed camera instrumentation was done by Jim Caywood of the Technical Information Department of LLNL.

GLOSSARY

BAe — British Aerospace (the "e" is added to distinguish it from British Airways).

Catastrophic Shattering — Global material failure characterized by complete separating and dispersing of a singular unit (such as an aircraft fuselage) into many small fragments due to dynamic loading through a combination of tensile, shear, and compression, which exceed the ultimate strength limits of the material.

FAA — Federal Aviation Administration.

Impact angle — The angle between the longitudinal axis of the model fuselage and the plane of the impact surface of the impacting projectile. By definition, this angle is restricted to values less than 90°.

NRC — United States Nuclear Regulatory Commission.

NUREG-0360 — An NRC Staff document which specifies criteria for qualification of a package for air transport of plutonium.

LLNL — Lawrence Livermore National Laboratory.

PAT — Plutonium Air Transport.

PAT package — The package for air transport of plutonium, including the plutonium itself, the inner and outer containment vessels, and all packaging components whose function relates to safety, protection, or aerodynamic drag enhancement.

PSA — Pacific Southwest Airlines.

Projectile — A cylindrical solid 63.62 mm (2.5-in.) diameter by 77.35 mm (3.0-in.) in length and made of Lexan polycarbonate.

Target — The model fuselage, generally fixed near the gas gun barrel exit, to be impacted (crashed) by the projectile.

1. Introduction

The purpose of this document is to describe the experimental methods and results employed in examining the mechanisms which cause shattering in a high-velocity aircraft crash. Of particular concern is the survivability of a plutonium air transport (PAT) package exposed to high-velocity impact crash conditions which could result from an accident.

Public Law 100-203 (Ref. 1) provides guidelines by which the United States Nuclear Regulatory Commission will regulate the transportation of plutonium from a foreign country to a foreign country through United States airspace. Section 5062 of that Law requires that a "worst-case" aircraft accident be considered to the maximum extent practicable. The NRC has specified that the conditions associated with the crash of PSA Flight 1771 on December 7, 1987, near Paso Robles, California, represents a "worst- case" crash. Catastrophic shattering of the fuselage skin, its contents, and appendages occurred. Fragments were scattered over a radius greater than 200 m from the point of impact. The aircraft type was a BAe-146-200. Figure 1a shows the broad dispersion of debris from the crash. Figure 1b shows a pile of collected fuselage fragmentation remnants from the crash.

An understanding of the various mechanisms which contributed to the disintegration of the aircraft is an essential element to the NRC satisfying conditions of Public Law 100-203. To that end, a brief, but intense, effort was initiated for the purpose of better understanding how the potential mechanisms of shattering applied to a high-velocity aircraft crash. Generalization of the results of this effort to less severe crashes was not attempted.

1.1 Shatter-Producing Phenomena

Five shatter-producing phenomenological candidates emerged through initial study. They were:

- high-strain rate in the fuselage skin,
- high-deformation rate of the fuselage skin,
- air pressure increase inside the fuselage due to volume collapse,
- rigid and semi-rigid mass (instrument panels, plastic and metal structure, seats, etc.) which shatters and produces "shrapnel" internal to fuselage,
- deformable mass (fluids) internal to the fuselage, which erupts under high pressure from impact.

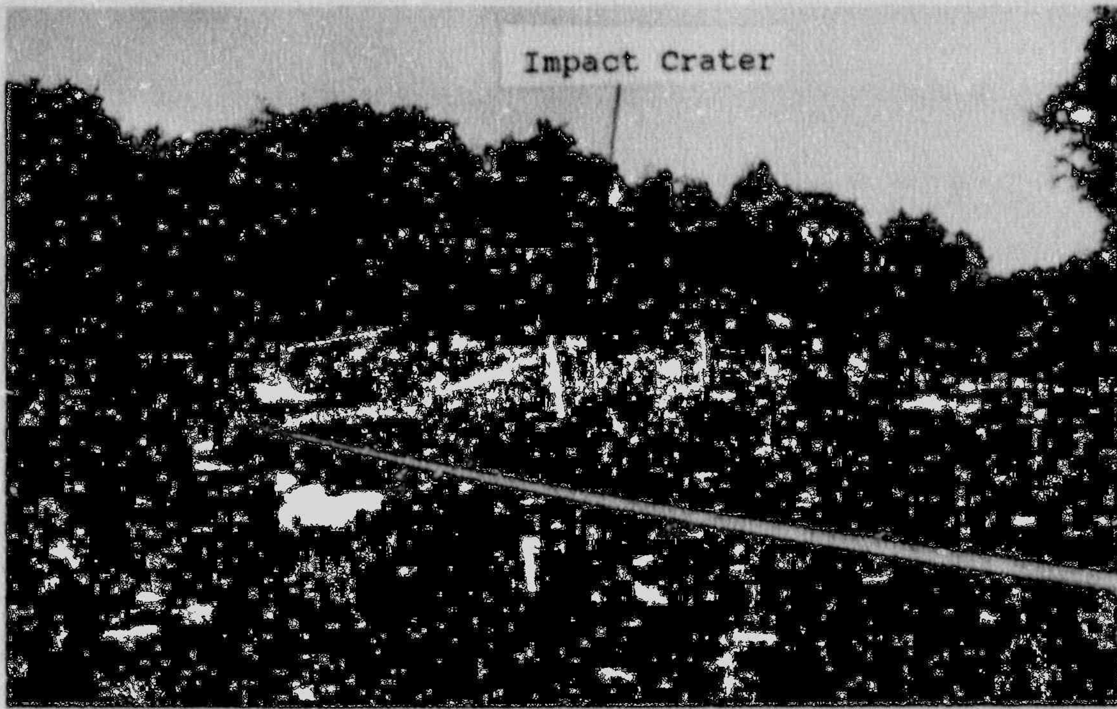

Figure 1a. Scattered debris from crash of PSA Flight 1771.

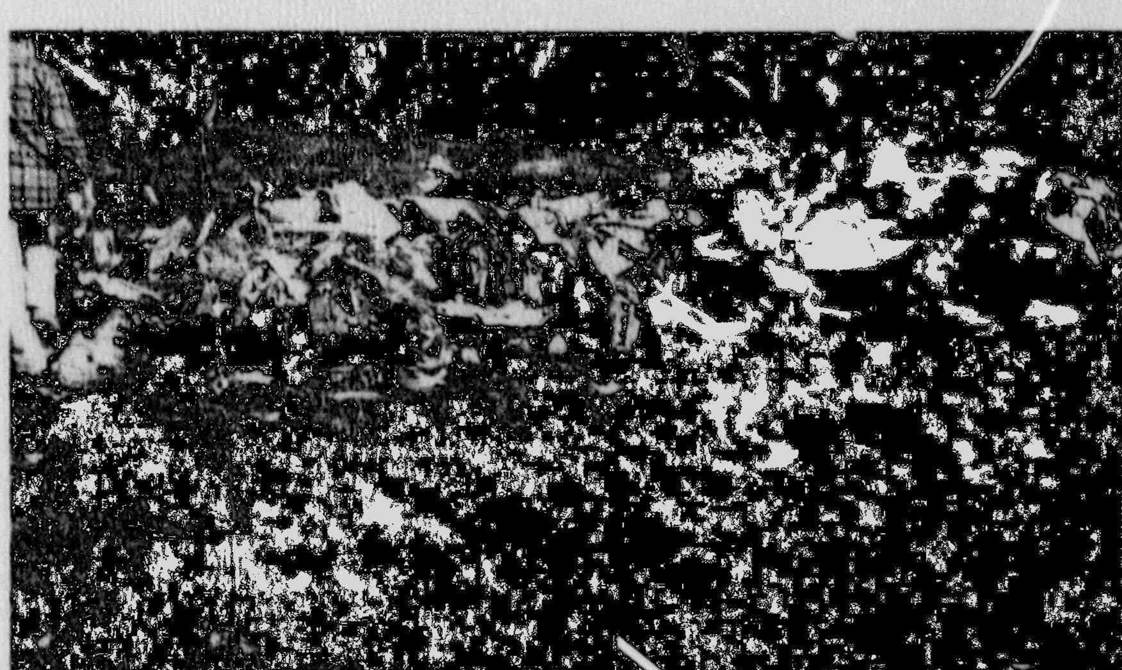

Figure 1b. Fragments collected from crash of PSA Flight 1771.

A series of high-velocity impact tests, designed to investigate each of the phenomenological candidates, was planned. A fundamental objective was that of reproducing the shattering conditions observed in the crash of PSA Flight 1771 with the crashing of small fuselage models. A secondary objective was that of delineating the relative effects of each potential shatter-producing candidate. A brief discussion of each candidate follows.

1.1.1 High-Strain Rate

The behavior of materials subjected to large strains and high-strain rates is of significant importance during metal forming, high-speed machining, high-velocity impact, and other similar conditions (Ref. 2). Very little data of modeling usefulness is currently available, and some conflict appears to exist with regard to the ultimate effect of strain-rate. Early investigators suggested that high-strain rates increased the yield strength (Ref. 3) while more recent investigators suggest that higher strain rates produce higher degrees of strain hardening and shorter "strain-to-failure" conditions (Ref. 4). Most investigators agree that more ductile materials are less sensitive to property modification due to strain rate (Refs. 2, 3, 4). LLNL experts in structural modeling believe that the effects of strain rate in aluminum, for dynamic conditions similar to the model crash tests and also for conditions of the PSA Flight 1771 actual crash, remain somewhat uncertain (Ref. 5). Results from LLNL model crash tests offer agreement to this assessment.

1.1.2 High-Deformation Rate

A high-velocity impact normal to the longitudinal axis of a ductile cylindrical shell produces an accordion type of buckling phenomena (Ref. 5). Such processes commonly occur when an empty aluminum soft drink can is "stomped". In the absence of internal mass, a similar buckling process might be expected to occur in the fuselage of an aircraft impacting the ground with a near-normal angle of impact. Buckling of this type was observed in fuselage models "crashed" in tests described in this report. Structural analysts (Ref. 5) have suggested that rapid buckling may induce large inertial forces as the walls of the cylindrical shell deform at a high rate. Two-dimensional rigid body kinematic analysis suggests that accelerations approaching 1.5E08 g's (see Appendix 11) are possible when the impact velocity is 290 m/s (950 ft/s). The resulting tensile loading, due to inertia, can exceed the ultimate stress limit of the fuselage skin, resulting in fragmentation.

1.1.3 Pressure Increase In Fuselage Due To Volume Collapse

As collapse of the fuselage progresses, following a near-normal impact, the volume of air inside the fuselage would be progressively compressed. The resulting pressure rise would, theoretically, become infinitely large with total collapse of the volume. At some point in the collapsing process the pressure would conceivably rise to the "burst" limit of the fuselage and result in catastrophic fragmentation.

1.1.4 Rigid and Semi-Rigid Mass Internal To Fuselage

Instrument panels, plastic and metal fixtures, partitions, seats and other similar internal appendages to the fuselage are subject to fragmentation upon impact, especially when the impact velocity is high. The consequence could be a "shrapnel"-like environment internal to the fuselage as the impact progresses from nose to tail, thus producing catastrophic fragmentation of the fuselage.

1.1.5 Deformable Mass Internal To Fuselage

Waterhammer-like phenomena is expected to occur when liquid or human mass is suddenly stopped by impact with the ground. Pressure within such mass may approach a magnitude as large as 344 MPa (50,000 psi) if the impact velocity is 290 m/s (950 ft/s). Pressure of this magnitude is expected to produce catastrophic eruption of deformable mass and contribute to the ultimate shattering of the aircraft fuselage.

1.2 Other Relevant Shatter-Influencing Parameters

The physical properties of the soil, the geometric properties of the terrain and the angle of impact are among other notable influences expected to affect the degree of shattering. The minimum angle of impact criteria specifies 60° (Ref. 9). That angle was developed from topographical surveys of the PSA 1771 crash site and near-impact data recorded on the flight data recorder.

Non-uniform distribution of mass along the length of the fuselage walls is expected to influence characteristics of fuselage shattering; windows and overhead storage bins are typical examples.

Of those influences mentioned in this section, only the angle of impact and the windows were examined experimentally.

1.3 The Need For Tests

The "worst-case" accident, as prescribed by the NRC, was an event which produced catastrophic shattering of the fuselage and its contents. A need to understand the mechanisms which produced shattering in that event, as it relates to the safety of shipping of plutonium by air, clearly emerged. The basic question which was first raised was, "can similar shattering of fuselage models be repeated in a laboratory environment, and further, can such tests be designed which will help delineate the effects of the phenomenological sources of shattering?" Because of the several shatter-producing candidates, and because of the availability of a 2.5-in. gas gun facility at the Laboratory, it seemed expedient that a few tests be designed which would provide better understanding of the shattering phenomena. Ten tests were conducted.

2. Gas Gun Facility

The history and engineering theory of high-speed gas-guns is well documented by Seigel (Ref. 6). Such guns utilize low molecular weight gas, compressed to high pressure, to propel a projectile. The projectile accelerates through a relatively long barrel, to impact a target fixtured inside an evacuated "catcher" chamber. The "catcher" chamber is usually appended to the exit end of the gun barrel, is closed, and can be made to sustain its own independent environmental pressure. Such a gun is shown in Figure 2.

The bore of the gun barrel is 2.5-in. in diameter. The barrel length is 8 ft. Helium is used to propel the projectile. Crash conditions were experimentally simulated by firing a 300 g projectile into fixed fuselage models positioned at the exit of the gun barrel. Thus, the projectile simulated "earth" crashing into the aircraft fuselage model; impact effects should be identical to that of the reverse case.

The test chamber, where impact occurred, had large side ports which permitted viewing with a high-speed camera. The pressure environment of the impact zone was controllable. Some tests were conducted in near-vacuum conditions; others were conducted with the model fuselage target contained in a 1-atm air pressure environment.

3. Experiment Design Considerations

To determine whether fuselage shattering could be duplicated in a laboratory setting, care was given to scaling the model fuselages, to the extent possible. The aircraft involved in the "worst-case" crash (PSA Flight 1771) was a BAe-146-200. Attention was also given to methods of partitioning the effects of the several shatter-producing phenomenological candidates.

3.1 Scaling

The fuselage dimensions of the BAe-146-200 aircraft (Ref. 7) were:

Overall Length:	28.60 m	(93.8 ft)
Fuselage Diameter:	3.56 m	(11.7 ft)
Effective Skin Thickness:	1.99 mm	(.078 in.)

The fuselage is made from aluminum alloy, series 2024.

Aluminum alloy tubing, series 6061-T6, was used for fuselage models because it was readily available. The dimensions of the fuselage models were:

Length:	178.2	mm	(7 in.)	
Diameter:	25.4	mm	(1 in.)	
Wall thickness:	0.087	mm	(0.0034 in.)	(Minimum)
Wall thickness:	0.127	mm	(0.0050 in.)	(Maximum)

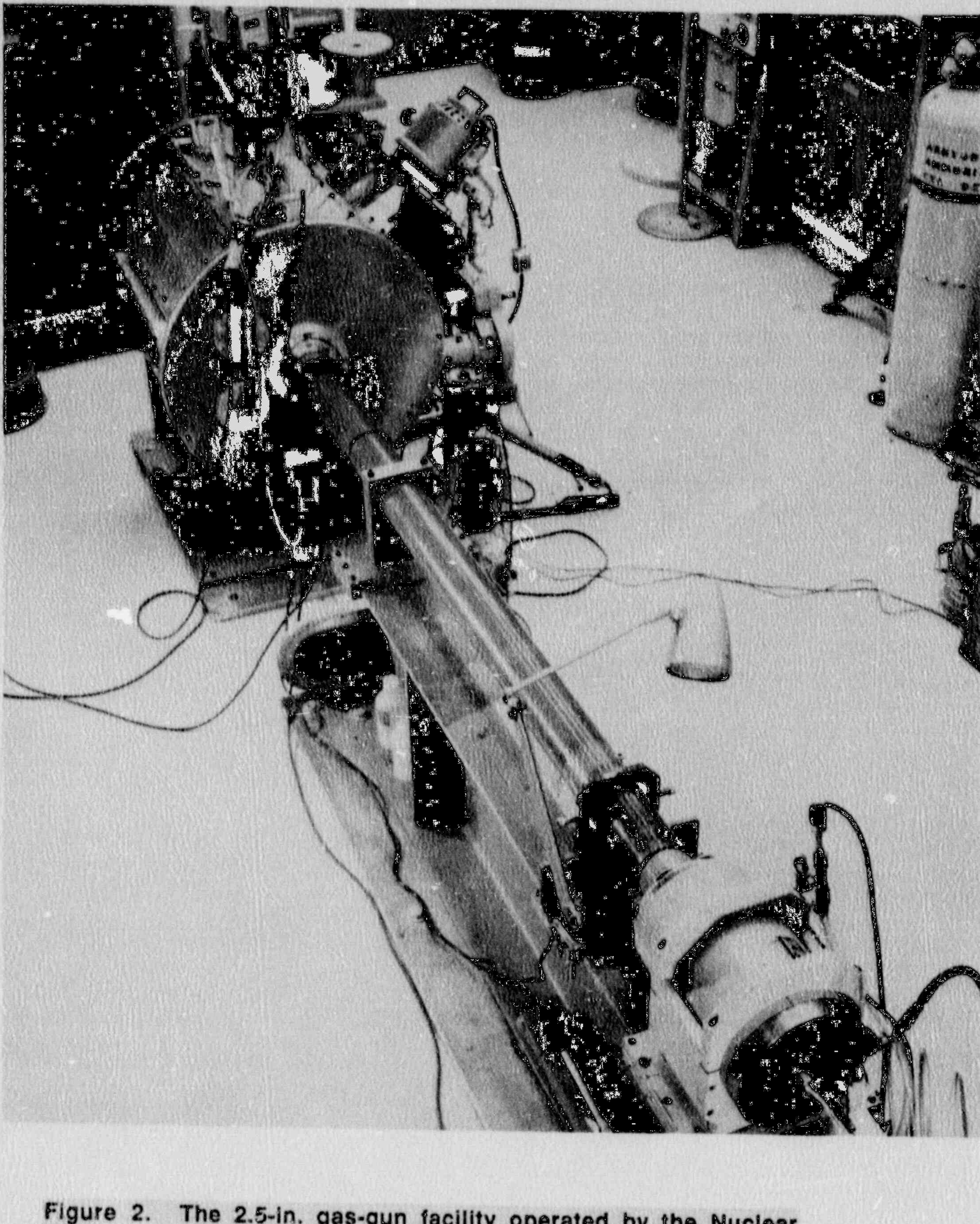

Figure 2. The 2.5-in. gas-gun facility operated by the Nuclear Chemistry Department.

The effective length of the cylindrical section of the BAe-146-200 was estimated to be slightly less than 25 m (82 ft). Thus the L/D (length/diameter) for the fuselage models are equal to that of the actual aircraft. The D/t (diameter to effective thickness) ratio of the actual aircraft fuselage is 1798. For the model fuselage, the maximum D/t-ratio was 294. The thinnest wall attainable by machining processes was that listed in the chart above. Efforts were made to produce models with a thinner wall by plating and subsequent chemical milling. Time and cost constraints precluded successful completion of that endeavor. Each fuselage model was closed at both ends by a thinly machined plug.

Other techniques for fabricating thin-wall fuselage models were considered, including laser welding of thin aluminum foil, hydro-forming, and spinning. They were not pursued because of high cost.

3.1.1 Scaling Of Rigid/Semi-Rigid Mass

Scaling of actual instrument panels, metal and plastic mass appendages internal to the fuselage was done purely qualitatively and without mathematical scale. It is speculated that a high-velocity impact of an aircraft will result in shattering of most of the fixtures internal to the fuselage. To experimentally simulate such physical conditions, miniature toy cars, fabricated from die cast metal and plastic, were purchased and used. The cars were small enough to fit inside a 1.59 cm (5/8-in.) diameter cylindrical shell. Their length was slightly more than 2.54 cm (1-in.). Four toy cars were glued together (front-to-rear) and placed inside the model fuselage to represent the rigid/semi-rigid mass internal to the BAe-146-200 aircraft. The "lead" toy car was glued to the nose-end of the model fuselage.

3.1.2 Scaling Of Deformable Mass

Scaling of liquid and human mass internal to the fuselage was purely qualitative and without mathematical proportioning. Several worthwhile ideas emerged. Thin-wall, flexible, medical capsules filled with jello (Ref. 8), and possibly containing dispersed rigid elements was considered for simulating human mass. Play gel, such as Ecto-Plazm (Kenner Parker Toys, Inc.), was also considered. A simple and expedient choice was to "cast" a relatively thin layer of jello, horizontally, the full length of the model fuselage. The jello occupied 33% of the internal volume of the model fuselage.

3.1.3 Simulating A 60° Impact Angle

The leading end of the projectile was fully beveled with a 30° angle as shown in Figure 3a. The 30° bevel produced the desired 60° angle of impact. Figure 3b shows the collision orientation of the projectile with a model fuselage.

3.1.4 Simulating Windows In Model Fuselage

Windows were scaled from actual size. Holes (26) were drilled in the model fuselage (on both sides). The holes were 2.4 mm (0.093-in.) and were drilled on 6.4 mm (0.25-in.) centers.

3.1.5 High-Speed Photography

High-speed photography was necessary. With an impact velocity of 290 m/s (950 ft/s), the impact event occurs over a period of slightly more than 0.5 ms. That is, the projectile drives through a 17.8 cm (7-in.) model fuselage in about 0.614 ms.

3.2 Partitioning Of Shatter-Producing Sources

Fuselage shattering effects caused by mass internal to the fuselage and also effects of air pressure buildup during fuselage collapse, were to be eliminated by impacting a fuselage model in a near-vacuum environment with no internal mass present. A small hole was drilled in the rear end plug to allow air to escape during the evacuation process.

The shattering effects of rigid and semi-rigid mass internal to the fuselage were partitioned from effects due to air pressure by impacting the fuselage in near-vacuum conditions. The tests that were performed resulted in superposition of rigid/semi-rigid mass effects on high-deformation rate and high-strain rate. A test was designed which utilizes a large diameter fuselage with open ends, permitting the projectile to pass through it; by impacting only the rigid mass internal to the fuselage it would be possible to further partition the singular effects of rigid and semi-rigid mass. This test may be conducted at some later date.

The shattering effects of deformable mass internal to the fuselage were partitioned only from the effects of rigid and semi-rigid mass.

3.3 Description of the Tests

Ten model crash tests were conducted. The fundamental objective was a "scoping" exploration of the phenomenological sources of shattering in high-velocity aircraft crashes. The ten tests are summarized in Table 1.

Table 1. Summary description of the model crash tests. All model fuselages were 25.4 mm diameter, 178 mm long.

Test	Wall Thickness, mm	Envir. Pres.	Remarks
1	0.127	vac.	no internal mass, no high-speed photograph
2	0.127	vac.	repeat of Test #1, but with high-speed camera
3	0.127	vac.	rigid/semi-rigid mass internal to fuselage
4	0.127	vac.	60°-impact angle, no internal mass
5	0.127	vac.	52 simulated windows, no internal mass
6	0.102	air, 1-atm	no internal mass, effect of air pressure buildup
7	0.102	air, 1-atm	deformable mass, jello occupying 33% of space
8	0.0865	vac.	repeat of Test #2, with thin wall model
9	0.0967	vac.	repeat of Test #3, with thin wall model
10	0.127	vac.	repeat of Test #2

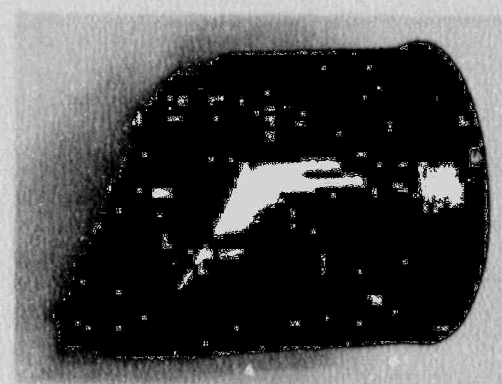

Figure 3a. Projectile, beveled to simulate 60° impact.

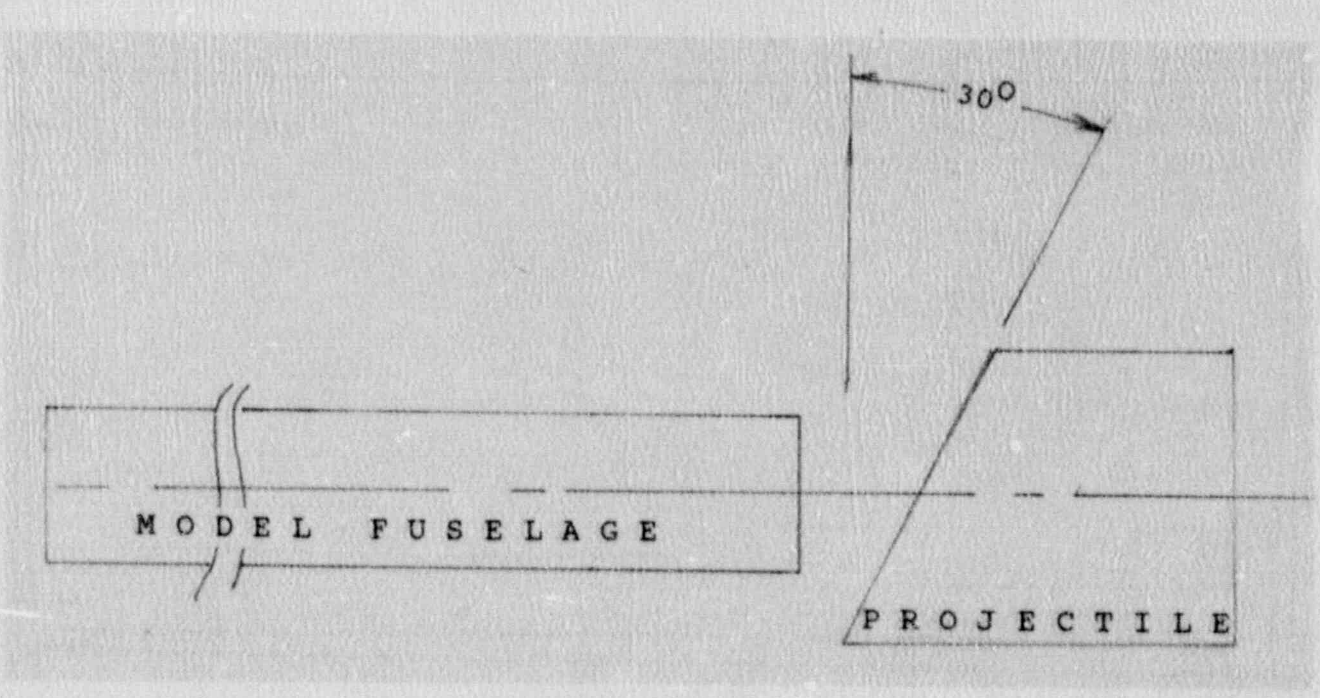

Figure 3b. Pre-impact configuration simulating 60° impact.

Test #1 was conducted without use of high-speed camera instrumentation. Because of the uncertainty of sources of resulting fragmentation, it was decided that high-speed camera instrumentation would be essential. Tests #2 and #3 were supported with high-speed camera, but triggering problems and lighting conditions were such that these tests needed to be repeated (Ref. Tests #9 and #10).

4. Results

It was deduced that some fragmenting of the fuselage occurred on impact in all ten tests. The criteria used to characterize and compare shattering effects due to the several potential sources were:

a) total number of fragments produced,

b) location of recovered fragments,

c) the size of the largest fragment,

d) the location of the largest fragment, and

e) observations of impact event from high-speed photography films (Ref. 10).

Table 2 provides a summary of details for each of the ten tests.

4.1 Base Case

The Base Case was a 90° impact angle in a vacuum environment at a velocity of 290 m/s (950 ft/s). No mass, other than the model fuselage skin, was involved in the impact with the projectile. Four very similar tests were conducted under Base Case conditions. The only significant variable was thickness of the fuselage skin wall. Results were essentially the same in all four events (Test #1, #2, #8, #10). A small amount of fragmentation occurred. High-speed camera was not in use for the first test. Lighting was inadequate in the second test. Fragmentation on impact was evident in the last two tests. There was no appreciable difference in the degree of fragmentation of a 0.127 mm (0.005-in.) wall thickness model fuselage and one with 0.086 mm (0.0034-in.) wall thickness. The 2-dimensional kinematic analysis of a buckling phenomena (Appendix 11) suggests that shattering due to high-deformation rate should be independent of wall thickness. Refer to Appendices 1, 2, 8, and 10 for detailed test results.

Table 2. Summary of results of the model crash tests.

Characteristic:	Test #1	Test #2	Test #3	Test #4	Test #5[1]	Test #6	Test #7	Test #8	Test #9	Test #10
Test Date	6/2	6/2	6/7	6/14	6/15	6/20	6/22	7/7	7/12	7/19
H.S. Camera Record	none	fair (slow)	better (dark)	good	good	good	fair	good	good	good
Target Environ. (milli-Torr)	40	135	135	74	85	1-atm	1-atm	70	70	90
Projectile Velocity (m/s)	303	292	292	425[2]	289	290	290	290	290	290
Projectile Mass (g)	314	314	314	232[2]	314	313	314	313	313	313
Angle of Impact (deg)	90	90	90	60	90	90	90	90	90	90
Model Fuselage Wall Thick., mm	.127 (.005")	.127 (.005")	.127 (.005")	.127 (.005")	.127 (.005")	.102 (.004")	.102 (.004")	.0865 (.0034")	.0967 (.0038")	.127 (.005")
Quantification of Fragmentation:										
Fragmentation on Initial Impact	no?[3]	no?[3]	yes	no?[3]	no?[3]	yes	yes	yes	yes	yes
Total Number of Alum. Fragments	62	35	128	54	42	139	143	24	186	124
Number of Alum. Fragments Recovered Outside Catcher	39	13	70	42	22	62	116	8	105	45
Number of Alum. Fragments Recovered Inside Catcher	23	22	58	12	20	77	27	16	81	79
Mass Analysis of Target:										
Mass of Fuselage Model (g)	8.2	8.2	6.7	7.3	7.34	6.2	6.4	4.62	4.91	6.84
Mass of Rigid and Semi-rigid Members (g)	--	--	17.79	--	--	--	--	--	17.71	--
Mass of Deformable Members (g)	--	--	--	--	--	--	35	--	--	--
Mass-% of Alum. Fragments Outside Catcher	14	3.3	44	87.7	8	8.9	89	9.5	39	9.8
Mass-% of Alum. Fragments OutsideCatcher	79	96.1	49	11.5	91.6	90	11	90.5	57	90.2
Mass-% of Alum. Frag. between Proj. and Foam	66	84	28	0[4]	79	82	0[4]	82	0[4]	0[4]
Mass-% of Largest Alum. Fragment	66	84	14	41	79	82	8	82	26	87

1 The fuselage model had holes drilled to simulate windows.
2 The steel peg separated from Lexan projectile; Lexan weight = 232 g.
3 Fragmentation was not detectable from high-speed film, due to poor lighting conditions; subsequent tests provided the basis for deducing that a small amount of fragmentation occurred on initial impact.
4 The projectile was disgorged from the catcher.

4.2 Rigid And Semi-Rigid Mass Effects

As described earlier, toy model cars fabricated of die cast metal and plastic parts, were glued together and then placed inside the model fuselage and glued to the nose end. The "crash" event occurred in near-vacuum conditions similar to that of the Base Case. The shattering effect on the model fuselage, due to the break-up of internal mass, was superimposed on the effects due to high-deformation rate and high-strain rate. Shattering of the model fuselage was catastrophic in both tests (Test #3 and Test #9). The only significant difference in the two tests was model fuselage wall thickness (as noted in Table 1). Fragmentation was slightly more severe in the case of thinner model fuselage wall. Refer to Appendices 3 and 4 for detailed test results.

4.3 Air Pressure Buildup Effects

The shatter-producing effects of air pressure were superimposed on high-deformation and high-strain rate effects. The result was a moderate degree of fragmentation. The presence of air made the model fuselage considerably "stiffer" than cases where a near-vacuum environment condition existed. As a consequence, less than half of the model fuselage collapsed during the initial impact event. Only one test of this type was conducted (Test #6). Refer to Appendix 6 for detailed test conditions and test results.

4.4 Deformable Mass Effects

The shattering effect of a relatively thin layer of jello, cast the full length of the fuselage (occupying 33% of the volume), was catastrophic. The impact occurred in a 1-atmosphere environment. Therefore, the event represented the combination of effects from: a) high-deformation rate, b) high-strain rate, c) air pressure buildup, as well as d) erupting deformable mass. Only one test involving deformable mass was conducted (Test #7). Refer to Appendix 7 for detailed test conditions and results.

4.5 Window Effects

Windows were expected to increase the potential of fuselage shattering, due to associated stress concentrations and mass concentration anomalies. However, no significant difference in model fuselage shattering was observed in comparison with results of the Base Case. Only one test involving simulated windows was conducted (Test #5). Refer to Appendix 6 for detailed test conditions and test results.

4.6 Angle Of Impact Effect

The angle of impact was expected to influence the degree of model fuselage shattering. One test was conducted where the angle of impact was 60° (Test #5). The model fuselage contained no concentrated masses of any kind. The impact occurred in a near-vacuum environment. The result of the one test indicates that angles of impact has little (if any) influence on model fuselage shattering, for conditions where no mass is concentrated internal to the fuselage or where no concentrated mass appendages to the fuselage structure exist. Refer to Appendix 6 for detailed test conditions and test results.

5. Discussion Of Results

It is noted in Table 2 that a relatively large number of fragments were recovered both inside the catcher and on the floor of the test chamber in each of the ten tests. Many of the fragments were produced by secondary impact of the model fuselage remnant with rigid foam placed in the catcher to decelerate the projectile. A means of "catching" the projectile and preventing it from crushing the model fuselage remnant was instituted for the last two tests (Tests #9 and #10).

5.1 Fragment Count And Distribution

High-speed photography shows fragments being disgorged from the catcher after the impact event is completed and the projectile has entered the catcher. Further, film shows some of the fragments created in the initial impact, entering the catcher ahead of the projectile. Thus, a simple count of fragments found outside the catcher cannot be attributed (solely) to fragmentation due to initial impact.

The crash tests producing the largest number of fragments were (186 fragments) in Test #9 (rigid and semi-rigid mass inside model fuselage) and (143 fragments) in Test #7 (deformable mass, jello). Generally, the fewest fragments resulted from "Base Case" conditions (vacuum, with internal mass). The number of fragments recovered from Test #10 appears anomalously high. A comparison of high-speed photography results of Test #10 (Base Case with 0.127 mm wall) with Test #8 (Base Case with 0.0865 mm wall), shows about the same amount of fragments being created during the initial impact event. It is deduced that the uncrushed model fuselage remnant (in Test #10) was driven into the catcher's steel conical insert in an adverse fashion, causing significant secondary fragmentation.

5.2 Significance Of "Largest" Fragment

The size of the largest fuselage remnant is a gauge of extent of global fragmentation. In all ten tests, a "largest piece" fuselage remnant was identified. In six of the ten tests the "largest" piece was more than 50% of the original mass of the model fuselage. The presence of concentrated mass internal to the model fuselage produced global shattering. Test #7 (deformable mass) produced the smallest "largest" fuselage remnant, 8% of the mass of the original model fuselage.

5.3 Effects of Fuselage Air Environment

The model fuselage in Test #6 behaved with considerably more stiffness during impact than any other test. It was stiffened by the presence of air both inside and outside the model. As a consequence, the projectile collapsed only about 50% of the model. The last 50% was crushed by the secondary impact with the decelerating foam. Shattering may have been more intense, locally, in this test than in any other, but the intensity diminished rapidly after impact as the velocity of the uncrushed target accelerated to the same velocity of the projectile.

A shock wave should be initiated in the air inside the fuselage upon impact. The peak pressure of the shock wave for conditions of Test #6 is calculated below (see page 3-72 of Ref. 11). The pressure wave would result from the sudden change in momentum of the air when it is decelerated by the impact.

$$P = \rho c V$$

$$= 0.12 \text{ MPa (17.5 psi)}$$

where:

ρ = standard air density (1.22 kg/m^3),
c = sonic velocity in standard air (340.4 m/s),
V = impact velocity (289.6 m/s, 950 ft/s).

Such a shock wave would more than double the local fuselage air pressure in the impact zone.

6. Conclusions

It was clearly established that "shattering", characteristic of that which occurred in the crash of PSA Flight 1771, could be replicated in a laboratory environment. It was determined that all of the phenomenological sources identified earlier contributed to shattering. While none of the five potential sources of shattering could be perfectly partitioned from the others, it is our qualitative judgment that internal mass (and external mass appendages), both rigid/semi-rigid and deformable, contribute most catastrophically to fuselage shattering. Further, these same two phenomenological shattering sources must be considered in assessing the survivability of a PAT package in the event of a "worst-case" crash.

7. References

1. United States Public Law 100-203, Title V - Energy and Environment Programs, Subtitle A - Nuclear Waste Amendments, Part F - Miscellaneous, Section 5062, December 22, 1987.

2. Johnson, G. R., et.al., "Response of Various Metals to Large Torsional Strains Over a Large Range of Strain Rates",. **TRANSACTIONS OF ASME**, Vol. 105, January 1983.

3. Juvinall, R. C., **ENGINEERING CONSIDERATIONS OF STRESS, STRAIN, AND STRENGTH**, McGraw-Hill Book Company, 1967.

4. Stout, M. G., et.al., "Strain Rate Sensitivity, Strain Hardening, and Yield Behavior of 304L Stainless Steel", **TRANSACTION OF ASME**, Vol. 108, October 1986.

5. Personal Communications, Monika Witte and martin Schwartz, Lawrence Livermore National Laboratory, July 1989.

6. Siegel, Arnold E., "The Theory of High-Speed Guns", United states Naval Ordnance Laboratory, White Oak, Silver Springs, Maryland, AGARDograph 91, NORTH ATLANTIC TREATY ORGANIZATION Advisory Group for Aerospace Research and Development, May 1965.

7. **JANE'S ALL THE WORLD'S AIRCRAFT 1987-88**, Jane's Publishing Company Limited, 238 City Road, London EC1V, England.

8. Personal Communications, Jim Van Sant, Lawrence Livermore National Laboratory, July 1989.

9. Walter, Carl E., Van Sant, James H., and Chou, C. K., **DRAFT CRITERIA FOR PACKAGE DROP AND AIRCRAFT CRASH TESTS** - An Interim Report, Lawrence Livermore National Laboratory, UCID-21697, June 28, 1989.

10. Caywood, J., Davis, B., Walter, C., Chou, C. K., "High-Velocity Impact Model Crash Experiments", (a video production of selected laboratory crash experiments), Lawrence Livermore National Laboratory, CS #2915, July 1989.

11. Baumeister & Marks, **STANDARD HANDBOOK FOR MECHANICAL ENGINEERS**, Seventh Edition, McGraw-Hill, 1967.

APPENDICES

Note: For all photos in Appendices 1 through 10, which show impact events, the time lapse between frames is 45 μs.

APPENDIX 1

Test #1

Test Results, Base Case

June 2, 1989

OBJECTIVE OF TEST:

The purpose of this test was that of determining whether shattering of a model fuselage could be produced by high-strain rate combined with high-deformation rate in a high-velocity impact, in the absence of concentrated mass internal to the fuselage.

TEST CONDITIONS:

The "Base Case" was a vacuum shot. A 1-in. thick x 8-in. OD cylindrical rigid foam shell encompassed the target. A 4-in. diameter steel pipe "catcher" was stationed behind the target. The purpose of the encompassing foam was to catch aluminum fragments, in the event of shattering. The purpose of the steel pipe was to catch the projectile. The target (fuselage model) had a blunt nose because time constraints did not allow forming of a rounded nose. We wanted to achieve an impact velocity of 283 m/s. The measured velocity was 303 m/s. Other specific test conditions are outlined below:

Time:	1.45 p.m.
Date:	June 2, 1989
Helium Pressure:	4.33 MPa (628 psi)
Chamber Pressure:	40 milli-Torr
Projectile Mass:	314 g
Projectile Velocity:	303 m/s
Target Dimensions: (Length x diameter x wall thickness)	178 mm x 25.4 mm x .127 mm (7 in. x 1 in. x 0.005 in.)
Target Material:	6061-T6 aluminum
Target Mass:	8.2 g
Impact Angle:	90°

RESULTS:

Following the shot a visual inspection was made through the acrylic site ports of the test chamber. The first indication that shattering might have occurred was given by observing that the foam encompassing the target had been destroyed. Upon opening the door of the test chamber, very small (approximately 2 mm x 7 mm) aluminum fragments were visible on the floor of the chamber.

Quantitative Observations:

1) Thirty-nine (39) fragments were recovered from the floor of the chamber. Fragment sizes ranged from about 1 mm x 2 mm to about 1 cm x 3 cm. By far, most of the fragments were very small, of the order of about 3 mm x 3 mm.

2) Twenty-three (23) fragments were recovered inside the catcher, with the sabot. Fragment sizes ranged from about 1 mm x 1 mm to about 1 cm x 1 cm. Additionally, a relative large portion of the target mass (about 70%) remained wedged between the face of the sabot and the foam shock absorber used to stop the sabot. That piece was clearly the largest fragmented piece. It appears to include both the "nose" end and the rear end of the target, as well as a portion of the wall of the target.

3) An exact accounting of fragment mass will be made soon and documented. It appears that fragments found on the floor came only from the walls of the target (both end pieces appear to have survived without fragmentation and were inside the catcher with the sabot). It is estimated that between 4 and 10% of the wall mass was recovered on the floor.

4) The largest single piece of the target was found inside the catcher, pressed between the face of the sabot and the shock absorbing foam. It is estimated that the piece represents about 70% of the mass of the original target.

DISCUSSION:

Observations 1), 2), and 3) suggest that shattering occurred on impact and that some tearing and ripping of the target also occurred during the stopping of the sabot by the rigid foam. Observation 4) indicates that some of the fragments found on the floor of the chamber could have come from shearing of the target by the foam as it was carried into a secondary impact condition with the foam by the sabot. Subsequent disgorging of fragments in the wake of the the sabot could possibly account for most of the fragments found on the floor of the chamber.

CONCLUSIONS:

Based on post-mortem observations, it is concluded that high-strain rate is likely the cause of some of the fragmentation of the "fuselage" model. It cannot be stated, however, that the majority of the fragmentation was caused by the initial impact of the sabot with the target. Future tests are expected to provide more precise delineation of shatter-producing phenomena.

APPENDIX 2

Test #2

Repeat of Base Case without H.S. Photo

June 12, 1989

OBJECTIVE OF TEST:

The purpose of the test was to determine whether a thin-wall fuselage model would fragment (due to high-strain rate) upon impact with a Lexan projectile having an impact velocity of 283 m/s (930 ft/s).

TEST CONDITIONS:

Test #2 was a repeat of Test #1 (Base Case). A high-speed camera (effective frame rate of 22,000 frames per second, maximum) was incorporated for the purpose of capturing the event (however, triggering of the camera was not properly synchronized). The test environment was partial vacuum. There were no concentrated masses and no surface irregularities designed into the model. The nose of the model was blunt. Other specific test conditions were:

Time:	10:45 a.m.
Date:	June 7, 1989
Helium Pressure:	3.86 MPa (560 psi)
Chamber Pressure:	135 milli-Torr
Projectile Mass:	314 g
Projectile Velocity:	92 m/s
Target Dimensions: (Length x diameter x wall thickness)	178 mm x 25.4 mm x 127 mm (7 in. x 1 in. x 0.005 in.)
Target Material:	6061-T6 aluminum
Target Mass:	8.2 g
Impact Angle:	90°

A foam collar was fitted over the forward end of the steel "catcher". Its purpose was to provide structure to support the target and catch some of the aluminum fragments. Most of the wall of the foam was cut away to permit camera viewing.

RESULTS:

The high-speed camera was triggered too late to effectively capture the entire impact event.

Quantitative Observations:

1) Four (4) impact "scars/holes" in the foam collar give indications that some fragmentation occurred on impact. One (1) fragment was recovered in the foam. Fragment dimensions were about 1 mm by 6 mm. It had penetrated about 2 inches of the foam, axially, before coming to rest near the outside surface.

2) Thirteen (13) fragments were recovered on the floor of the test chamber. The fragments ranged in size from small (1 mm x 1 mm) to large (6 mm x 15 mm).

3) Twenty-two (22) fragments were recovered inside the catcher. The fragments ranged in size from 1 mm x 1 mm to about 15 mm x 15 mm, except for one massive piece which remained pressed between the projectile and the foam inside the catcher. That one piece included both the nose cap and the end cap, in addition to some of the target wall. This largest piece weighed 6.9 g, representing 84.1% of the original target.

4) A mass analysis of fragments found is given below:

a)	Fragments outside catcher (13)	=	0.27 g (3.3%)
b)	Fragments inside catcher (22)	=	7.88 g (96.1%)
c)	Mass of original target	=	8.2 g

DISCUSSION:

Observation "1)" above suggests that fragmentation occurred on impact. It is noted, however, that the "scars/holes" in the foam may have been caused by fragments disgorged from the catcher. (The film showed disgorged fragments and foam "flying about" inside the chamber.) Only four useful frames of film caught the initial impact. Careful review of these frames yielded no evidence that fragmentation of the fuselage model occurred upon initial impact. It is significant that most of the original mass (84.1%) of target was recovered as one fragment, pressed between the face of the projectile and the absorbing foam inside the catcher. Again, as in the first test, evidence that some of the target was sheared away upon secondary impact with the foam in the catcher was clearly observed.

CONCLUSION:

It is concluded that the strain rate produced by initial impact of the Lexan projectile with the target was not great enough to induce fragmentation. For sure, the degree of fragmentation (if any at all) due to initial impact was insignificantly small.

APPENDIX 3

Test #3

Effect of Concentrated Rigid Mass on Fuselage Model Fragmentation

June 13, 1989

OBJECTIVE OF TEST:

The purpose of this test was to investigate the influence of concentrated rigid and semi-rigid masses (within a fuselage model) on fragmentation of model "fuselage" walls when model is impacted by a high-velocity projectile.

TEST CONDITIONS:

Four small toy cars, made of metal and plastic, were glued together (end-to-end), as detailed in Figure A.3.1, and were placed inside the model fuselage. The string of cars were glued to the front end of the tube. A high-speed camera (22,000 frames/sec, max.) was stationed such that the impact event could be recorded. The test environment was partial vacuum. The nose of the model was blunt. Other specific test conditions were:

Time:	2:45 p.m.
Date:	June 7, 1989
Helium Pressure:	.83 MPa (555 psi)
Chamber Pressure:	135 milli-Torr
Projectile Mass:	314 g
Projectile Velocity:	292 m/s
Target Dimensions: (Length x diameter x wall thickness)	178 mm x 25.4 mm x .127 mm (7 in. x 1 in. x 0.005 in.)
Target Material:	6061-T6 aluminum
Target Mass:	6.7 g
Total Mass of 4 Toy Cars:	17.79 g
Impact Angle:	90°

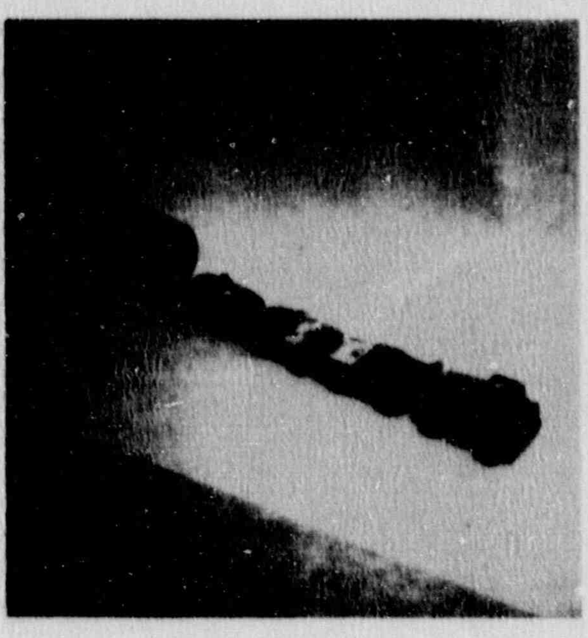

Figure A.3.1. Metal and plastic toy cars represent rigid and semi-rigid mass internal to the fuselage.

RESULTS:

The high-speed camera was properly triggered for this event. Lighting was insufficient, however. Seven frames show the impact event for about each half-inch of travel of the projectile. Catastrophic fragmentation occurred on impact. Small pieces of toy cars could be identified flowing radially from the point of impact, having apparently crashed through the walls of the model "fuselage". Refer to the sequence of frames, labeled Figures A.3.2 through A.3.8.

Quantitative Observations:

1) Four (4) impact "scars/holes" in the foam collar give indications that some fragmentation occurred on impact. Four (4) fragments was recovered in the foam. Fragment dimensions were about 4 mm by 5 mm.

2) Seventy (70) aluminum "fuselage" fragments were recovered on the floor of the test chamber. The fragments ranged in size from small (1 mm x 1 mm) to large (10 mm x 50 mm). Numerous small toy car fragments were recovered on the floor of the chamber. The toy fragments were not counted. It is estimated they numbered about 100 pieces. The rear end-cap was among the pieces found on the floor of the chamber. In all previous tests, the rear end piece was found inside the catcher pressed between the projectile and the shock absorbing foam.

3) Fifty-eight (58) fragments were recovered inside the catcher. The fragments ranged in size from 1 mm x 1 mm to about 15 mm x 15 mm, except for four pieces (total mass = 1.88 g) which remained pressed between the projectile and the foam inside the catcher. One of the larger pieces was the nose cap of the target. The largest piece (0.94 g) was part of the target walls and represents about 14% of the original mass of the fuselage target (without toy cars). In addition to the aluminum fragments recovered inside the catcher, a large number of small fragments of toy cars were also inside the catcher. They were not counted. It is estimated that about 50 pieces were recovered.

4) A mass analysis of fragments found is given below:

a)	Fragments outside catcher (70)	=	2.92 g (44%)
b)	Fragments inside catcher (58)	=	3.31 g (49%)
c)	Mass of original target	=	6.7 g

DISCUSSION:

By comparing the fragment counts with previous tests and by observation of film records, clearly the concentrated rigid and semi-rigid masses inside the fuselage produced considerably more shattering of the "fuselage" model. The film showed toy car fragments "flowing" radially from the point of impact early in the event. It is significant also that only 28% of the total original mass was recovered from the interface of the projectile and the shock absorbing foam, and further, that it was in four pieces. In previous tests more than 80% was recovered from that spot, and it was one piece. Total fragments (of aluminum "fuselage") inside and outside the catcher were 128. In two previous cases the count was 62 (Test #1, vel = 303 m/s) and 35 (Test #2, vel = 292 m/s).

CONCLUSION:

Concentrated rigid and semi-rigid mass inside the model "fuselage" represent a major contributor to fuselage shattering on initial impact. It is likely this conclusion can be extrapolated with confidence to PSA Flight 1771, where the concentrated masses would be in the form of seats, instruments, panels, and miscellaneous fixtures.

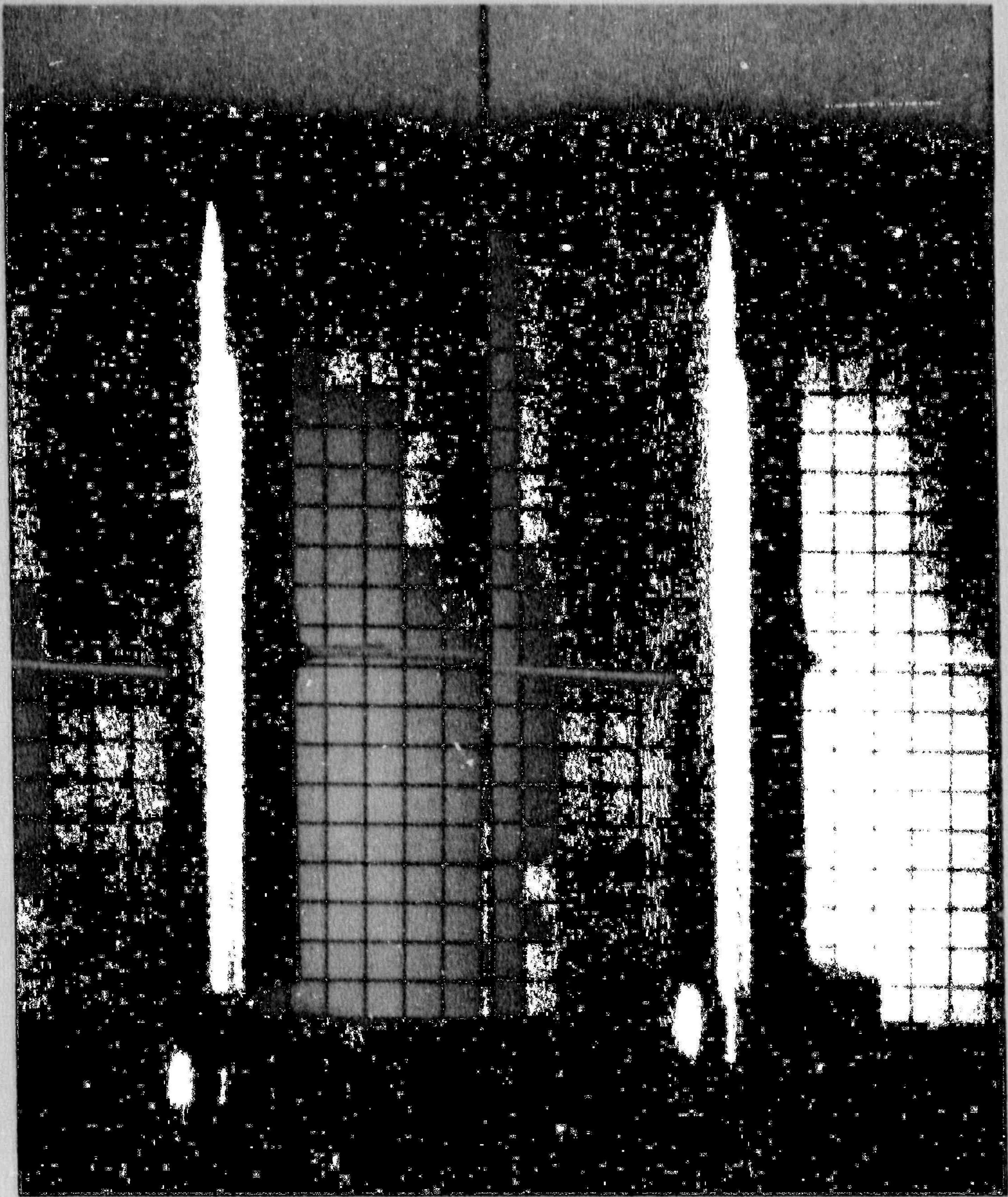

Figure A.3.2. Impact event with rigid and semi-rigid mass.

Figure A.3.3. . . . . Rigid and semi-rigid mass impact.

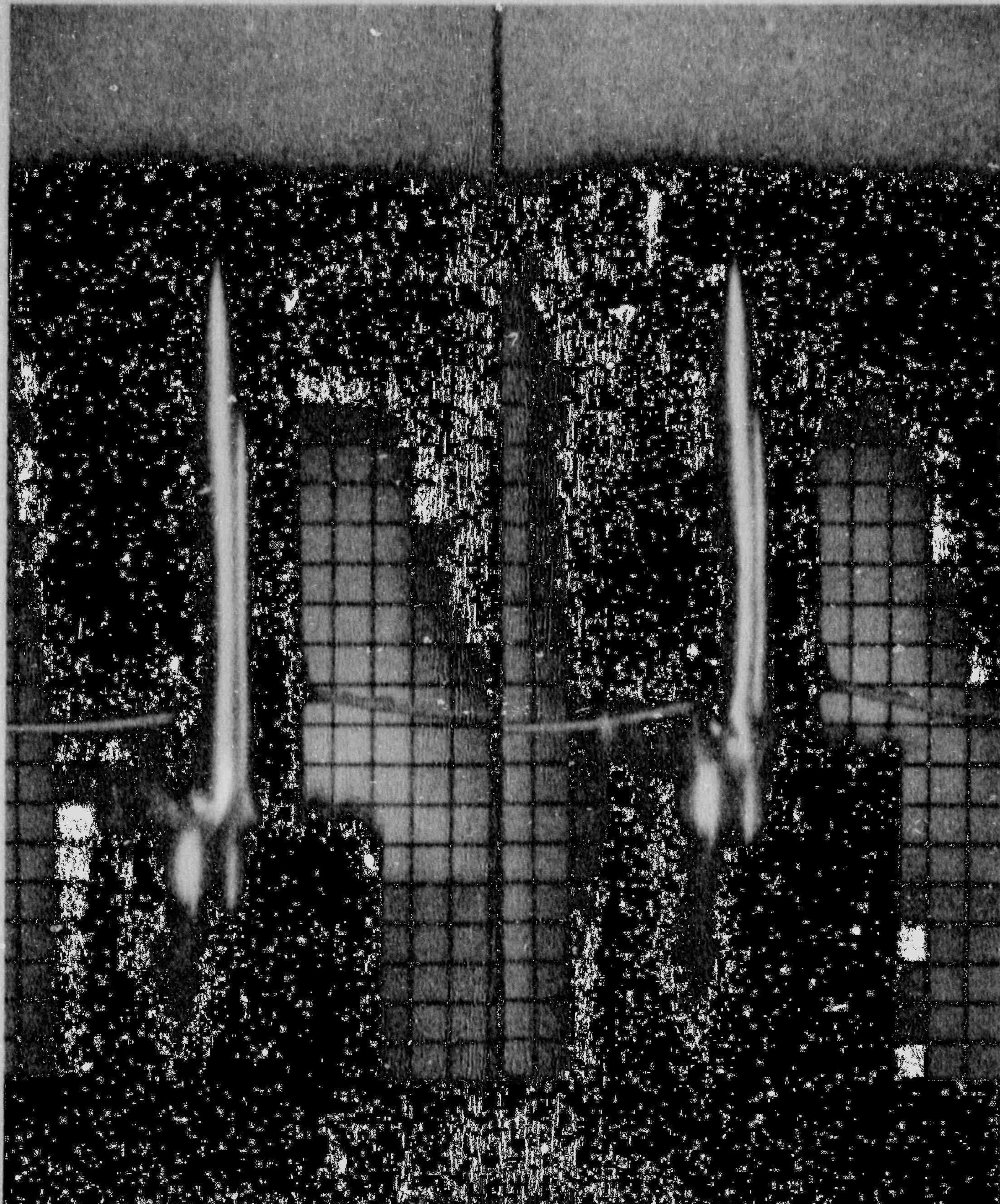

Figure A.3.4. . . . . Rigid and semi-rigid mass impact.

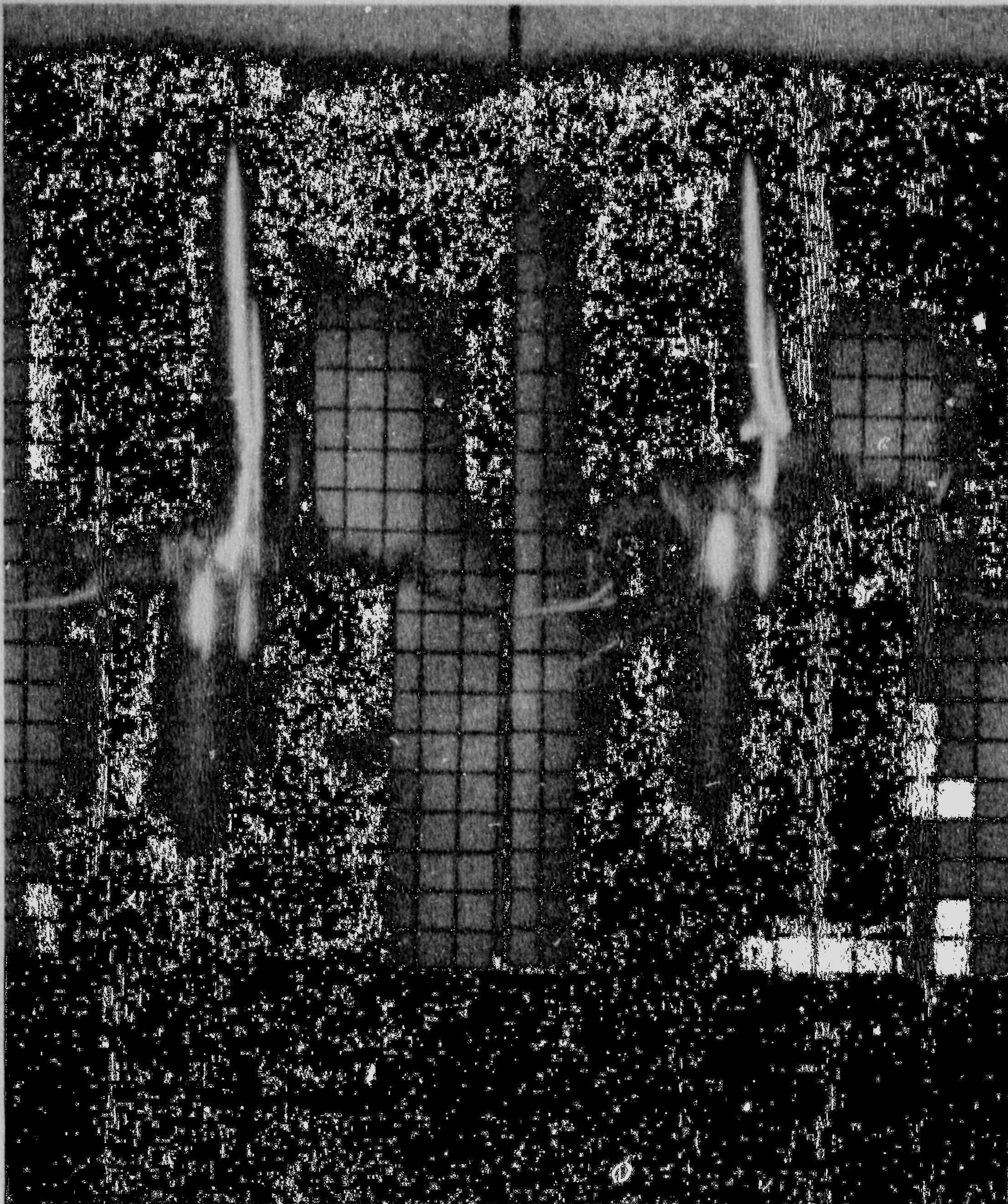

Figure A.3.5. . . . . Rigid and semi-rigid mass impact.

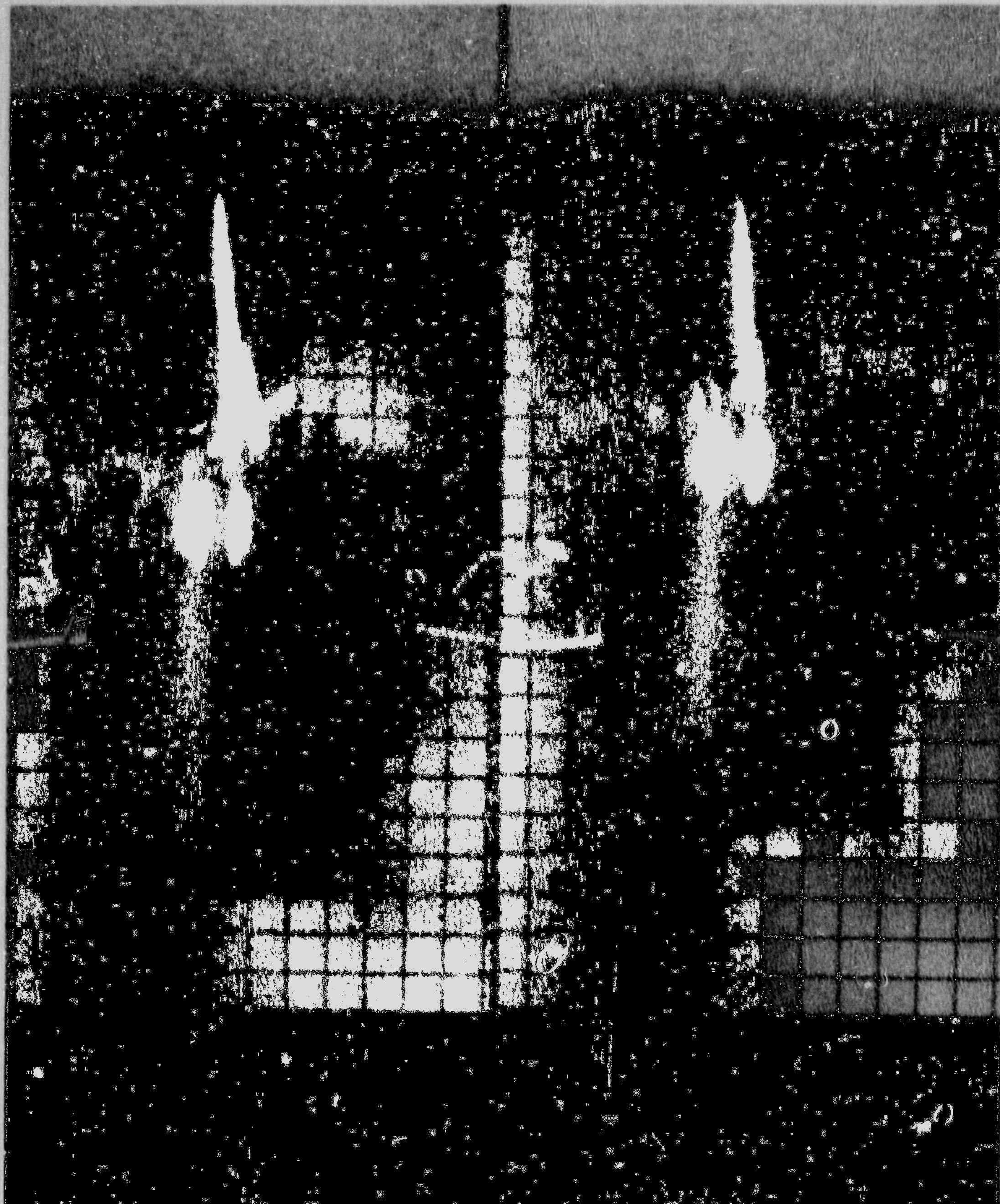

Figure A.3.6. . . . . Rigid and semi-rigid mass impact.

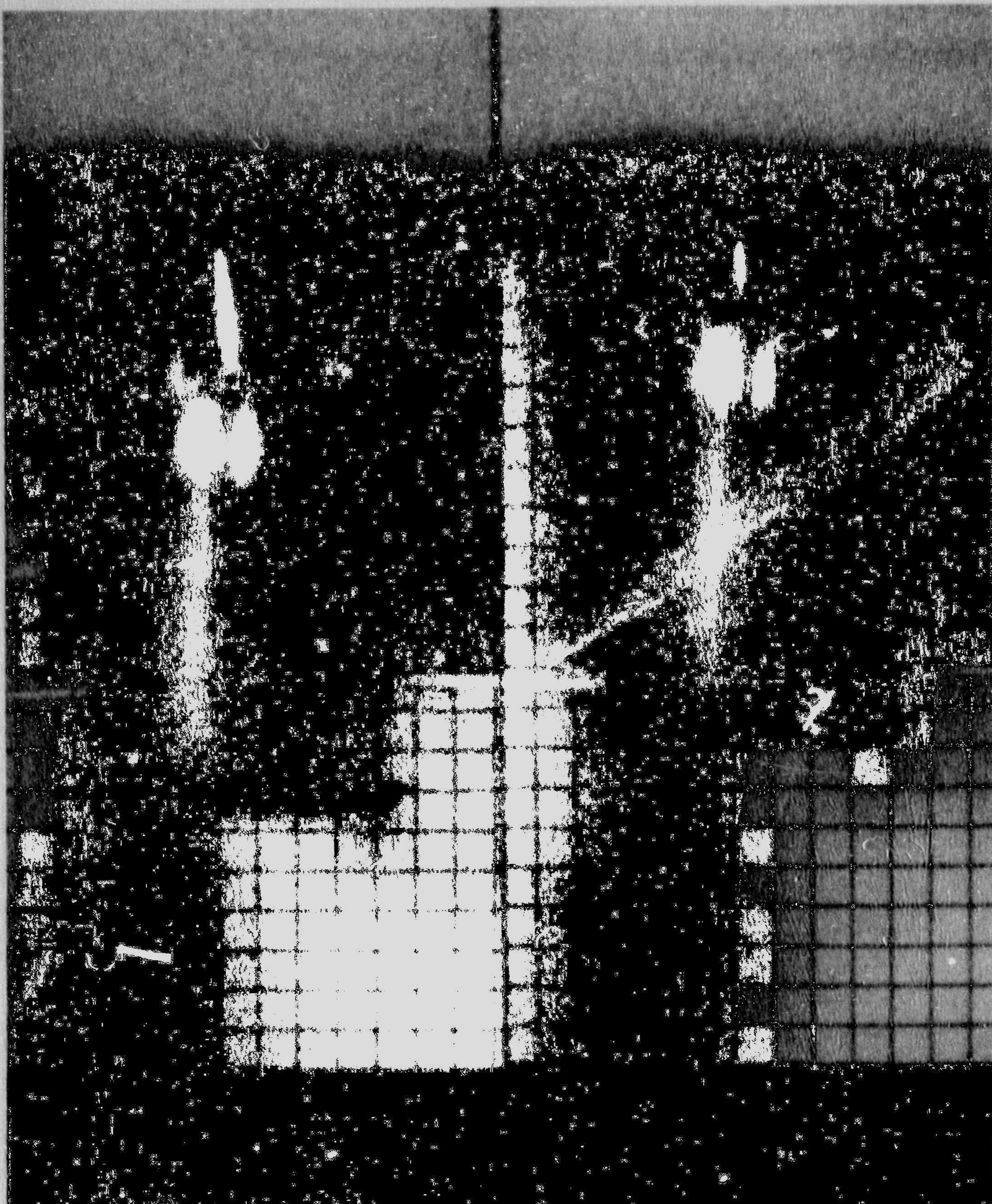

Figure A.3.7. . . . . Rigid and semi-rigid mass impact.

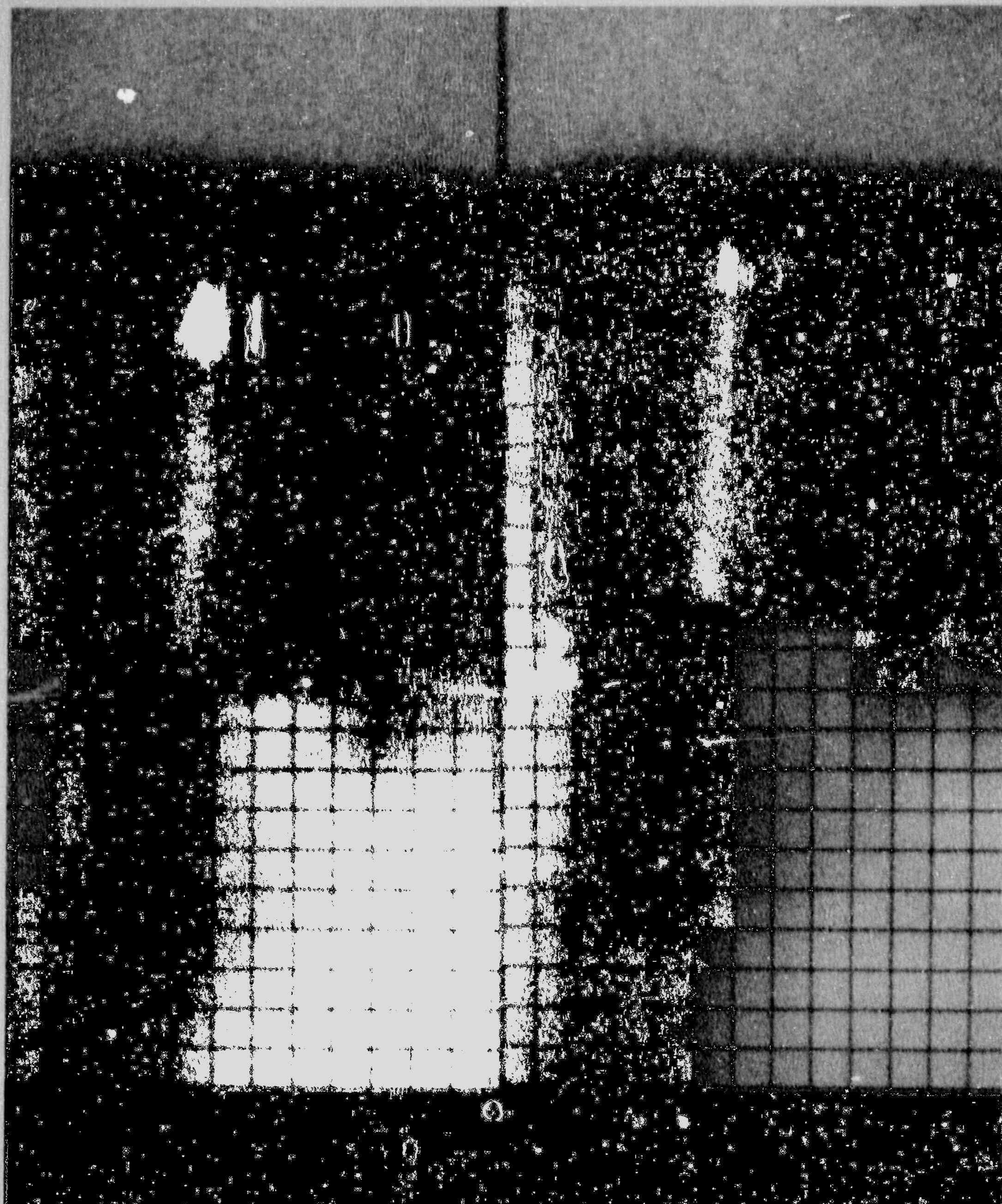

Figure A.3.8. . . . . Rigid and semi-rigid mass impact.

APPENDIX 4

Test #4

Crash Test in Vacuum with 60° Impact Angle

June 15, 1989

OBJECTIVE OF TEST:

The purpose of this test was to determine whether shattering of a "fuselage" model would occur on initial impact when the impact angle was 60° and the impact velocity was 283 m/s (930 ft/s).

TEST CONDITIONS:

The test environment was partial vacuum. The projectile was placed in the gun breech with knife-edge of beveled projectile oriented downward. The high-speed camera was electronically instrumented to fire the gun at optimum camera speed (22,000 frames per second). A steel peg was pressed into a drilled hole in the rear of the projectile to bring its weight to 313 g. During the event the steel peg became dislodged from the Lexan projectile, permitting the Lexan part to achieve velocities higher than the 283 ms intended. The impact velocity was estimated to be about 425 m/s from the high-speed photography record. Other specific test conditions were:

Time:	1:15 p.m.
Date:	June 14, 1989
Helium Pressure:	3.76 MPa (545 psi)
Chamber Pressure:	74 milli-Torr
Projectile Mass:	311 g
Projectile Velocity:	425 m/s
Target Dimensions: (Length x diameter x wall thickness)	178 mm x 25.4 mm x .127 mm (7 in. x 1 in. x 0.005 in.)
Target Material:	6061-T6 aluminum
Target Mass:	7.3 g
Impact Angle:	60°

A foam collar was fitted over the forward end of the steel "catcher". Its purpose was to provide structural support for the target fixture and catch some of the aluminum fragments. Most of the foam wall was cut away to permit camera viewing. The projectile was painted black and the target was painted flat yellow for this test. The reason for so doing was to improve the contrast. Another problem was created by the paint; it flaked off during impact, making it difficult to discern whether fragmentation was occurring.

RESULTS:

No large pieces of aluminum fragments remained inside the catcher. Many pieces were seen being disgorged after the projectile entered the catcher. The projectile was also disgorged in this event.

Quantitative Observations:

1) The beveled projectile entered the steel catcher off-center, slightly impinging on the lip of the catcher. It (projectile) was stopped by the shock absorbing foam and subsequently disgorged, coming to final rest on the floor of the test chamber. No scars were observed in the pieces of foam collar (outside the catcher) and no fragments were recovered in the pieces of foam collar.

2) Forty-two (42) aluminum "fuselage" fragments were recovered on the floor of the test chamber. The fragments ranged in size from small (1 mm x 1 mm) to two relatively large crumpled masses, each weighing about 3 g. The high-speed photography print showed the two large masses being disgorged from the catcher.

3) Twelve (12) fragments were recovered inside the catcher. The fragments ranged in size from 1 mm x 1 mm to about 15 mm x 25 mm. Unlike previous tests, no large single fragment remained in the catcher.

4) A mass analysis of fragments found is given below:

a)	Fragments outside catcher (42)	=	6.4 g (87.7%)
b)	Fragments inside catcher (12)	=	0.84 g (11.5%)
c)	Mass of original target	=	7.3 g

DISCUSSION:

The high-speed camera was properly triggered for this event. Seven frames show the impact event for about each inch of travel of the projectile. Fragmentation on impact was not clearly evident from either the quantity/location of fragments nor from the high-speed photography. The two large pieces, mentioned in "Observation 2.", were seen being disgorged from the catcher after the projectile entered the catcher. The photography showed a large number of small aluminum fragments being disgorged after the projectile entered the catcher. It is noted that the velocity at impact was significantly higher than that of other similar events (for reasons explained earlier). What appeared to be small "fuselage" fragments being cast upward during initial impact was later concluded to be paint, which flaked off the target and the beveled face of the projectile during collision. The series of photos, labeled Figures A.4.1 through A.4.7, show the initial impact event.

CONCLUSION:

In the absence of concentrated masses internal to the model "fuselage", the 60° impact angle does not appear to increase the degree of fragmentation. Further, the degree of fragmentation (if any) on initial impact was negligibly small.

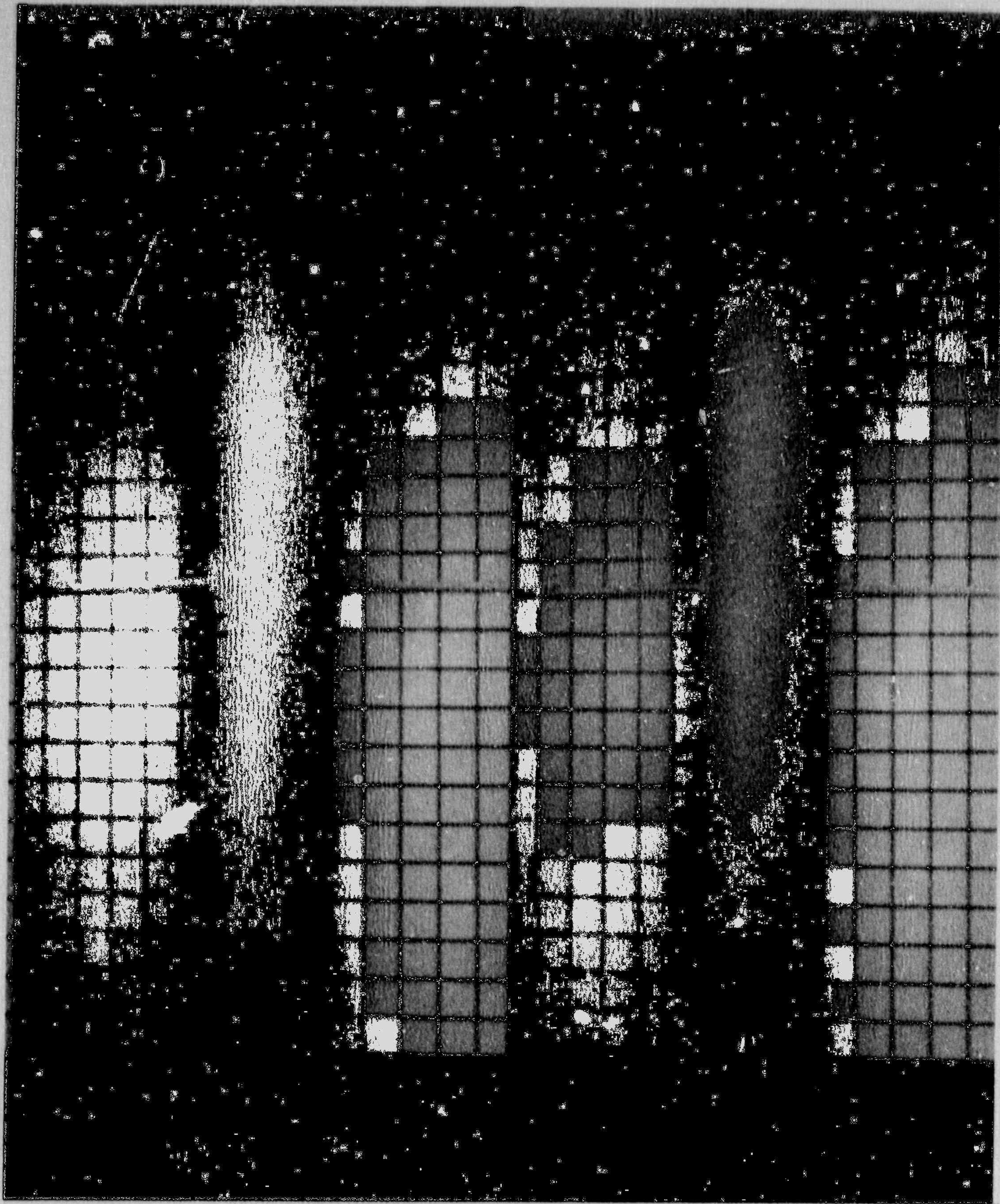

Figure A.4.1. 60° angle of impact.

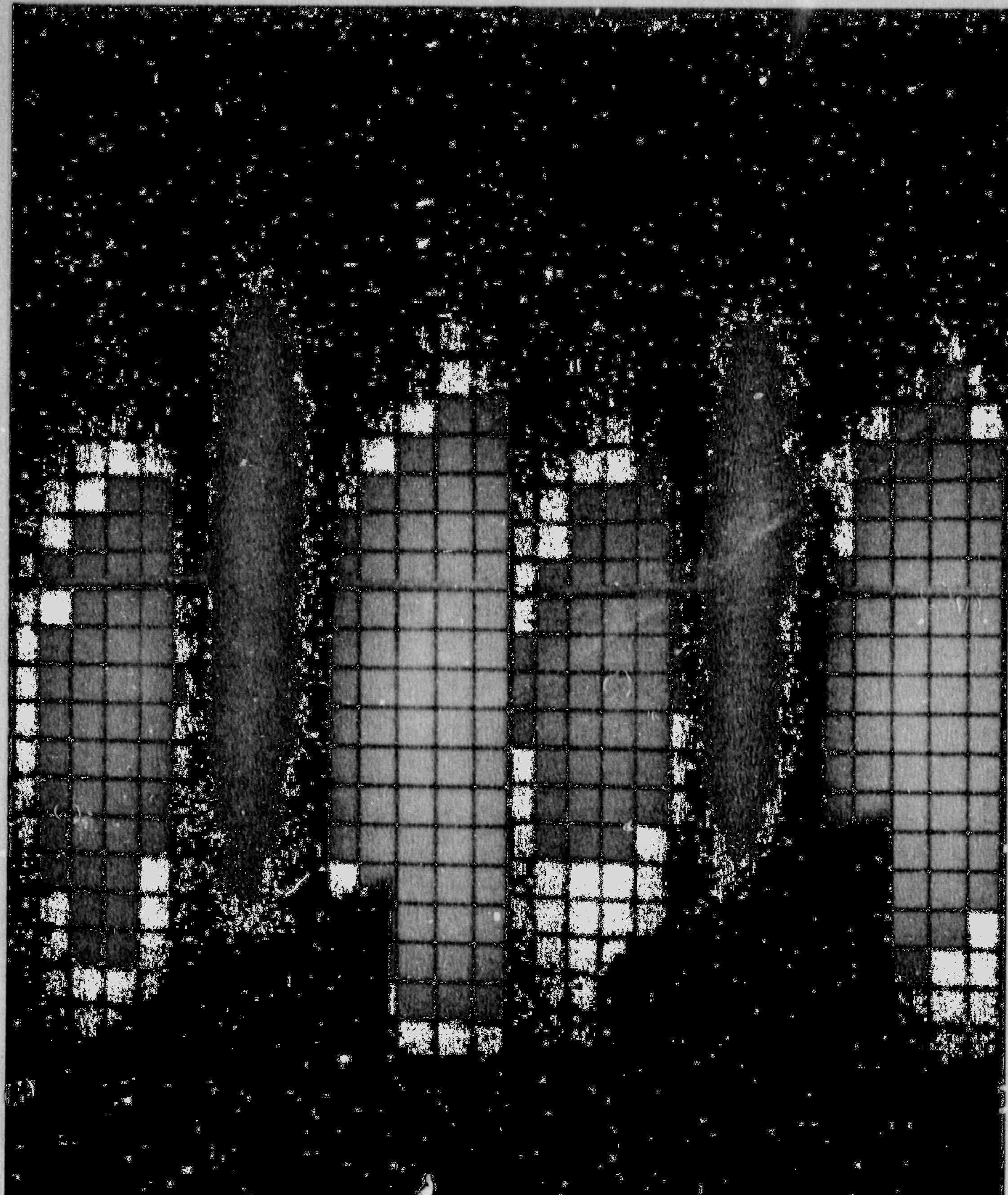

Figure A.4.2. . . . . 60° impact.

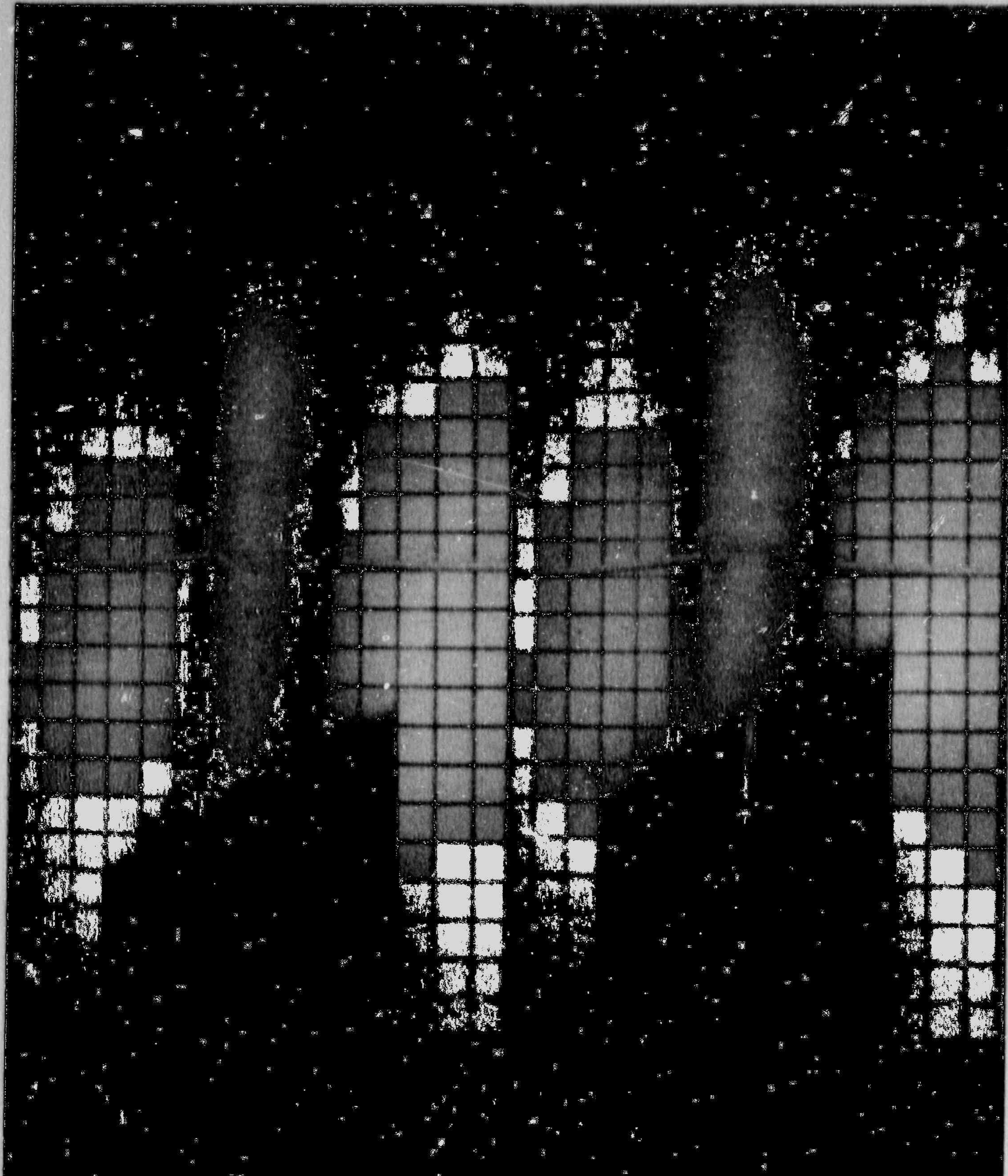

Figure A.4.3. . . . . 60° impact.

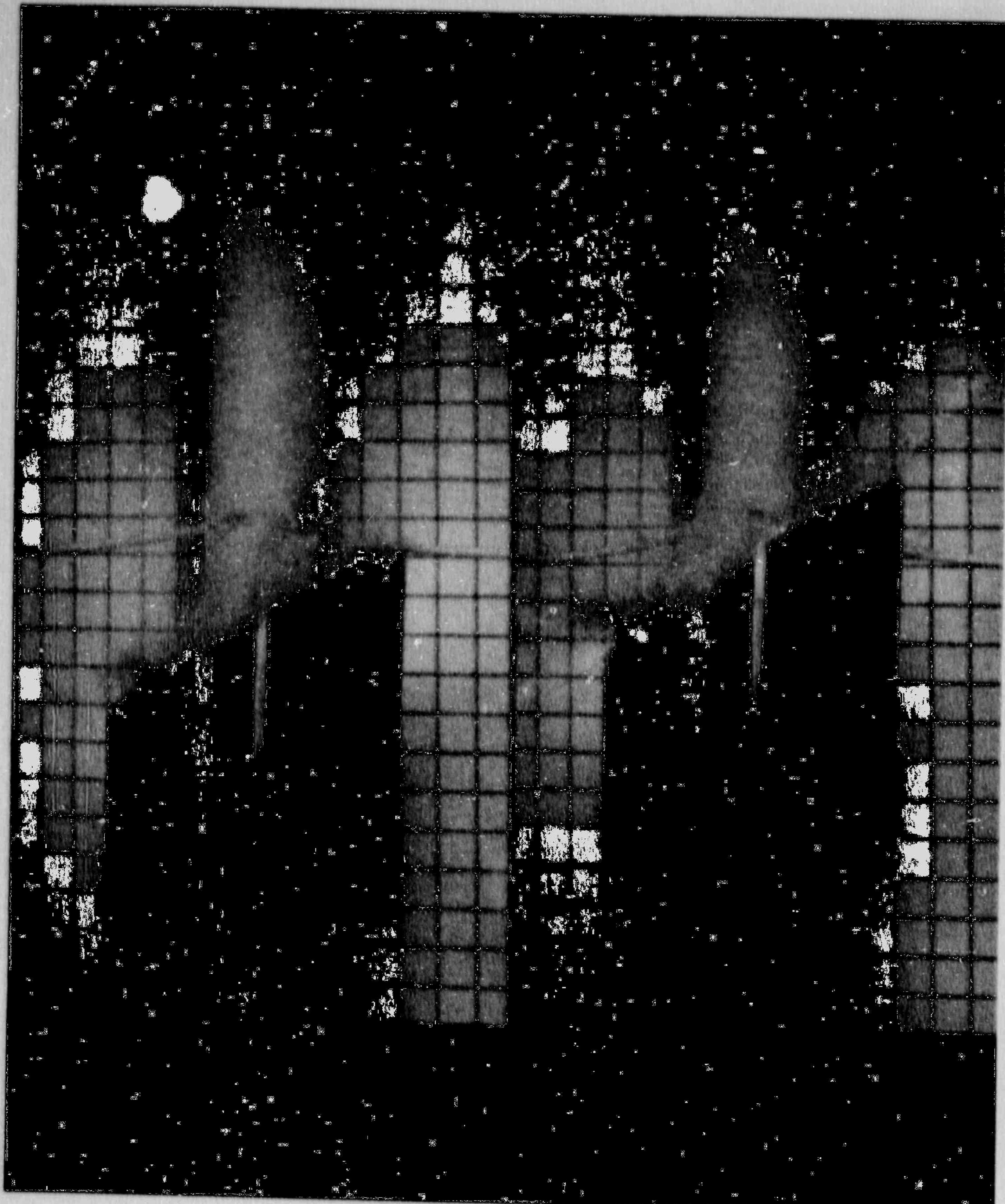

Figure A.4.4. . . . . 60° impact.

Figure A.4.5. . . . . 60° impact.

Figure A.4.6. . . . . 60° impact.

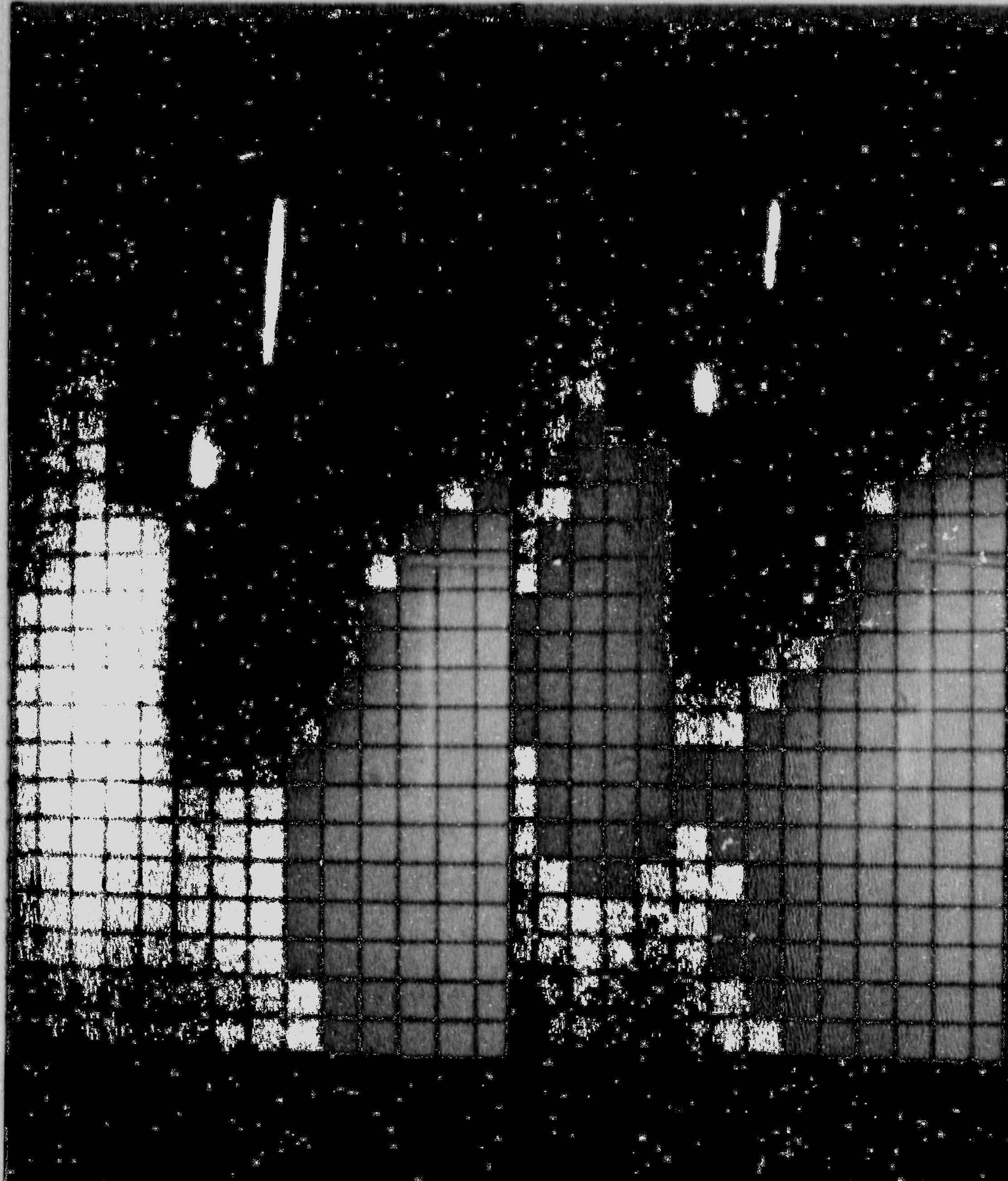

Figure A.4.7. . . . . 60° impact.

APPENDIX 5

Test #5

Crash Test in Vacuum with Windows, 90° Impact Angle

June 19, 1989

OBJECTIVE OF TEST:

The purpose of this test was to determine whether simulated "windows" in the model "fuselage" would contribute to fragmentation of the fuselage when impacted at about 283 m/s by a Lexan projectile.

TEST CONDITIONS:

The test environment was a partial vacuum. Holes (0.0937-in. dia.) were drilled on 0.25-in. centers in the target walls. There were 26 holes (windows) on each side of the target. The target was suspended by small sticks from two foam "fingers" which were attached to a foam collar, as shown in Figure A.5.1. The projectile, also shown in Figure A.5.1, is solid Lexan. It was painted black and the target was painted a flat yellow, in order to provide photographic contrast. Other specific test conditions were:

Time:	1:30 p.m.
Date:	June 15, 1989
Helium Pressure:	3.76 MPa (545 psi)
Chamber Pressure:	85 milli-Torr
Projectile Mass:	313.7 g
Projectile Velocity:	289 m/s
Target Dimensions: (Length x diameter x wall thickness)	178 mm x 25.4 mm x .127 mm (7 in. x 1 in. x 0.005 in.)
Target Material:	6061-T6 aluminum
Target Mass:	7.34 g
Impact Angle:	90°

The high-speed camera properly triggered the firing of the projectile.

RESULTS:

A large piece of target mass (5.8 g) remained trapped between the projectile and the shock absorbing foam. The large piece was crumpled and flattened. It represented 79% of the original target mass.

APPENDIX 5

Test #5

Crash Test in Vacuum with Windows, 90° Impact Angle

June 19, 1989

OBJECTIVE OF TEST:

The purpose of this test was to determine whether simulated "windows" in the model "fuselage" would contribute to fragmentation of the fuselage when impacted at about 283 m/s by a Lexan projectile.

TEST CONDITIONS:

The test environment was a partial vacuum. Holes (0.0937-in. dia.) were drilled on 0.25-in. centers in the target walls. There were 26 holes (windows) on each side of the target. The target was suspended by small sticks from two foam "fingers" which were attached to a foam collar, as shown in Figure A.5.1. The projectile, also shown in Figure A.5.1, is solid Lexan. It was painted black and the target was painted a flat yellow, in order to provide photographic contrast. Other specific test conditions were:

Time:	1:30 p.m.
Date:	June 15, 1989
Helium Pressure:	3.76 MPa (545 psi)
Chamber Pressure:	85 milli-Torr
Projectile Mass:	313.7 g
Projectile Velocity:	289 m/s
Target Dimensions: (Length x diameter x wall thickness)	178 mm x 25.4 mm x .127 mm (7 in. x 1 in. x 0.005 in.)
Target Material:	6061-T6 aluminum
Target Mass:	7.34 g
Impact Angle:	90°

The high-speed camera properly triggered the firing of the projectile.

RESULTS:

A large piece of target mass (5.8 g) remained trapped between the projectile and the shock absorbing foam. The large piece was crumpled and flattened. It represented 79% of the original target mass.

Quantitative Observations:

1) The projectile struck the target squarely and entered the catcher near the center opening. It remained in the catcher. Two scars were observed on the foam collar which were caused by fragments.

2) Twenty-two (22) aluminum "fuselage" fragments were recovered on the floor of the test chamber. The fragments ranged in size from small (2 mm x 5 mm) to medium large (10 mm x 10 mm). The total mass of the fragments found outside the catcher was 0.6 g.

3) Twenty (20) fragments were recovered inside the catcher. The fragments ranged in size from 1 mm x 1 mm to the large piece, previously described. The nose piece was recovered inside the catcher, but not trapped by the projectile. It was relatively undamaged.

4) A mass analysis of fragments found is given below:

a)	Fragments outside catcher (22)	=	0.6 g (8%)
b)	Fragments inside catcher (20)	=	6.72 g (91.6%)
c)	Mass of original target	=	7.34 g

DISCUSSION:

The one large piece which was trapped inside the catcher by the projectile is evidence that significant fragmentation did not occur. Further evidence that fragmentation on initial impact did not occur is given by the small mass of fragments found outside the catcher (8%). The high-speed photography shows no clear evidence of fragmentation occurring upon initial impact. Unfortunately, the paint flaked off during impact and, thus obscured any visual evidence of fragmentation. The series of photographic frames labeled Figures A.5.2 through A.5.4 show some of the impact event.

CONCLUSION:

In the absence of concentrated masses internal to the model "fuselage", windows do not appear to appreciably influence the degree of fragmentation. Further, the degree of fragmentation on initial impact was small.

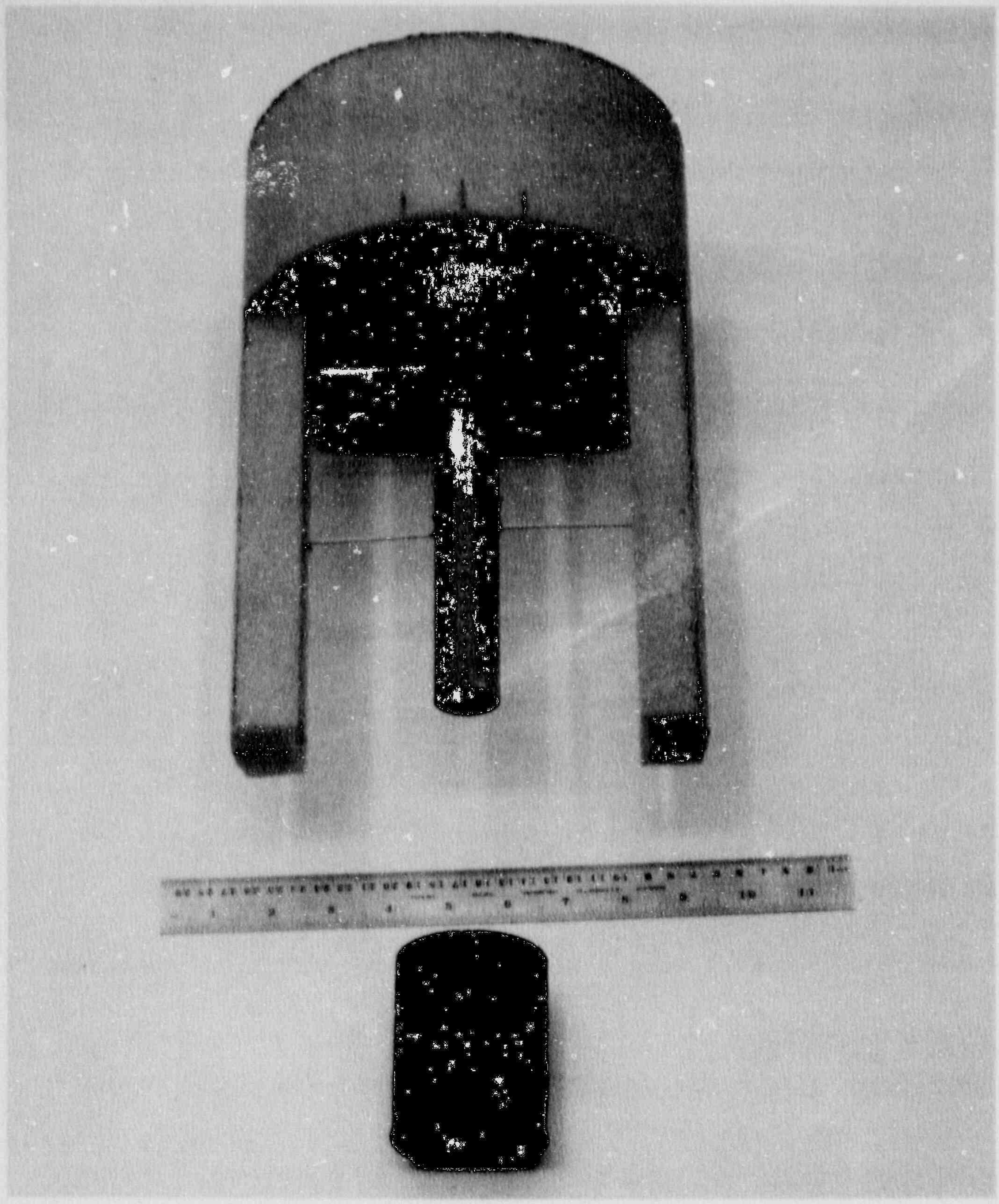

Figure A.5.1. Fuselage model shown with projectile.

Figure A.5.2. First frame of the impact sequence with windows.

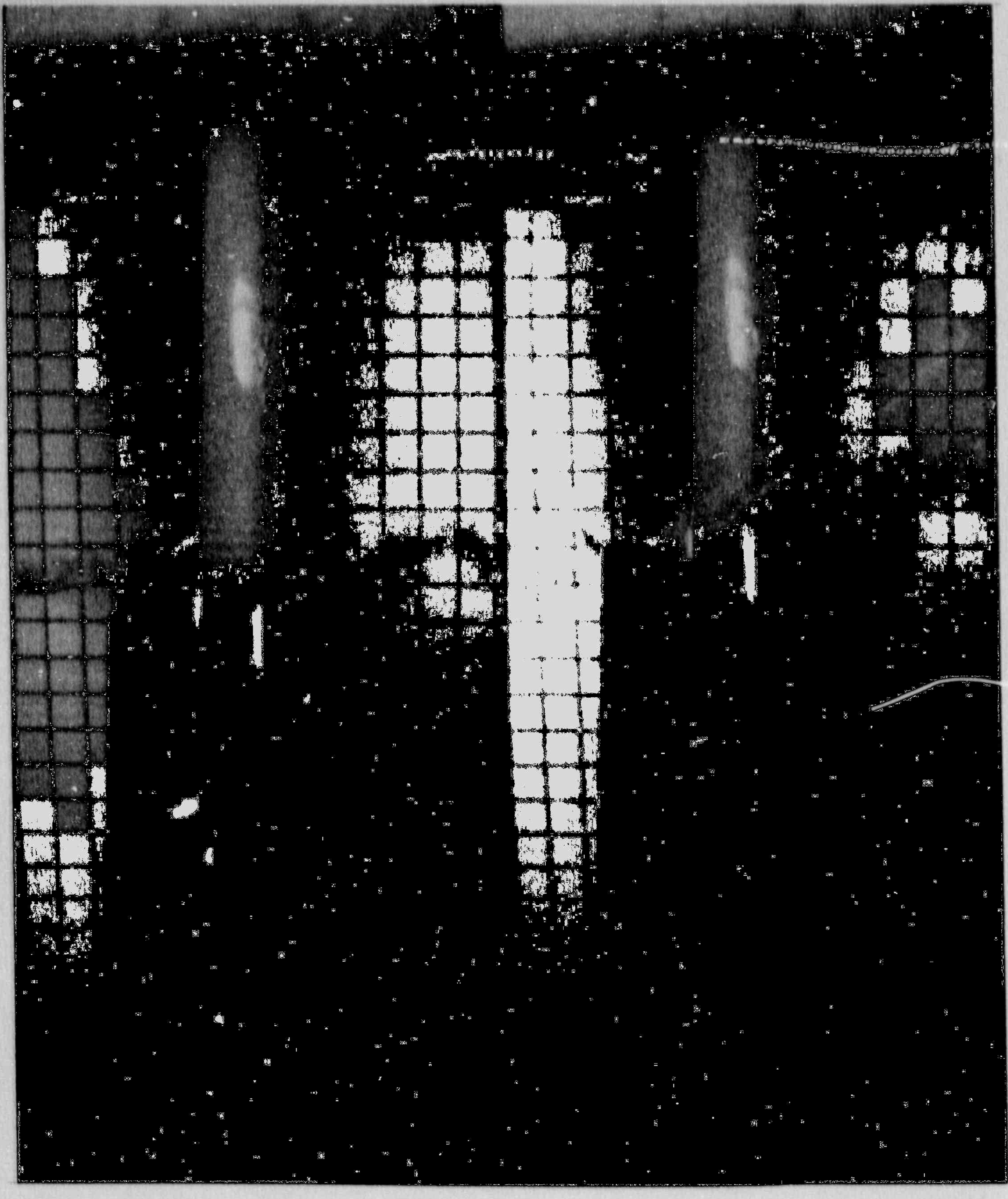

Figure A.5.3. . . . . Impact with windows.

Figure A.5.4. . . . . Impact with windows.

APPENDIX 6

Test #6

Crash Test, with 1-Atm of Air in "Fuselage", 90° Impact Angle

June 28, 1989

OBJECTIVE OF TEST:

The purpose of this test was that of determining whether air pressure buildup inside fuselage, as collapse of volume occurred, would be sufficient to produce shattering when impacted by a Lexan projectile moving at 283 m/s.

TEST CONDITIONS:

A new "catcher" design was employed. The new catcher provided a means for maintaining a 1-atmosphere pressure condition around the model "fuselage". In this test the target was sealed with epoxy. Air inside was at approximately 1 atmosphere. The target was glued to the front diaphragm. The need for sticks to hold the target in place was eliminated. Painting of target and projectile were eliminated for this test and for all future tests because "flaking" of the paint during impact tended to obscure post-event analysis. Other specific test conditions were:

Time:	2:00 p.m.
Date:	June 20, 1989
Helium Pressure:	3.76 MPa (545 psi)
Chamber Pressure:	150 milli-Torr
Projectile Mass:	313.4 g
Projectile Velocity:	290 m/s
Target Dimensions: (Length x diameter x wall thickness)	178 mm x 25.4 mm x .102 mm (7 in. x 1 in. x 0.004 in.)
Target Material:	6061-T6 aluminum
Target Mass:	6.2 g
Impact Angle:	90°

The high-speed camera was properly triggered the firing of the projectile.

RESULTS:

A large piece of target mass (5.1 g) remained trapped between the projectile and the shock absorbing foam. The large piece was crumpled and flattened. It represented 82% of the original target mass. The projectile struck the target squarely and entered the catcher near the center opening. It remained in the catcher. Analysis of the film of the event clearly showed that shattering occurred upon initial impact. The film also showed that the model fuselage was considerably stiffer than vacuum tests, due to the presence of air inside the fuselage. As a consequence, it was observed that the velocity of the rear of the fuselage was approaching the same velocity of the projectile before the projectile had crushed the first half of the fuselage model. An unusually large number of fragments were recovered (139). Their source is discussed later.

Quantitative Observations:

1) Sixty-two (62) aluminum "fuselage" fragments were recovered outside the steel section of catcher. The fragments ranged in size from small (1 mm x 1 mm) to medium large (10 mm x 10 mm). The total mass of the fragments found outside (inside the acrylic chamber) was 0.55 g.

2) Seventy-seven (77) fragments were recovered inside the catcher. The fragments ranged in size from 1 mm x 1 mm to about 5 mm x 15 mm.

3) A mass analysis of fragments found is given below:

a)	Fragments outside stl. sect. (62)	=	0.55 g (8.9%)
b)	Fragments inside stl. sect. (77)	=	5.58 g (90%)
c)	Mass of original target	=	6.2 g

DISCUSSION:

The film showed that both fragmentation and crushing of the fuselage model had ceased by the time the projectile had collapsed the first 50% of the fuselage model. Shattering of the fuselage model was of maximum intensity during the first inch of travel after impact. It is deduced that the remaining 50% of the target was collapsed by secondary impact with the diaphragm at the exit end of the acrylic viewing chamber. The film suggests three phases for the impact event:

1) Crushing, with associated fragmentation.

2) Crushing with little or no associated fragmentation.

3) Carrying of the remaining fuselage model without crushing. Phase transition was smooth. Shattering occurred with decreasing intensity the first 1.5-in. of travel after impact. Shattering ceased but crushing continued for the next 2 inches. Finally, neither shattering nor crushing occurred for the remaining several inches of travel, until the fuselage target made contact with the final diaphragm. The mass analysis is

consistent with observations from the film. The large single fragment (82% of original target mass) trapped by the projectile and the foam was carried by the projectile through the final diaphragm. It is noted that the stiffness of the fuselage model was significantly greater than vacuum tests. It is also deduced that intense fragmentation occurred with the impact of the fuselage model and the secondary diaphragm, as the remaining 50% of the fuselage model was rapidly collapsed. This likely accounts for the unusually large number of fragments (139). It is noted that drag force on crushed fuselage model elements will produce large tearing/shearing forces. Considering the early observance of fragmentation, it may be much easier to defend the postulation that drag, instead of pressure buildup, produced fragmentation in the air environment. The impact event sequence is shown in the seven photo frames labeled Figures A.6.1 through A.6.7.

CONCLUSION:

The presence of air produced shattering of the fuselage model when impacted by a blunt-nosed Lexan projectile with a velocity of 290 m/s. It is likely that the combination of:

a) increased internal pressure,

b) high-deformation rate,

c) drag forces on collapsing skin folds,

was sufficient to produce shattering early in the impact event.

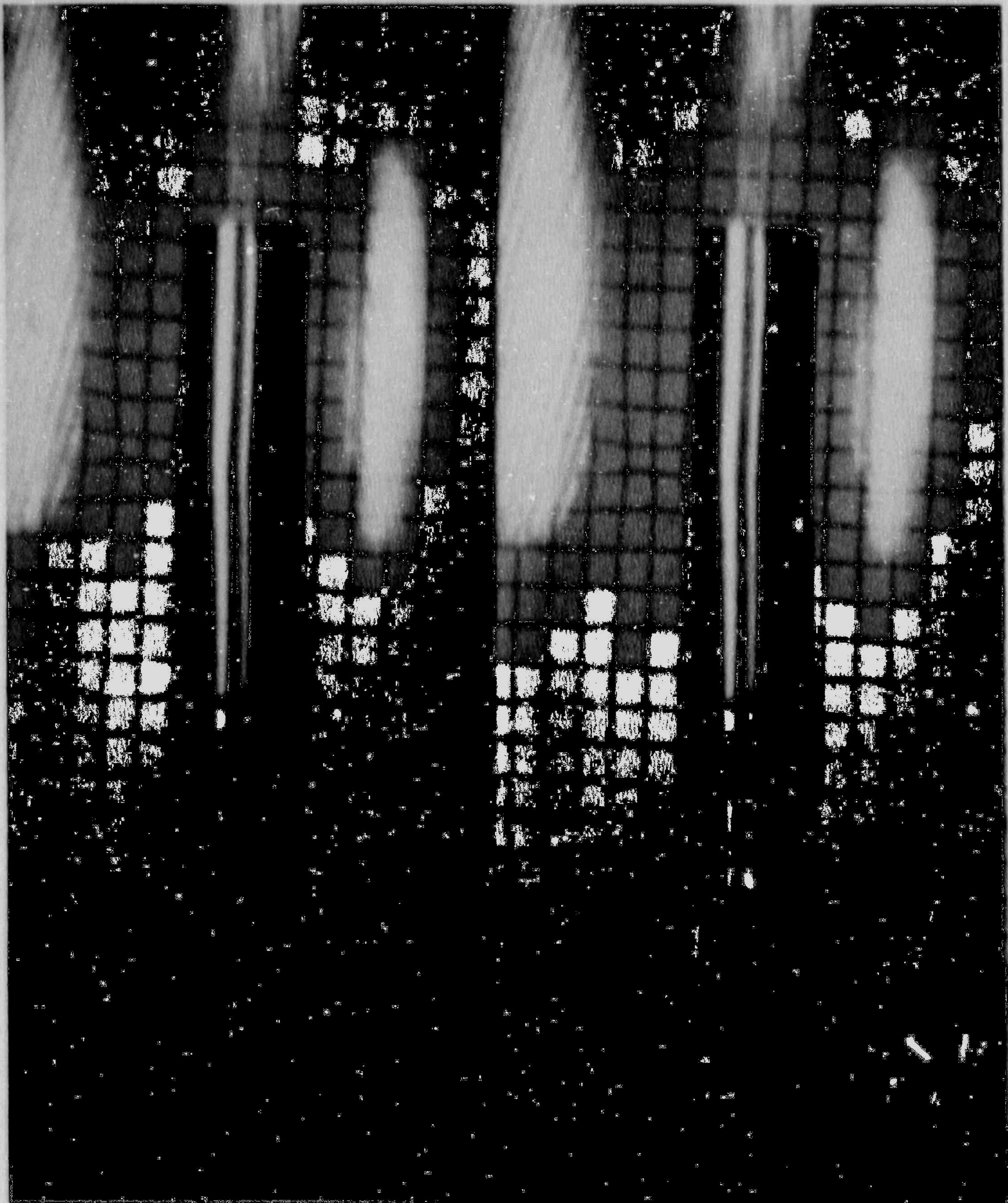

Figure A.6.1. Impact sequence in a 1-atm air environment.

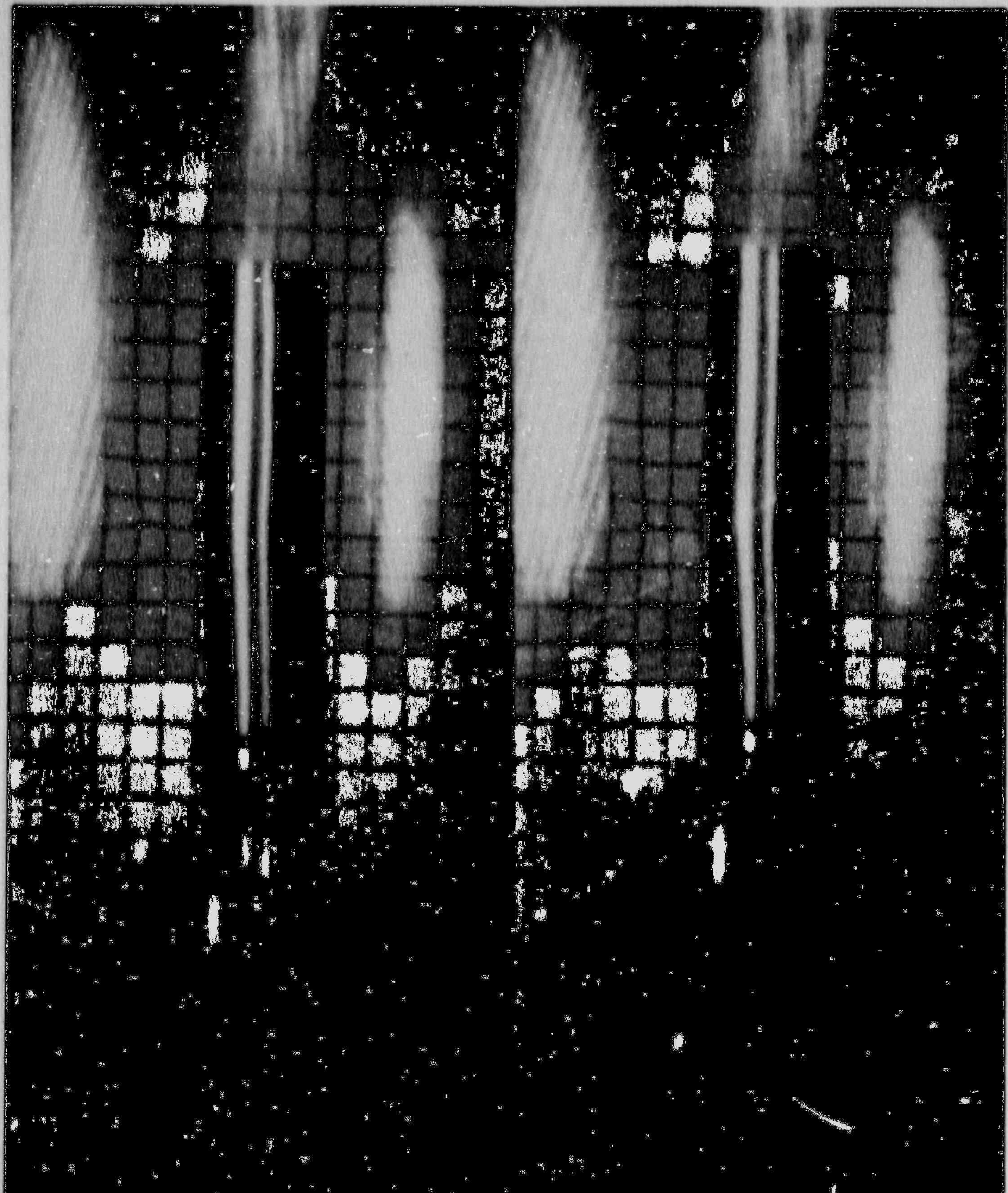

Figure A.6.2. . . . . 1-atm air.

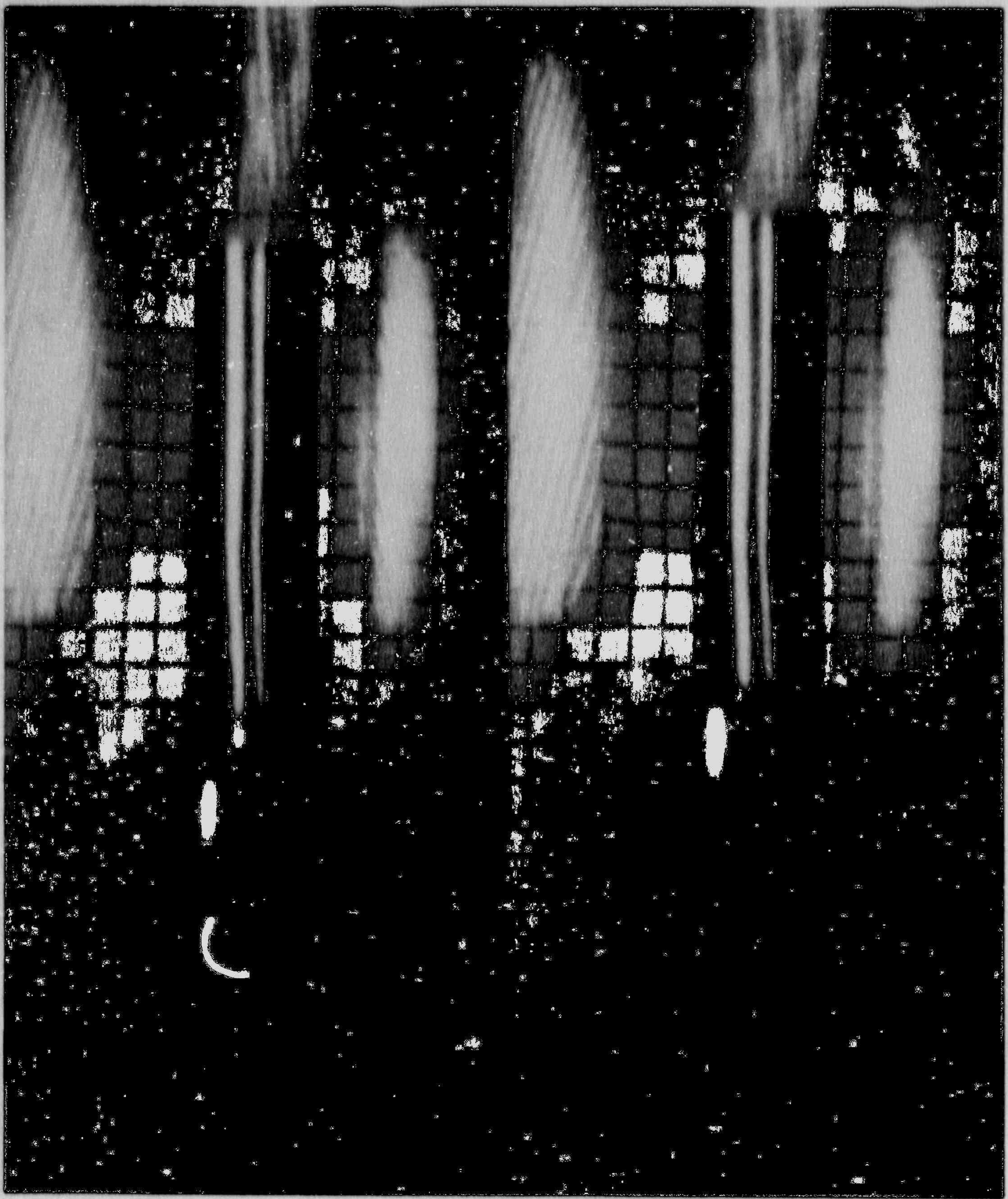

Figure A.6.3. . . . . 1-atm air.

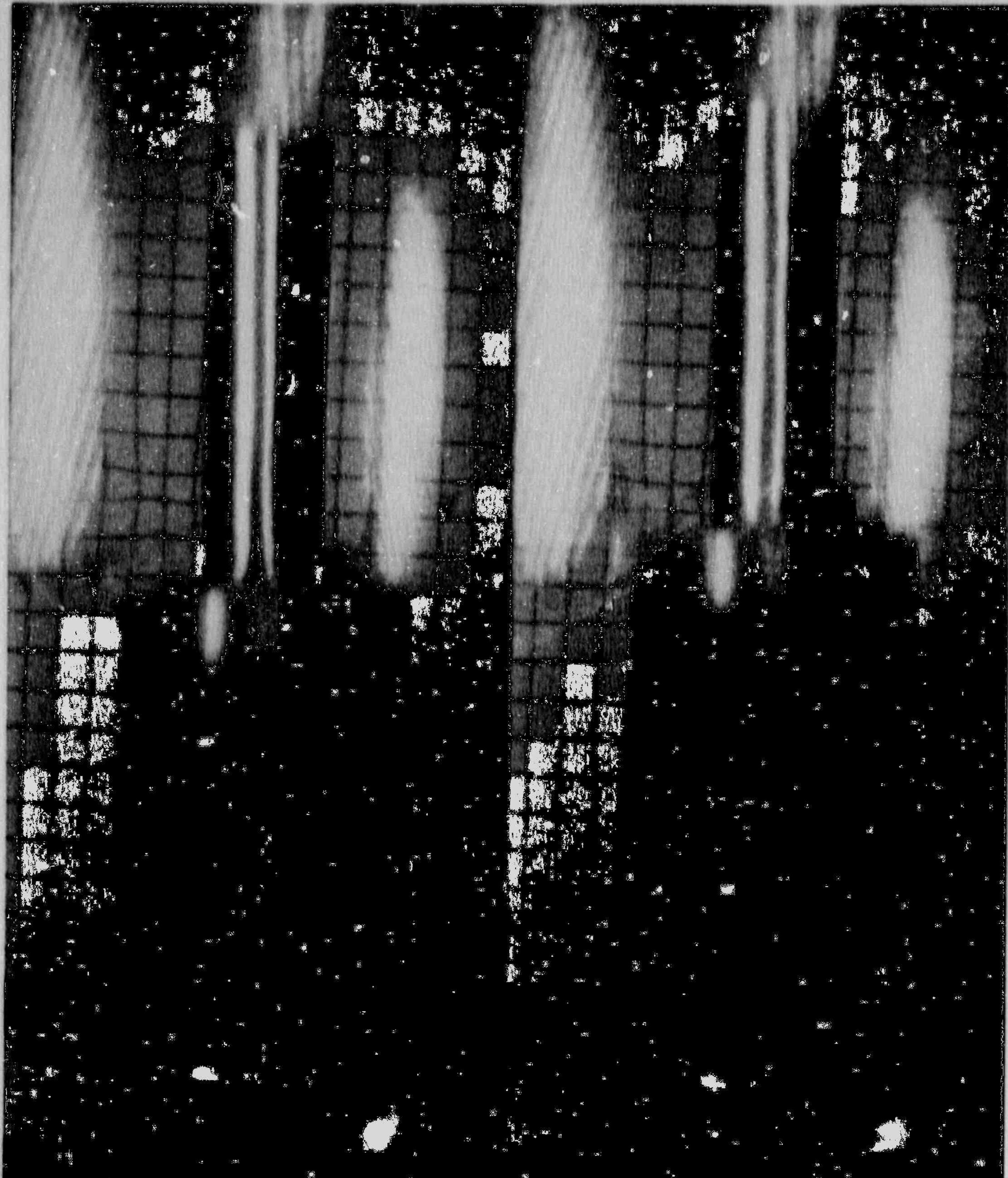

Figure A.6.4. . . . . 1-atm air.

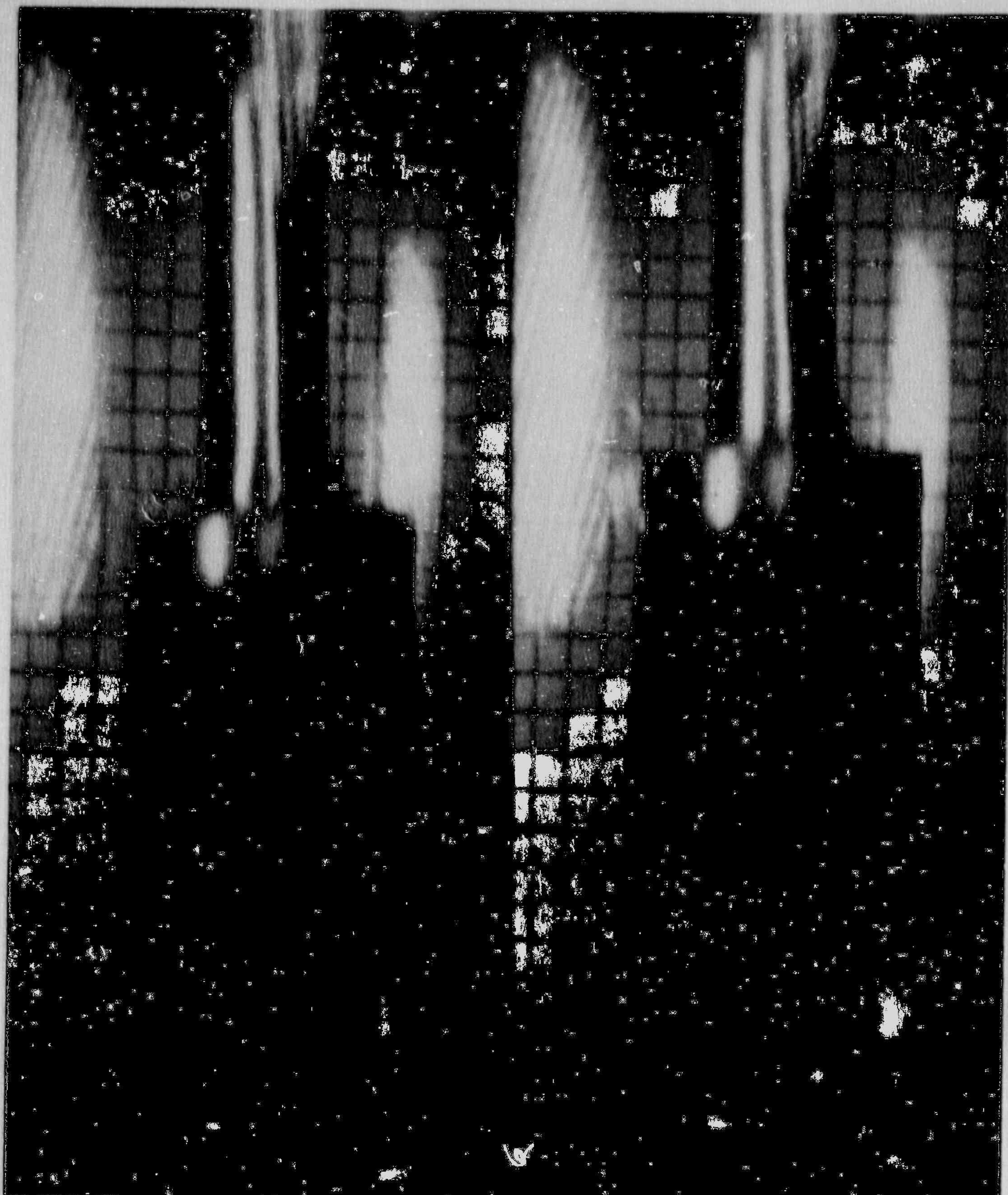

Figure A.6.5. . . . . 1-atm air.

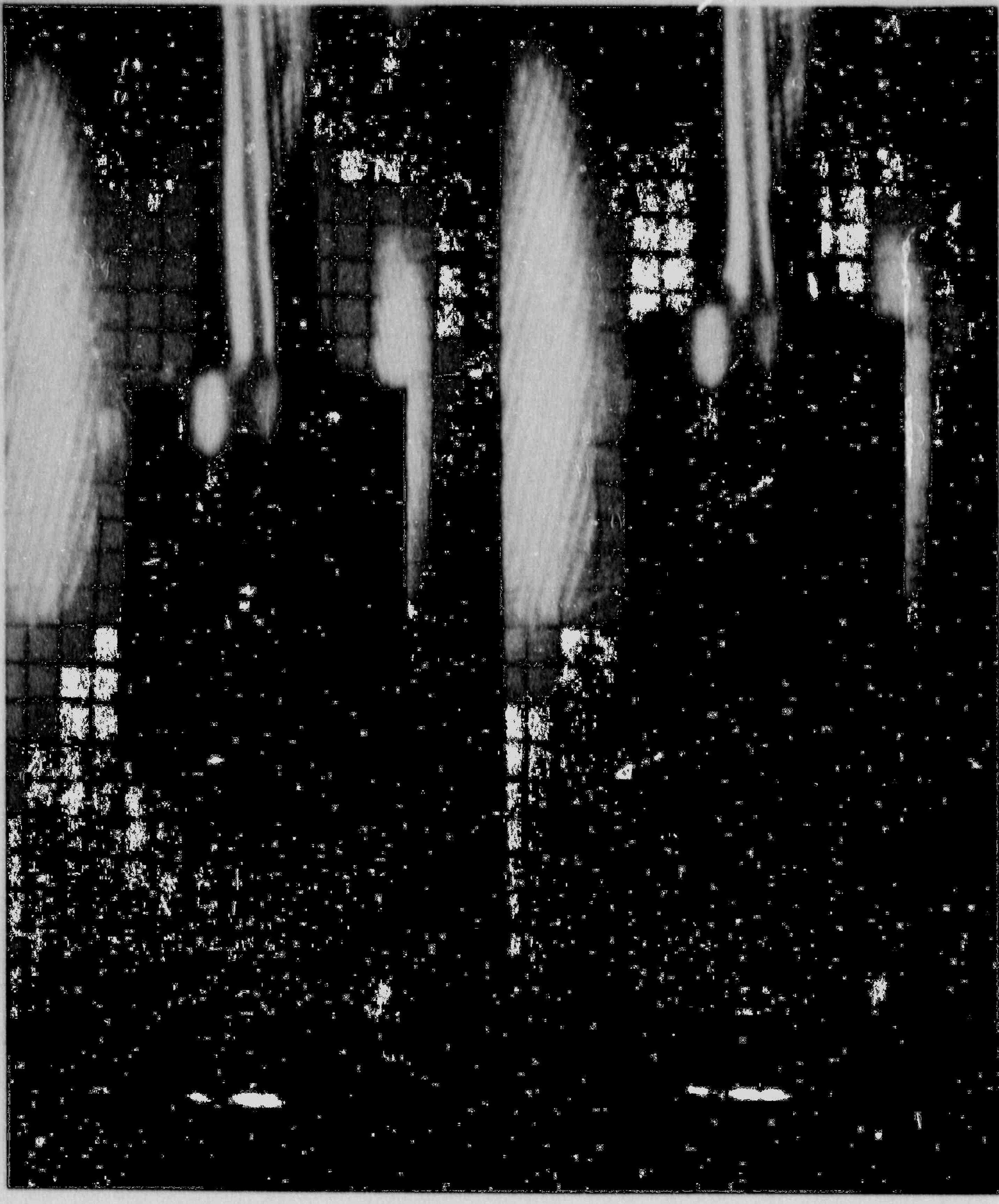

Figure A.6.6. . . . . 1-atm air.

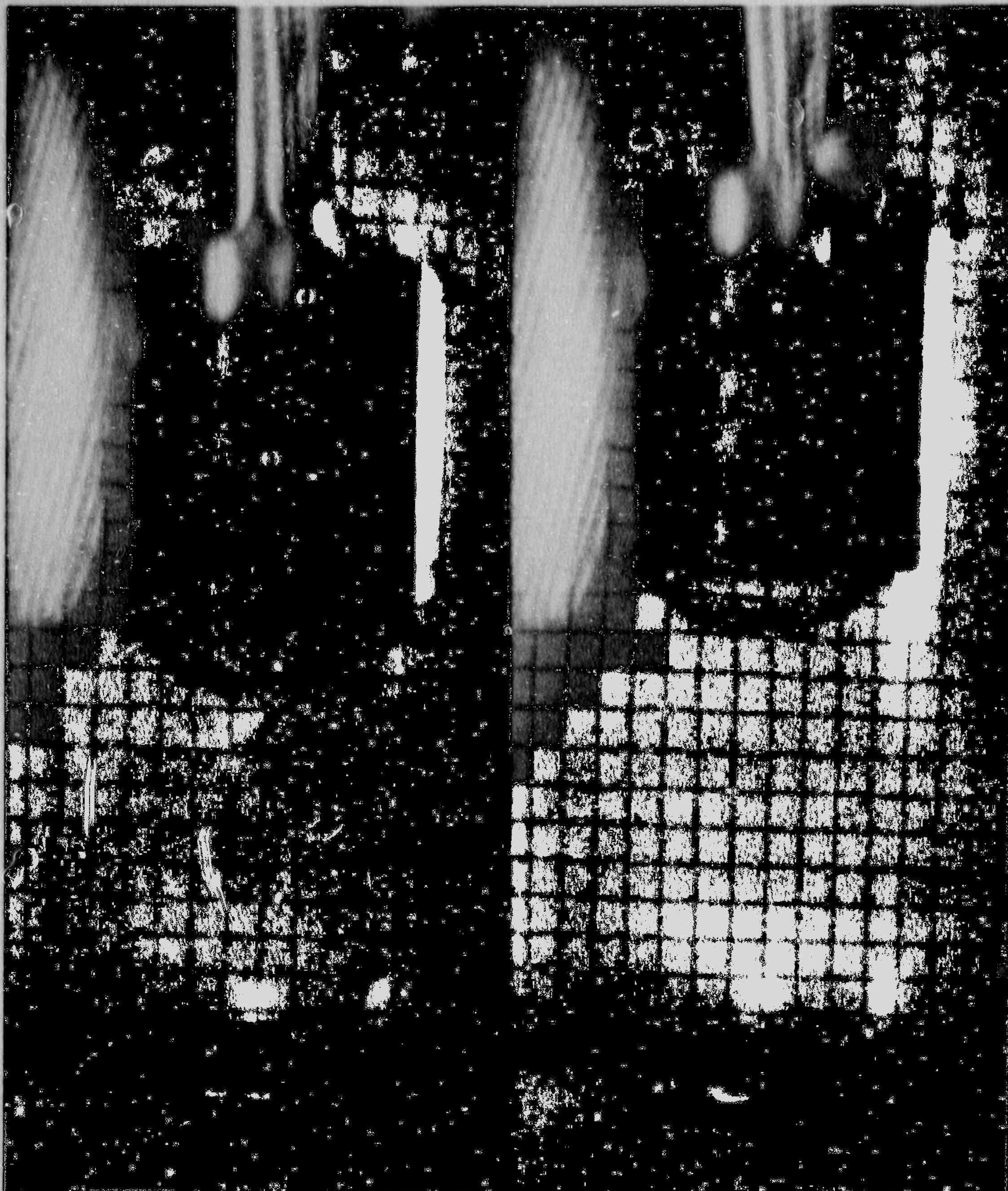

Figure A.6.7. . . . . 1-atm air.

APPENDIX 7

Test #7

Crash Test, with Deformable Mass, 90° Impact Angle

June 29, 1989

OBJECTIVE OF TEST:

The purpose of this test was that of determining whether deformable mass was capable of inducing shattering of a model fuselage when impacted by a Lexan projectile with an impact velocity of 283 m/s.

TEST CONDITIONS:

The new catcher was used for the second time. The catcher provided a means for maintaining a 1-atmosphere pressure condition around the model fuselage. In this test 35.5 g of jello was jelled inside the model fuselage. The fuselage model was maintained in a horizontal position during jelling. The jello occupied 33% of the internal volume of fuselage model. The jello contained no rigid or semi-rigid elements, as originally planned. The fuselage model was sealed with thin end-plugs, epoxied in place. Teflon sheet was wrapped around the acrylic viewing chamber to reduce the glare from flood lamps. Other specific test conditions are outlined below:

Time:	1:45 p.m.
Date:	June 22, 1989
Helium Pressure:	3.76 MPa (545 psi)
Chamber Pressure:	70 milli-Torr
Projectile Mass:	313.4 g
Projectile Velocity:	290 m/s
Target Dimensions: (Length x diameter x wall thickness)	178 mm x 25.4 mm x .102 mm (7 in. x 1 in. x 0.004 in.)
Target Material:	6061-T6 aluminum
Target Mass:	6.4 g
Impact Angle:	90°

The high-speed camera properly triggered the firing of the projectile.

RESULTS:

The model fuselage appeared to shatter on impact. The viewing zone was sprayed with jello on impact. The projectile entered the steel portion of the catcher, but did not come to rest inside the catcher. The acrylic viewing chamber shattered. The acrylic wall was 0.5-in. thick; the first crack was visible 1 ms after the projectile entered the steel section. Some of the jello evaporated on impact. Evidence of this observation is supported by the haze observed in the test chamber after the event and also by uniformly distributed rust which accrued throughout the test chamber during the 16 hours following the event. The chronology of the impact event and subsequent fracturing, as observed from the film, is given below:

1) 0.0 ms .... Impact: eruption of model fuselage walls at impact and spraying of the viewing chamber.

2) 0.5 ms after impact: projectile had driven through the fuselage model.

3) 1.5 ms after impact: projectile should have made contact with shock absorbing foam in steel section.

4) 2.5 ms after impact: first crack in the acrylic wall is visible.

5) 4 ms after impact: second crack in acrylic wall is visible.

6) 5.5 ms after impact: third crack in acrylic wall is visible.

7) 9.5 ms after impact: acrylic viewing tube begins to break apart.

8) 19 ms after impact: shattering of acrylic chamber is complete, fragments observed falling toward test chamber floor.

9) 43 ms after impact: camera view is completely obscured by vapor/fog from jello.

10) 185 ms after impact: camera view begins to clear.

It cannot be confirmed that the jello impacting on the walls of the acrylic chamber induced fracturing of the acrylic. It seems more likely that the impacting jello combined with the bending stresses induced during the impact of the projectile with foam in the catcher to produce shattering of the acrylic. It is noteworthy that large fragments did not occur. (The largest was 0.5 g, a fragment from the fuselage model skin, recovered outside the catcher.) It is also noteworthy that this test produced the largest number of fragments (143). Further, there were no really small fragments. (The smallest was about 2 mm x 4 mm.) Most of the fragments were about 4 mm x 6 mm. The film showed the entire length of model fuselage being crushed/fragmented on initial impact. That is, the rear end of the fuselage model appeared to be "driven through" by the projectile before carrying remnants into the diaphragm at the acrylic viewing chamber exit.

Quantitative Observations:

1) One hundred sixteen (116) aluminum fragments were recovered outside the steel section of catcher. The fragments ranged in size from small (2 mm x 4 mm) to medium large (12 mm x 30 mm). The total mass of the fragments found outside the steel catcher section) was 6.3 g.

2) Twenty-seven (27) fragments were recovered inside the catcher. The fragments ranged in size from 2 mm x 3 mm to about 10 mm x 20 mm.

3) A mass analysis of fragments found is given below:

a)	Fragments outside stl. sect. (116)	=	5.7 g (89%)
b)	Fragments inside stl. sect. (27)	=	0.7 g (11%)
c)	Mass of original target	=	6.4 g

DISCUSSION:

The film showed that the jello erupted the fuselage model walls on impact. The jello was ejected radially from the axis of impact. The sequence of photos, Figures A.7.1 through A.7.7 show the progression of the radial spray of jello as the projectile moves through the fuselage model. Because of poor lighting the fragments cannot be seen. Aluminum fragments likely "flowed" radially with the jello. The projectile did not remain inside the steel portion of the catcher. It is noted that the presence of 35 g of jello in the lower section of the fuselage caused the center of mass of the fuselage model to be slightly off-center of the projectile. This condition should initiate tumbling. The projectile probably did not strike the shock absorbing foam squarely, resulting in a pitching motion and ultimate disgorging of the projectile. A secondary result was likely an inertial bending stress imposed on the acrylic viewing chamber. The bending stress coupled with reactions from impacting jello probably combined to produce shattering of the viewing chamber.

The large number of fragments (143) is significant. That fact, combined with the observation of very few small fragments, suggests that the deformable imposed a "dampening" condition to the shock.

CONCLUSION:

The presence of deformable mass produced fragmentation of the model fuselage on impact with a Lexan projectile when impact velocity was 290 m/s. The fragmentation was more severe than any of the other six tests (143 fragments). The characteristics of the fragment shapes suggest that the jello induced "ripping" of the fuselage skin parallel with the longitudinal axis (across the buckled folds) of the fuselage model.

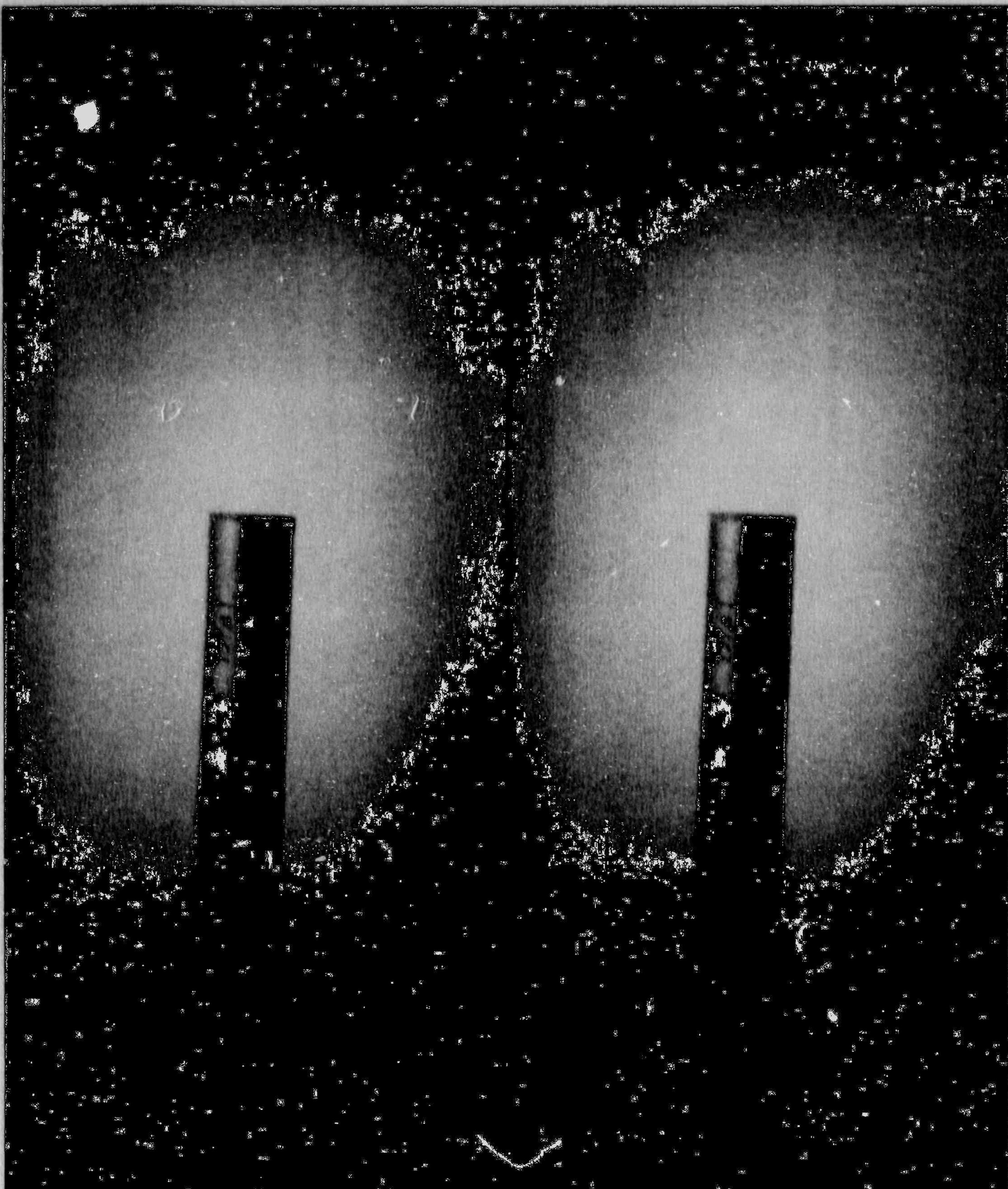

Figure A.7.1. Impact sequence w/deformable mass (jello).

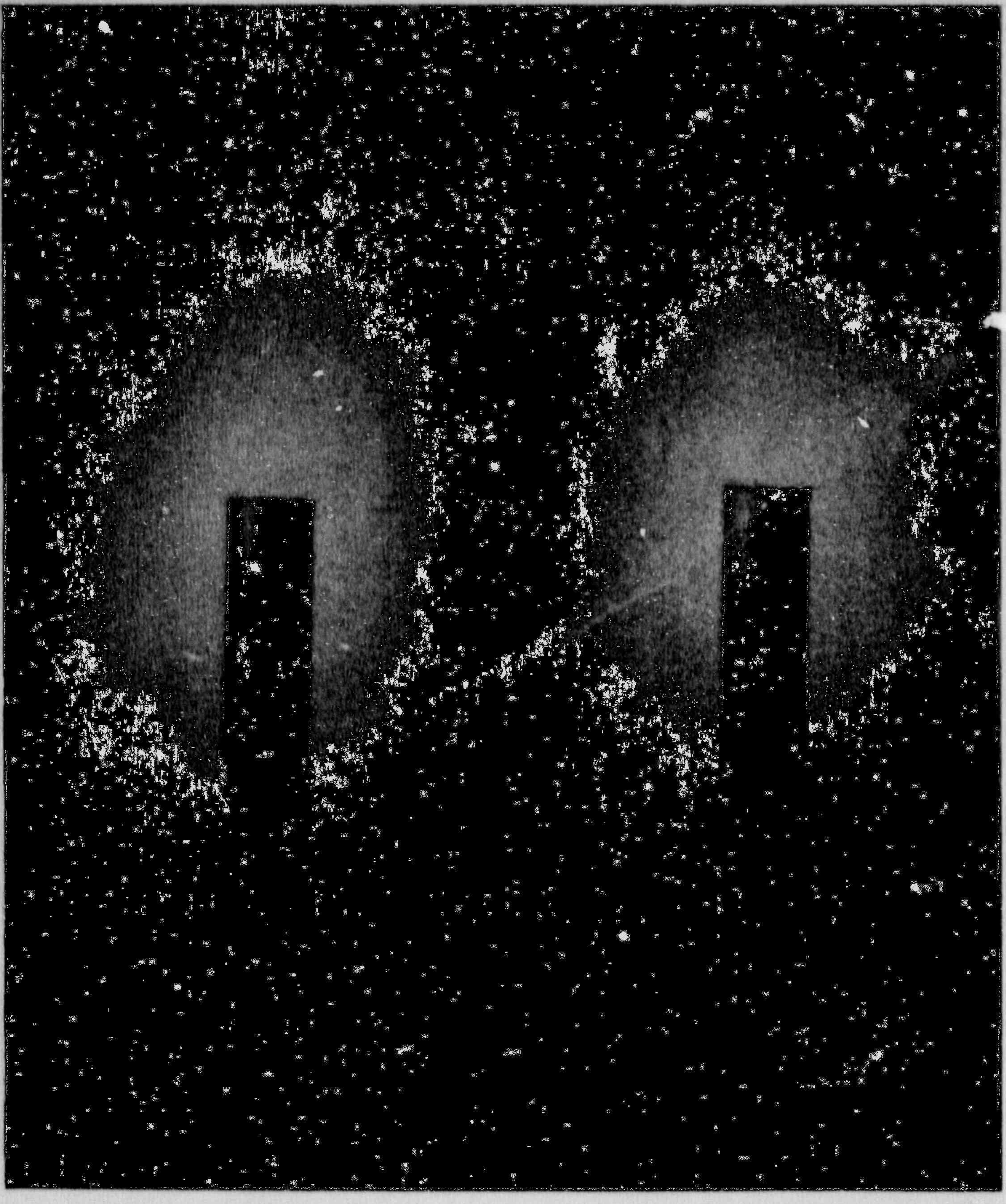

Figure A.7.2. . . . . Deformable mass (jello).

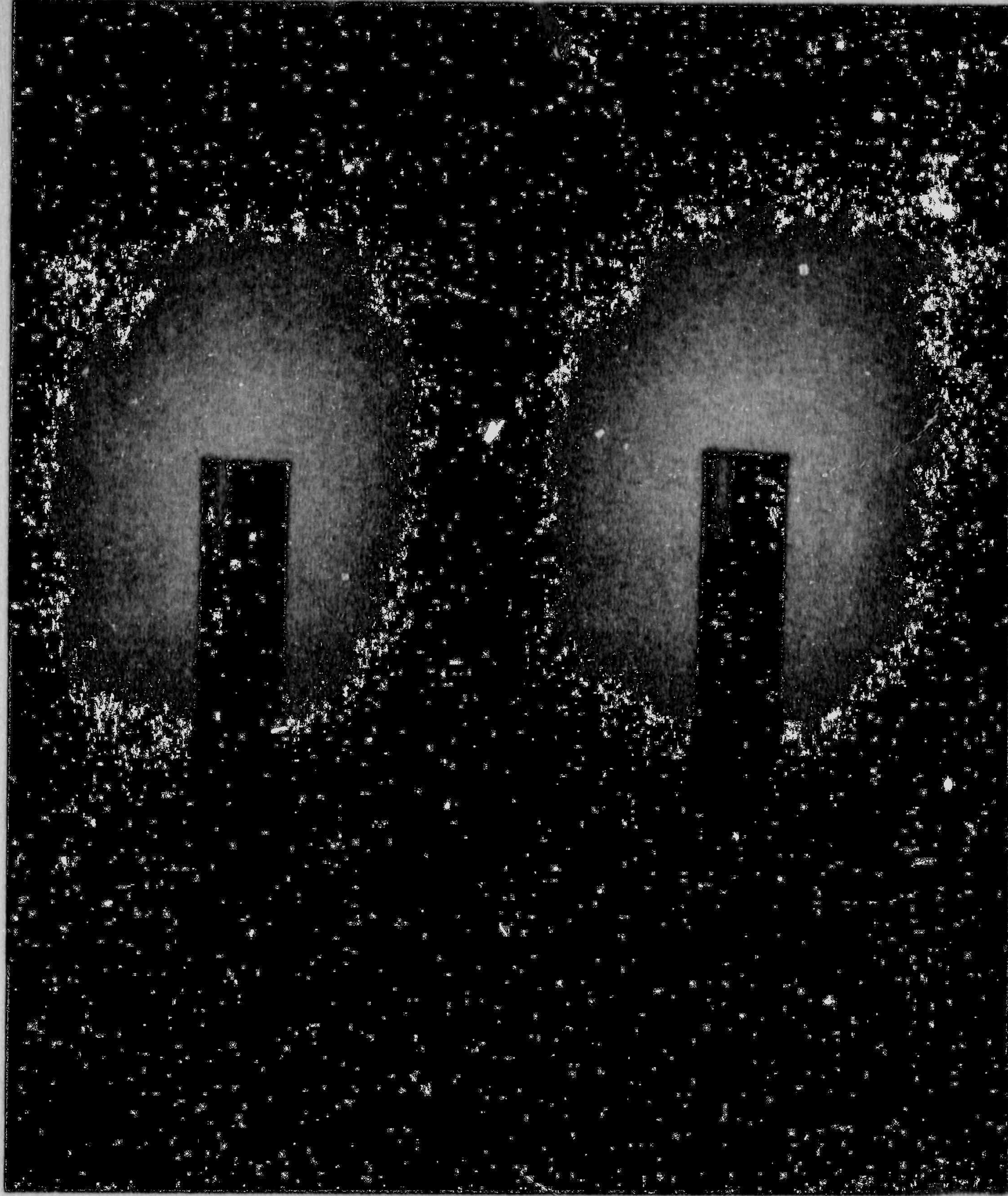

Figure A.7.3. . . . . Deformable mass (jello).

Figure A.7.4. . . . . Deformable mass (jello).

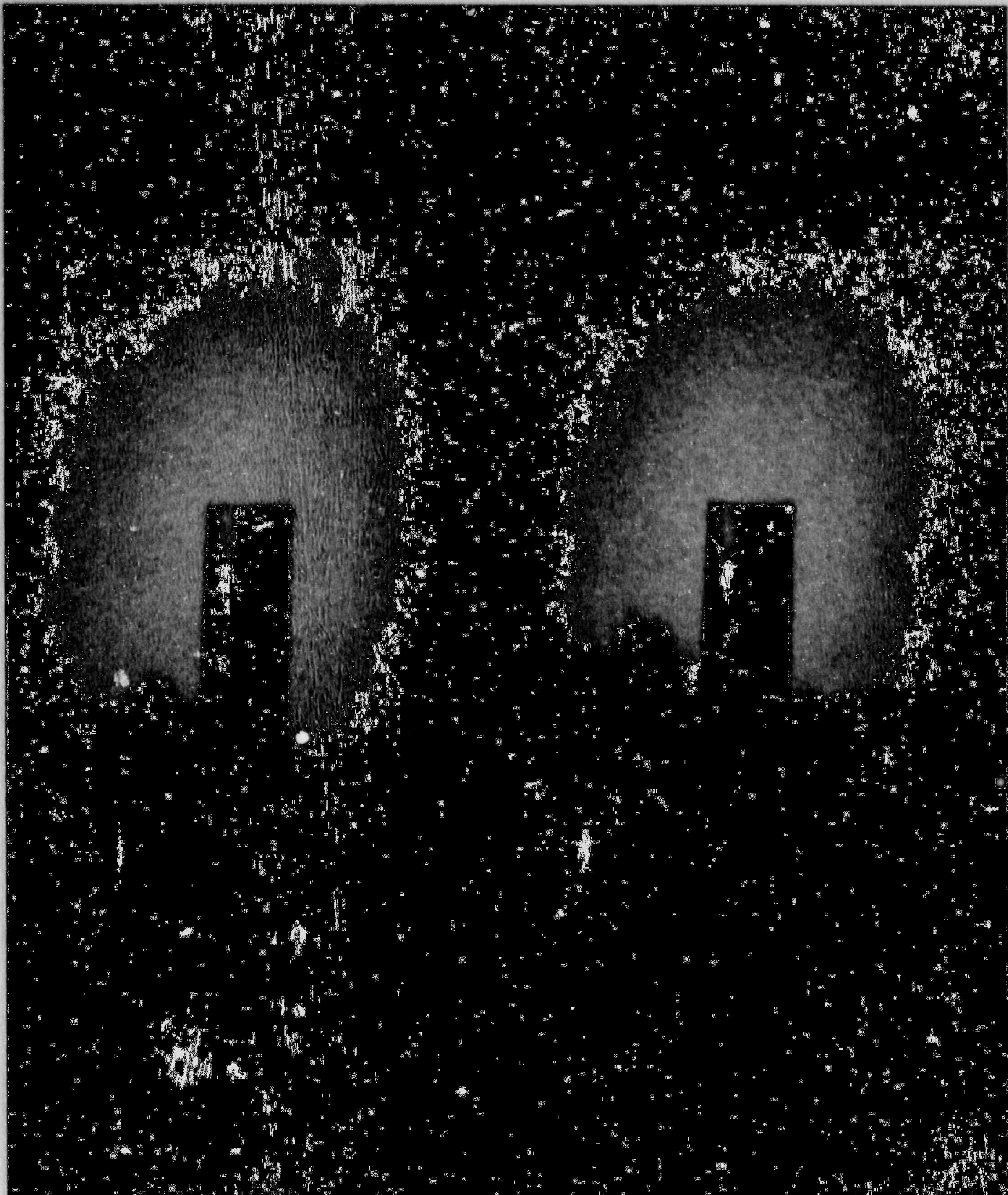

Figure A.7.5. . . . . Deformable mass (jello).

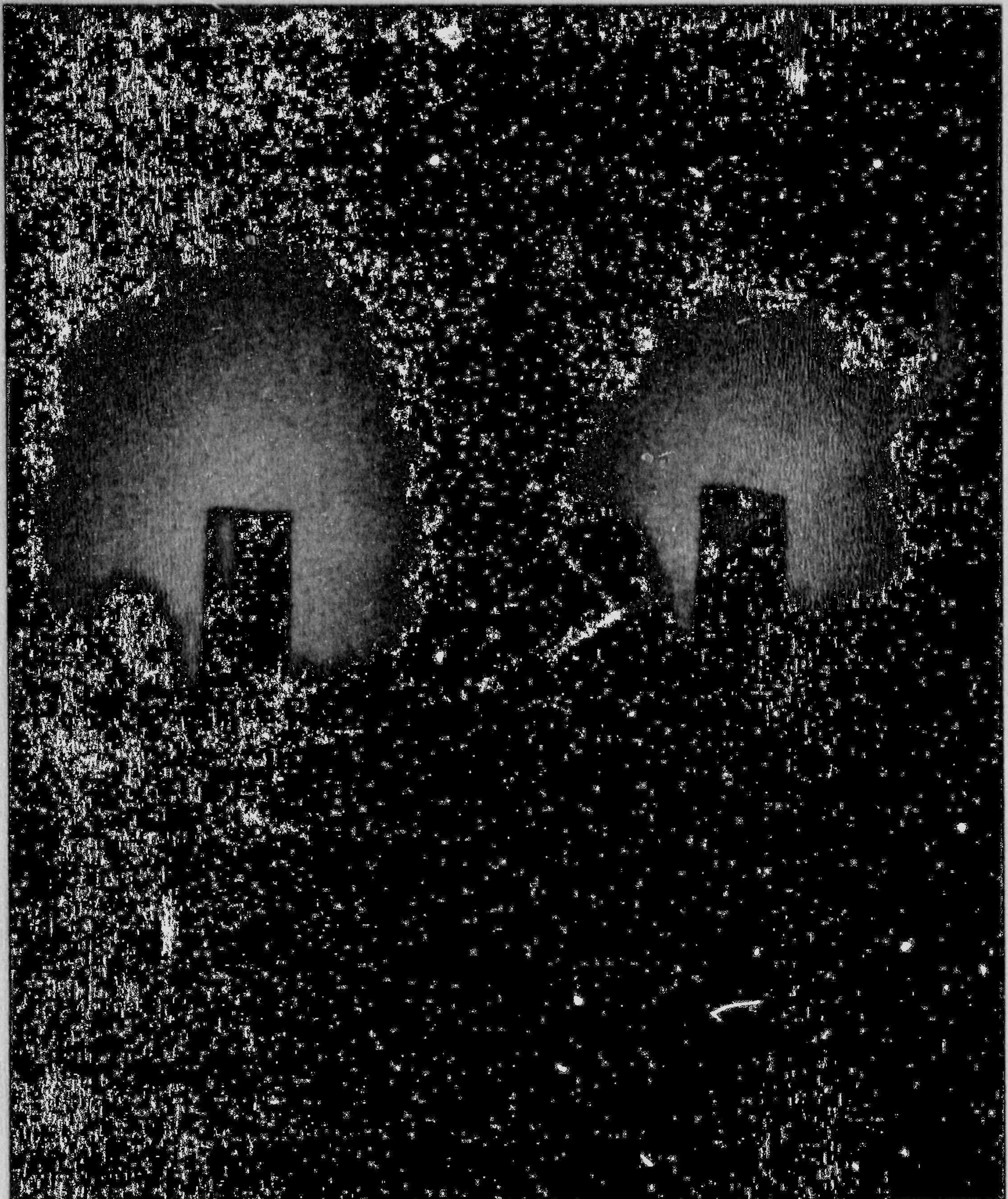

Figure A.7.6. . . . . Deformable mass (jello).

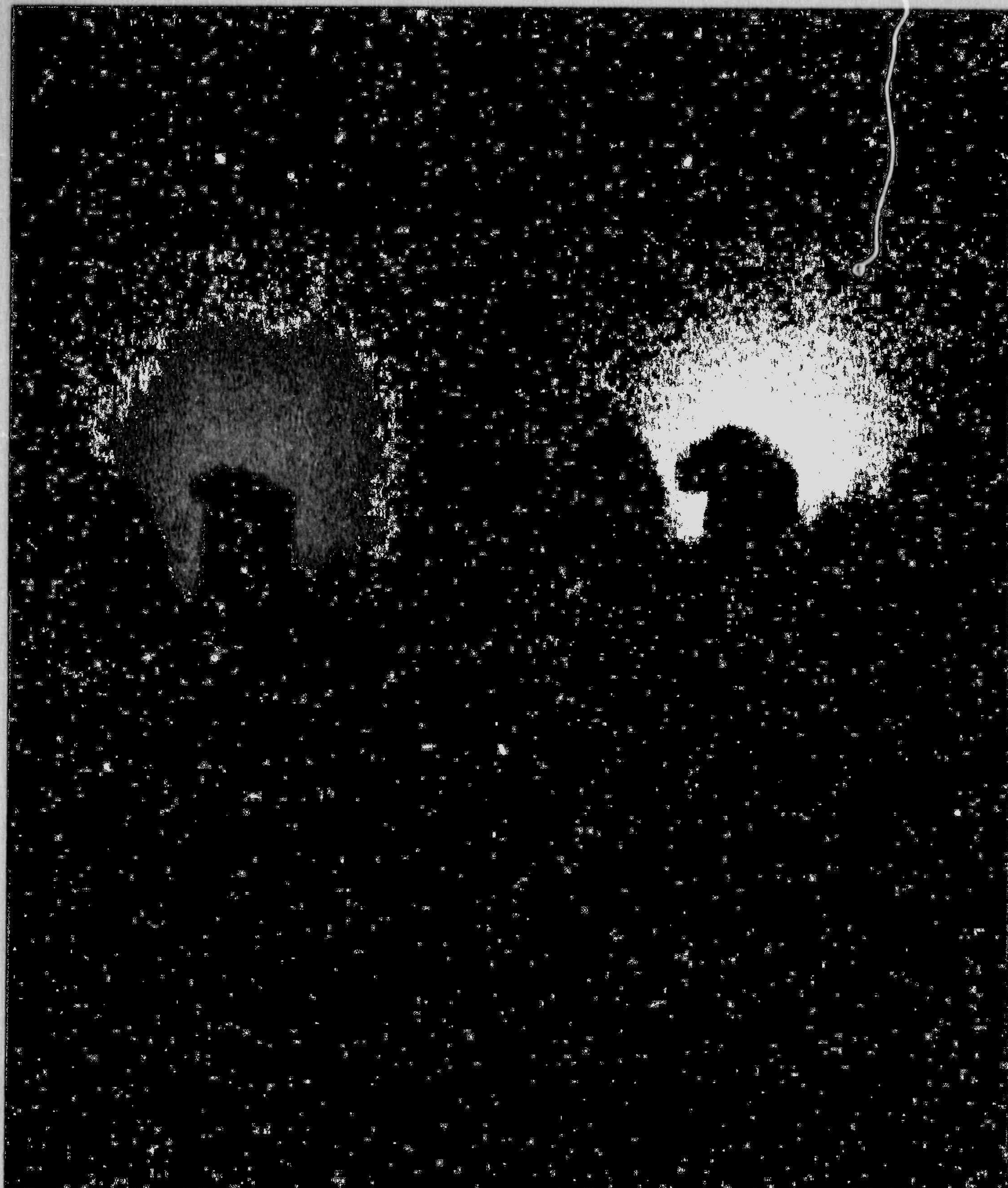

Figure A.7.7. . . . . Deformable mass (jello).

APPENDIX 8

Test #8

Crash Test, Base Case without .0034-in. Wall, 90° Impact Angle

July 10, 1989

OBJECTIVE OF TEST:

The purpose of this test was that of repeating Base Case conditions with a thinner wall to determine if shattering could be produced by high-strain rate. A second objective was to test the ability of a modified catcher design to "catch" the projectile, preventing it from crushing the model fuselage remnant during deceleration.

TEST CONDITIONS:

The test environment was near vacuum (70 milli-Torr). The target wall thickness was 0.0034-in. The catcher had a steel insert at its entrance; it tapered from a 3.75-in. diameter to a 2.125-in. diameter at its throat. The purpose of the steel insert was to catch the Lexan projectile and allow the model fuselage fragment to pass on through the throat and be gently stopped by soft rubber foam. The target mass (4.62 g) was the smallest of all tests conducted to date. Other specific test conditions are outlined below:

Time:	2:00 p.m.
Date:	July 6, 1989
Helium Pressure:	3.76 MPa (545 psi)
Chamber Pressure:	70 milli-Torr
Projectile Mass:	313.3 g
Projectile Velocity:	290 m/s
Target Dimensions: (Length x diameter x wall thickness)	178 mm x 25.4 mm x .0865 mm (7 in. x 1 in. x 0.0034 in.)
Target Material:	6061-T6 aluminum
Target Mass:	4.62 g
Impact Angle:	90°

The high-speed camera properly triggered the firing of the projectile.

RESULTS:

Local shattering in the zone of impact occurred. The high-speed film record of the impact event had the best clarity of all tests conducted to date. The film showed that the projectile crushed the first 4.25-in. of the target before the rear section of the target could be accelerated to the same velocity of the projectile. The 2.75-in. long uncrushed rear section was observed being driven into the catcher. The 2.125-in. throat of the catcher insert was not small enough to stop the Lexan projectile. The 2.5-in. diameter projectile was extruded through the throat and came to rest after crushing the fuselage model remnant against the rubber foam. The crushed remnant had a mass of 3.81 g, and was the largest fragment. The photos, Figures A.8.1 through A.8.7, show the impact event.

Quantitative Observations:

1) Eight (8) aluminum fuselage fragments were recovered outside the catcher. The fragments ranged in size from small (1 mm x 2 mm) to medium small (3 mm x 10 mm). The total mass of fragments recovered outside the catcher was 0.44 g.

2) Sixteen (16) fuselage fragments were recovered inside the catcher. The fragments ranged in size from 1 mm x 1 mm to about 30 mm x 40 mm (the crushed tail section).

3) A mass analysis of fragments found is given below:

   a) Fragments outside stl. sect. (8) = 0.44 g (9.5%)

   b) Fragments inside stl. sect. (16) = 4.18 g (90.5%)

   c) Mass of original target = 4.62 g

DISCUSSION:

The total number of fragments (24) was smallest of all eight tests. The absence of decelerating foam is likely the reason. The film showed fragments flying from the point of impact with initial contact. The intensity of shattering diminished throughout the crushing process. More than 70% of the fuselage model was crushed during initial impact. It was noted that the fuselage model was not perfectly "square" with the colliding projectile (model appeared to be tilted upward about 5°. It is also noted that the wall thickness of this fuselage model was the thinnest yet tested (0.0034"). Based on results of Test #4 (60° impact angle) it does not seem likely that the slight off-normal angle of impact contributed to shattering. In view of the determination that shattering did occur on initial impact, and in consideration of the problems with camera speed in the Test #2 (Base Case Test w/0.005-in. thickness), it is recommended that Test #2 be re-run with a model fuselage having a thickness of 0.005-in. to verify whether shattering occurred in the thicker model.

The throat of the conical section steel insert, adapted to the catcher, was too large (2.125-in. dia.) to stop/catch the projectile. The throat will be reduced to 1.75-in. diameter for the next test.

CONCLUSION:

It was determined that fragmentation of the model fuselage (0.0034-in. wall thickness) occurred on impact with a projectile having a velocity of 290 m/s. Fragmentation was relatively local and was not catastrophic, but definitely occurred.

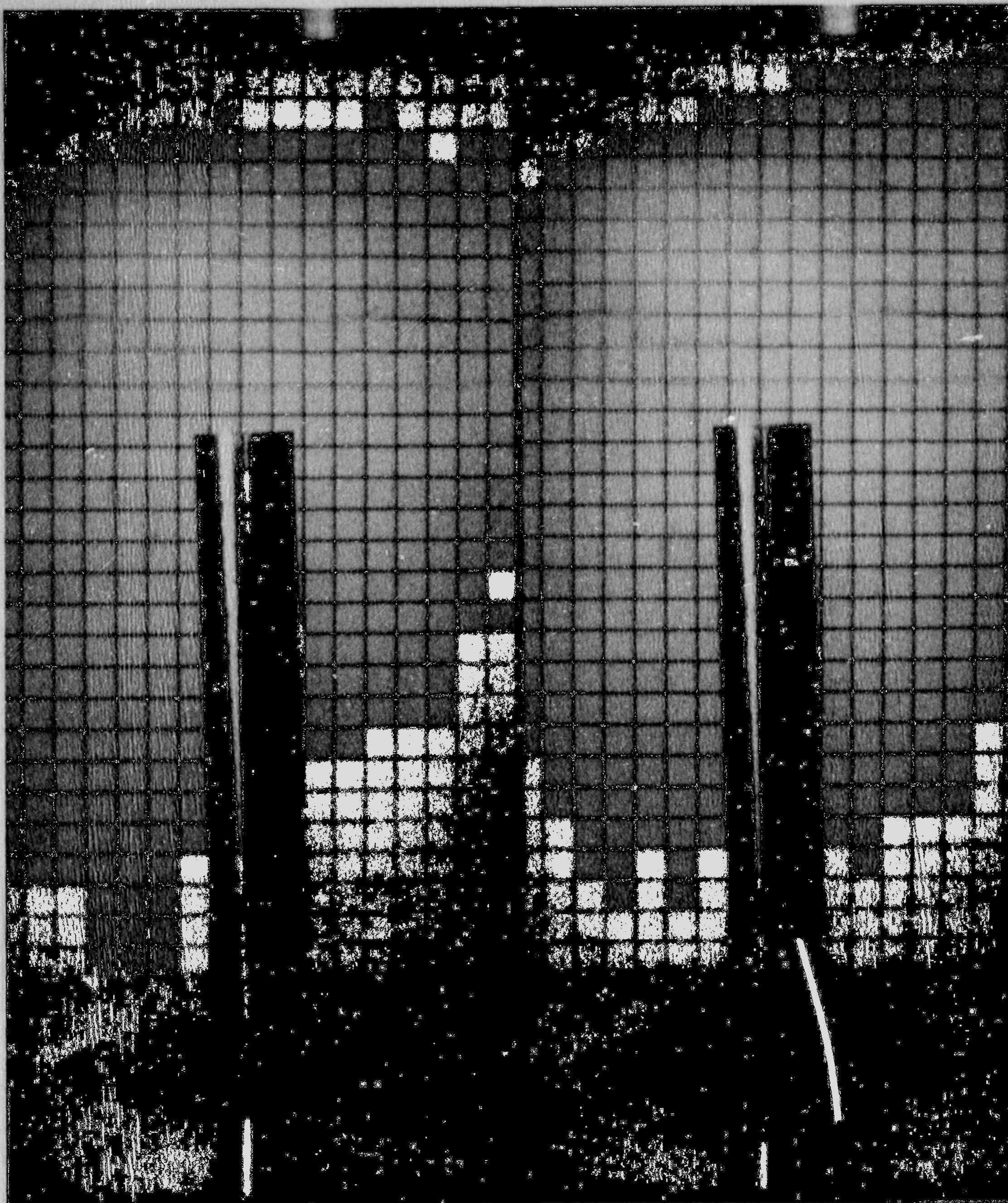

Figure A.8.1. Impact sequence, Base Case w/thin wall.

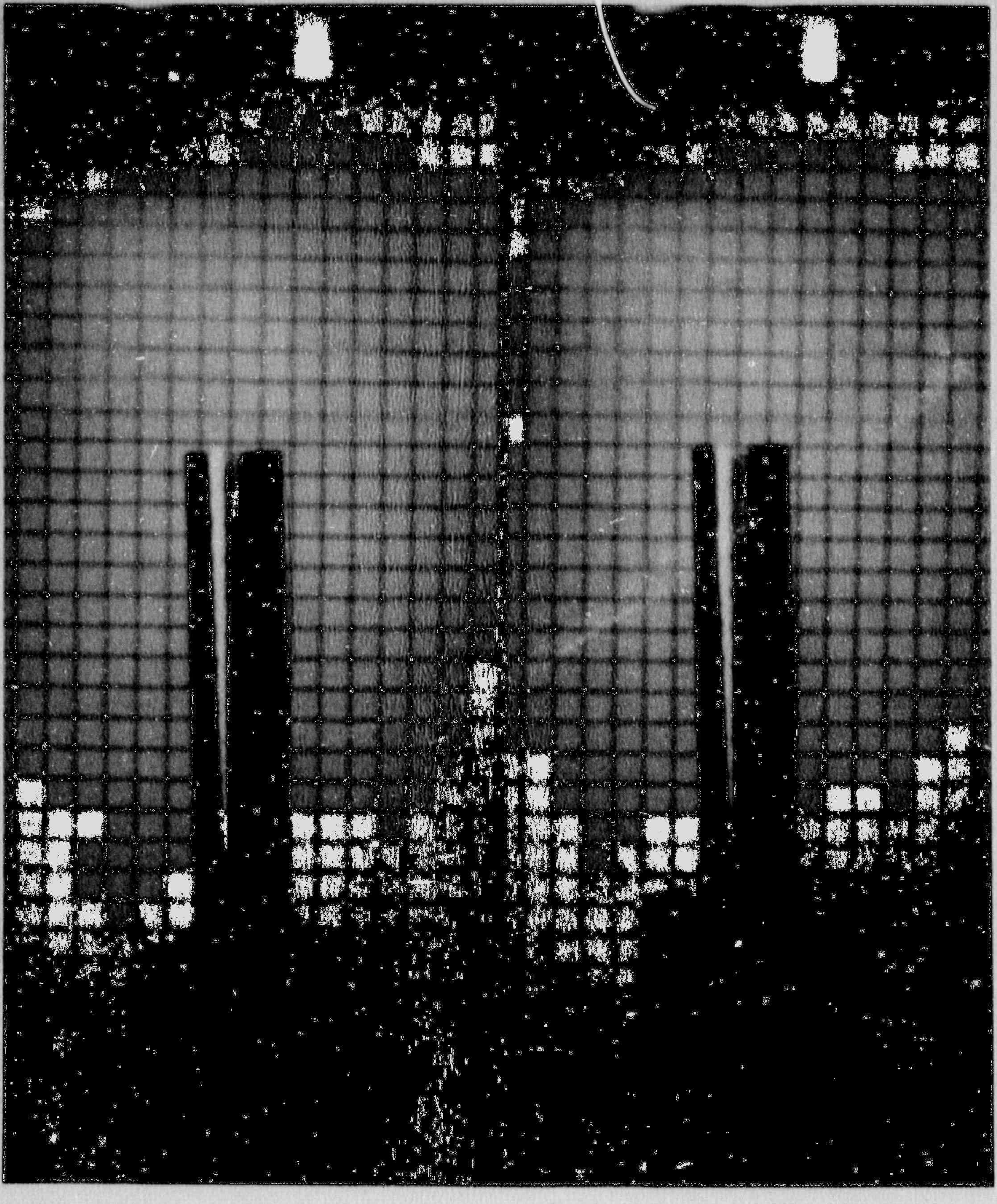

Figure A.8.2. . . . . Base Case w/thin wall.

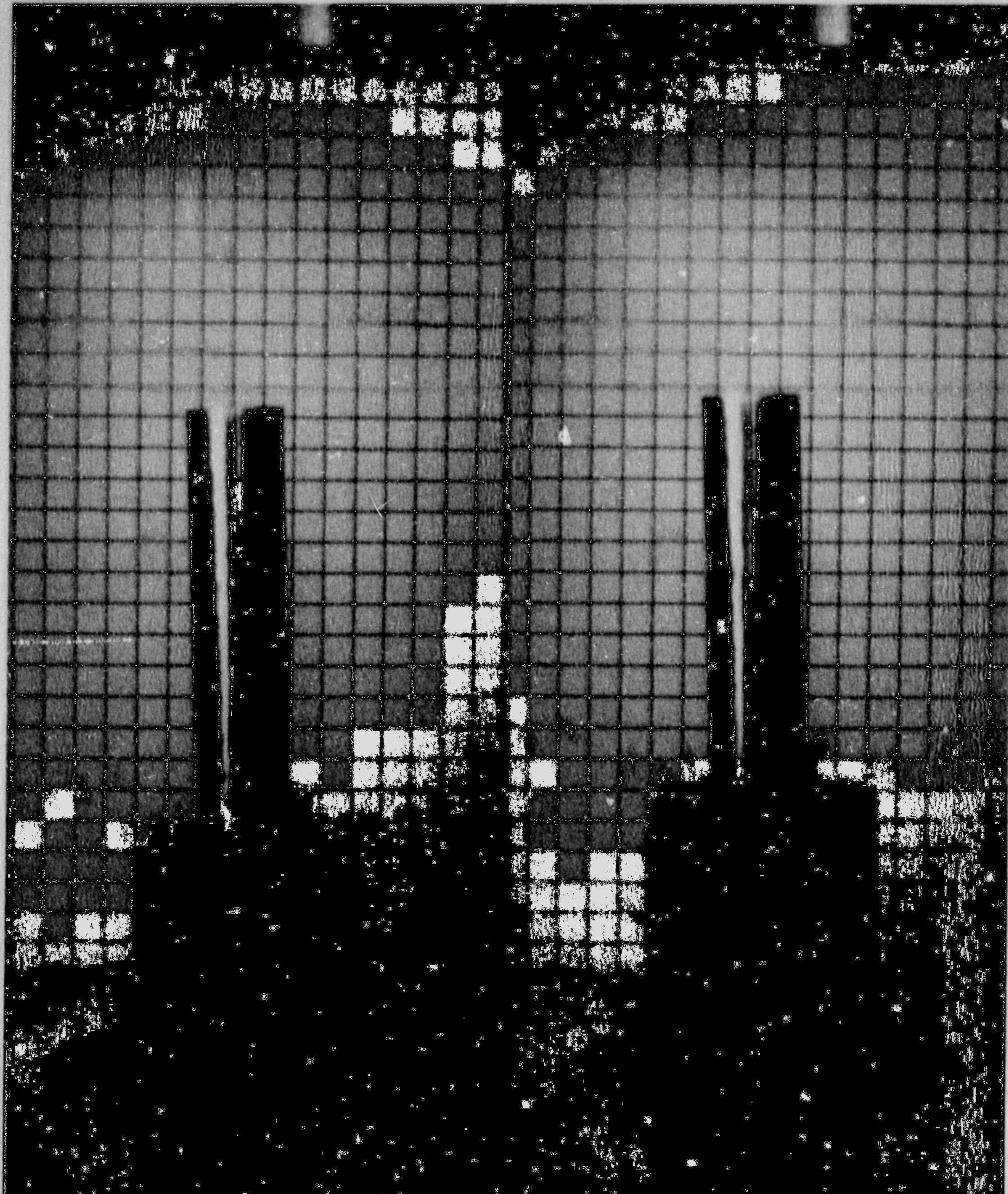

Figure A.8.3. . . . . Base Case w/thin wall.

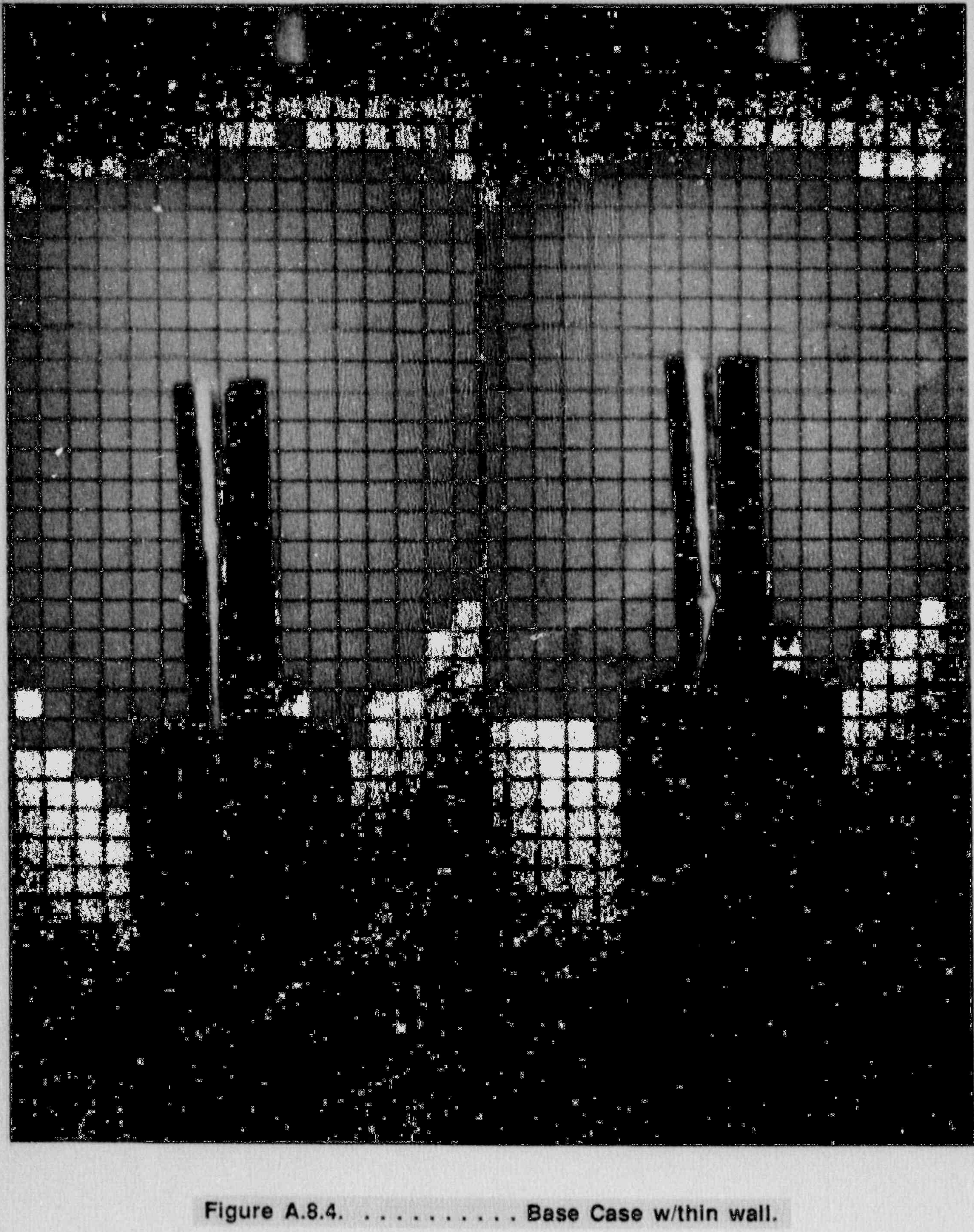

Figure A.8.4. . . . . Base Case w/thin wall.

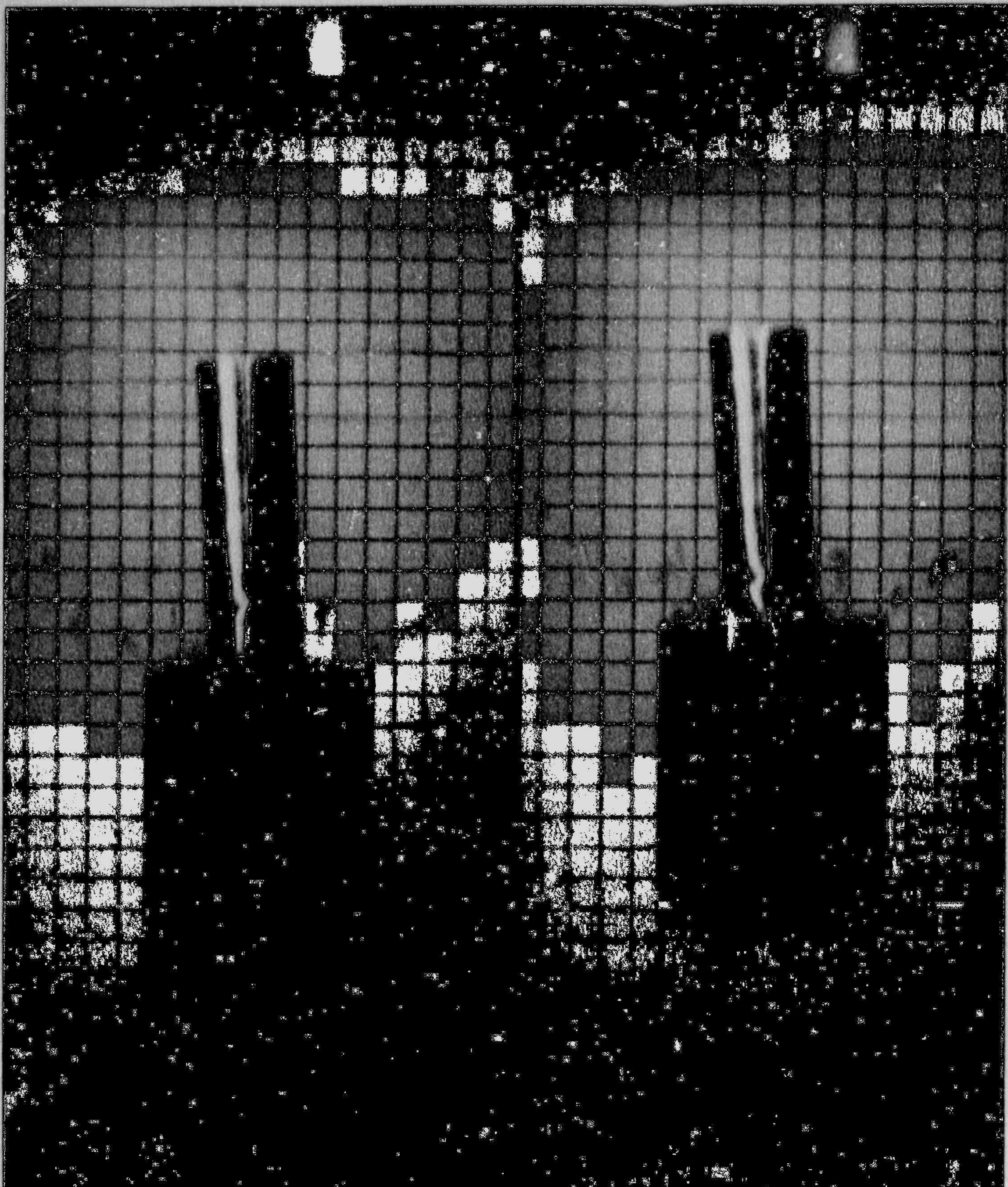

Figure A.8.5. . . . . Base Case w/thin wall.

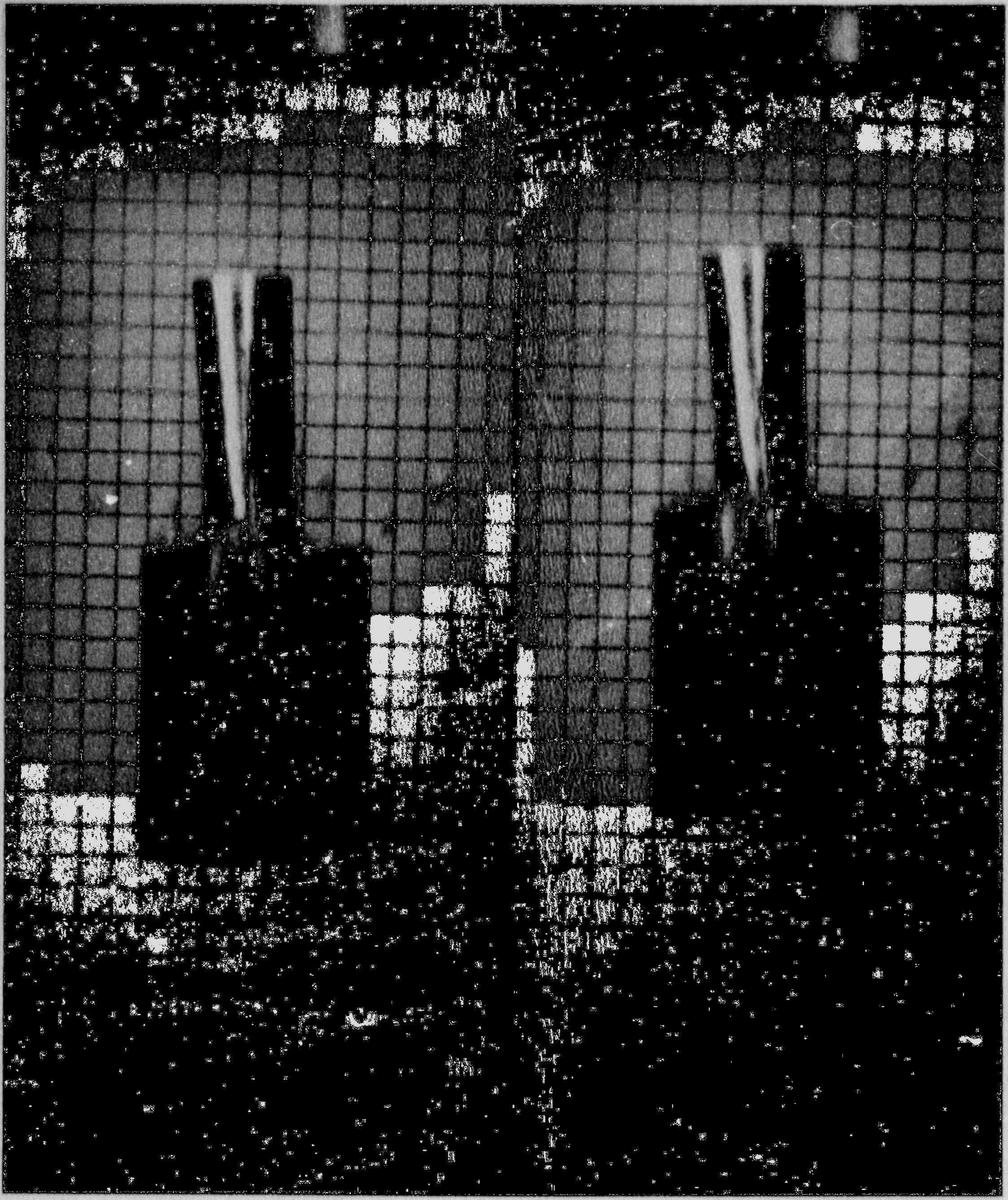

Figure A.8.6. . . . . Base Case w/thin wall.

Figure A.8.7. . . . . Base Case w/thin wall.

APPENDIX 9

Test #9

Rigid/Semi-Rigid Internal Mass Crash Test without 0.0038-in. Wall Thickness

July 14, 1989

OBJECTIVE OF TEST:

The purpose of this test was to investigate the influence of concentrated rigid and semi-rigid masses (within a fuselage model) on fragmentation of model "fuselage" walls when model is impacted by a 290 m/s projectile. The wall thickness (0.0038-in.) for this test is 24% thinner than the wall for Test #3 (0.005-in.). A secondary purpose for this test was to investigate sensitivity of wall thickness to shattering. (All other conditions were essentially the same as Test #3.)

TEST CONDITIONS:

Four small toy cars, made of metal and plastic, were glued together (end-to-end), and were placed inside the model fuselage. The string of cars were glued to the front end of the tube. A high-speed camera (22,000 frames/sec, max.) was stationed such that the impact event could be recorded. The test environment was partial vacuum. The nose of the model was blunt. Other specific test conditions were:

Time:	10:00 a.m.
Date:	July 12, 1989
Helium Pressure:	3.76 MPa (545 psi)
Chamber Pressure:	70 milli-Torr
Projectile Mass:	313 g
Projectile Velocity:	290 m/s
Target Dimensions: (Length x diameter x wall thickness)	178 mm x 25.4 mm x .0967 mm (7 in. x 1 in. x 0.0038 in.)
Target Material:	6061-T6 aluminum
Target Mass:	4.91 g
Total Mass of 4 Toy Cars	17.71 g
Impact Angle:	90°

The fuselage model was fixed (glued) to a 0.020-in. thick aluminum plate which was pressed against the gun barrel exit by a fixture. The catcher was modified, again, in an attempt to "catch" the projectile and avoid crushing the model fuselage remnant during deceleration. The throat of the steel insert was reduced to 1.75-in. diameter.

RESULTS:

Catastrophic fragmentation occurred on impact. Small of toy cars and model fuselage wall can be identified flowing radially from the point of impact, having apparently crashed through the walls of the model fuselage. Refer to the sequence of frames, labeled Figures A.9.1 through A.9.7. The mass of the largest fragment was 1.35 g (26%); it was a remnant the rear section of model fuselage, which was unoccupied by toy cars. The steel insert placed inside the catcher succeeded in stopping the projectile and, thereby, avoided crushing the tail section remnant. However, the remnant was crushed by the 6-in. of soft rubber foam as it brought the remnant to rest.

1) One hundred five (105) "fuselage" fragments were recovered on the floor of the test chamber. The fragments ranged in size from small (1 mm x 1 mm) to large (20 mm x 30 mm). Numerous small toy car fragments were recovered on the floor of the chamber. The toy fragments were not counted. (It is estimated they numbered more than 200 pieces.)

2) Eighty-one (81) fragments were recovered inside the catcher. The fragments ranged in size from 1 mm x 1 mm to about 30 mm x 40 mm; the largest fragment was the 1.35 g piece mentioned above.

3) A mass analysis of fragments found is given below:

a)	Fragments outside catcher (105)	=	1.92 g (39%)
b)	Fragments inside catcher (81)	=	2.81 g (57%)
c)	Mass of original target	=	4.91 g

DISCUSSION:

By comparing the fragment counts with previous tests and by observation of film records, clearly the concentrated rigid and semi-rigid masses inside the fuselage produced considerably more shattering of the "fuselage" model. The film showed toy car fragments "flowing" radially from the point of impact, early in the event. Shattering appears to be quite sensitive to the thickness of the model fuselage wall. It is noted that the number of fragments in Test #3 was 128, while the number in Test #9 was 186. The only significant difference in the two tests was the slightly thinner wall in Test #9. It is also significant that the final 2 inches of the fuselage model remained uncrushed by the initial impact; further, toy cars did not occupy the final 2 inches of model fuselage. In all tests where concentrated mass existed (Tests #3, #7, #9), disintegration of the model fuselage always occurred in the zones where the mass was present.

CONCLUSION:

Concentrated rigid and semi-rigid mass inside the model "fuselage" represent a major contributor to fuselage shattering on initial impact. It is likely this conclusion can be extrapolated with confidence to PSA Flight 1771, where the concentrated masses would be in the form of seats, instruments, panels, and miscellaneous fixtures.

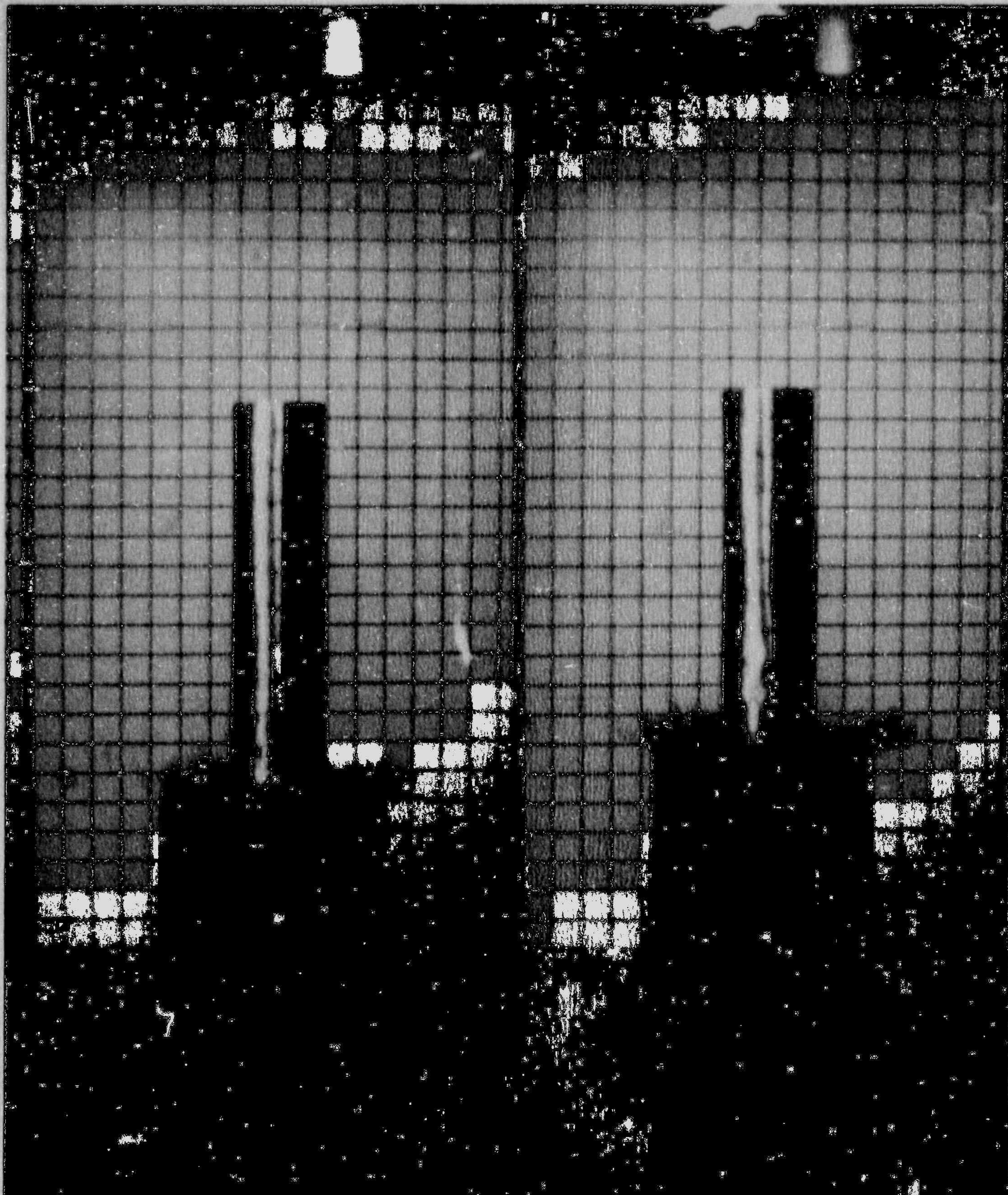

Figure A.9.1. Impact sequence, rigid and semi-rigid mass.

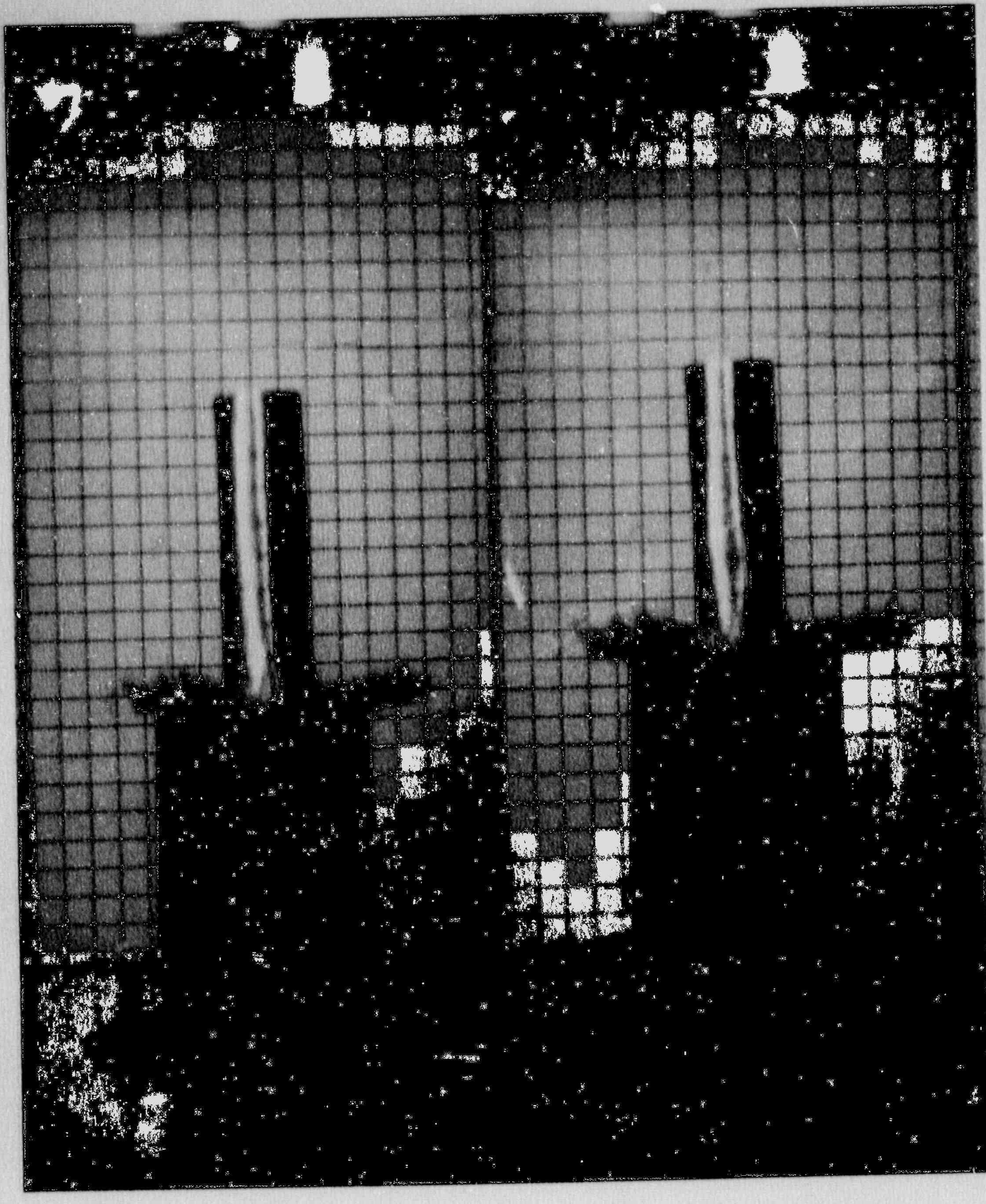

Figure A.9.2. . . . . Rigid and semi-rigid mass

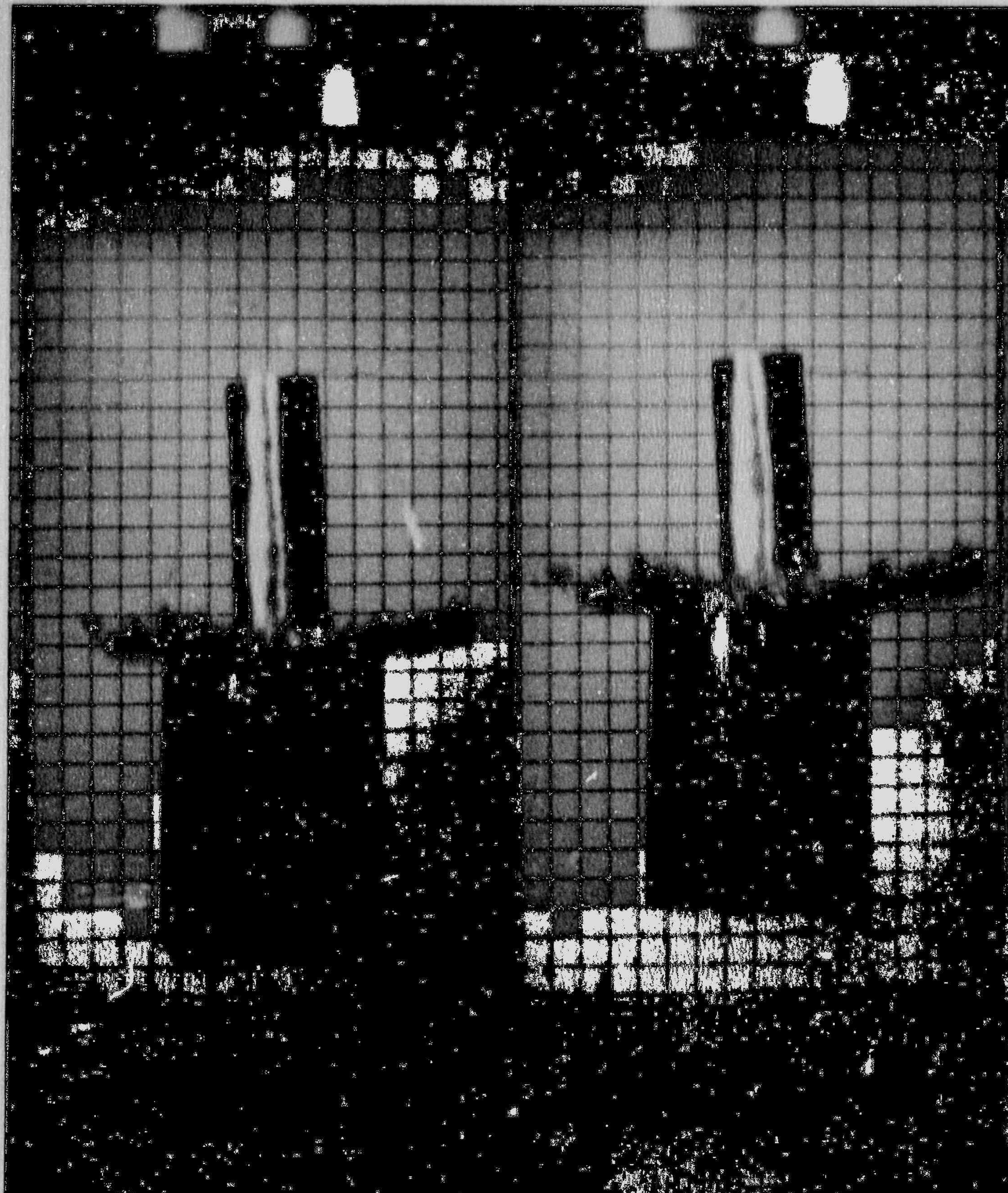

Figure A.9.3. . . . . Rigid and semi-rigid mass.

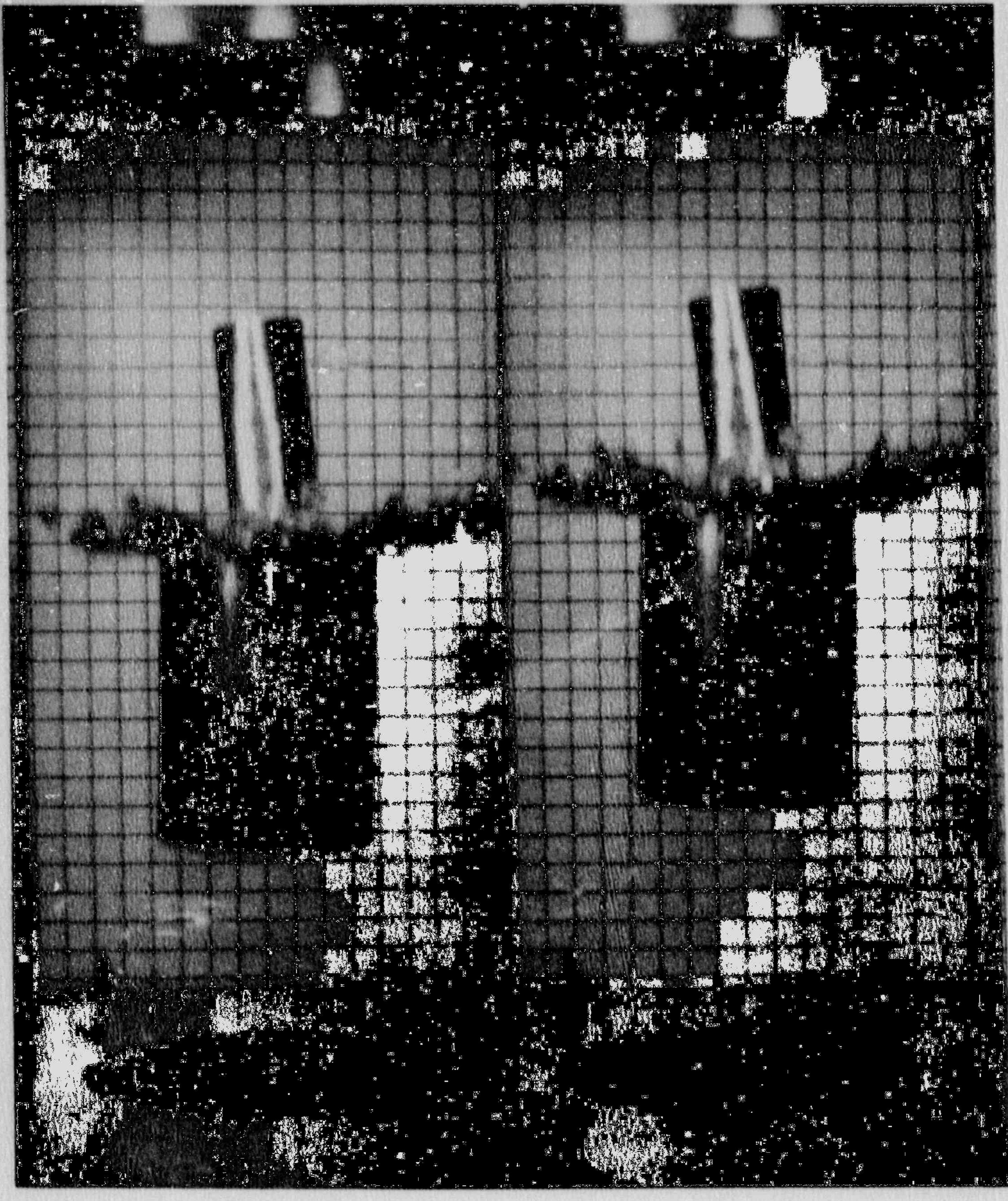

Figure A.9.4. . . . . Rigid and semi-rigid mass.

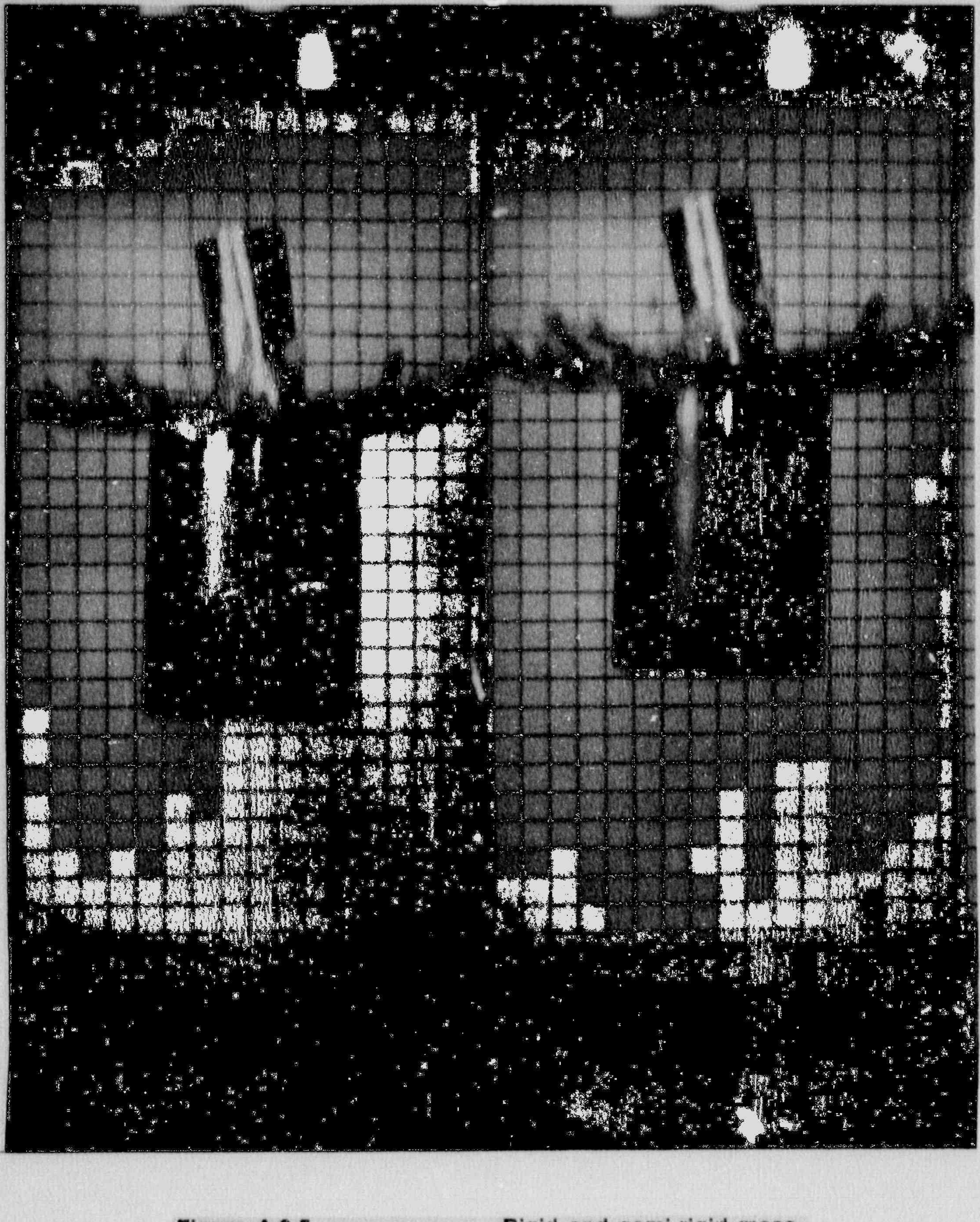

Figure A.9.5. . . . . Rigid and semi-rigid mass.

Figure A.9.6. . . . . Rigid and semi-rigid mass.

APPENDIX 10

Test #10

Base Case, Repeat without 0.005-in. Wall

July 19, 1989

OBJECTIVE OF TEST:

The purpose of this test was that of repeating conditions of the Base Case (Tests #1 and #2), with improved camera lighting and speed, to verify whether fragmentation occurred upon initial impact.

TEST CONDITIONS:

Conditions for this test were identical to that of Tests #1 and #2, except for improved lighting techniques and electronic triggering of the camera. Other specific test conditions were:

Time:	10:00 a.m.
Date:	July 19, 1989
Helium Pressure:	3.76 MPa (545 psi)
Chamber Pressure:	90 milli-Torr
Projectile Mass:	313 g
Projectile Velocity:	290 m/s
Target Dimensions: (Length x diameter x wall thickness)	178 mm x 25.4 mm x .127 mm (7 in. x 1 in. x 0.005 in.)
Target Material:	6061-T6 aluminum
Target Mass:	6.84 g
Impact Angle:	90°

The fuselage model was fixed (glued) to a 0.020-in. thick aluminum plate which was pressed against the gun barrel exit. The catcher was modified, again, in an attempt to "catch" the projectile and avoid crushing the model fuselage remnant during deceleration. The throat of the steel insert was reduced to 2.0-in. diameter.

RESULTS:

Fragmentation occurred with initial impact; the number of fragments was quite small, as observed from the film record of the event. The impact event is shown in the photos attached, labeled Figures A.10.1 through A.10.7. The results fo this test leads to the deduction that fragmentation, of a moderate degree, also occurred with Tests #1, #2, #4, and #5, but the lighting and timing of the camera was such that fragments were not observable in the earlier tests. It is significant that the mass of the largest remnant was 5.97 g (87.3%) of the original fuselage mass. The projectile was caught and retained in he throat of the steel conical insert in the catcher, thus preventing the secondary crushing of the model fuselage remnant. The remnant was brought to rest by 12-in. of soft rubber foam in the rear of the catcher.

1) Forty-five (45) model fuselage fragments were recovered on the floor of the test chamber. The fragments ranged in size from small (1 mm x 1 mm) to 5 mm x 10 mm.

2) Seventy-nine (79) model fuselage fragments were recovered inside the catcher. The smallest was less than 1 mm square and the largest was 5.96 g, as described in he paragraph above.

3) A mass analysis of fragments found is given below:

a)	Fragments outside catcher (45)	=	0.67 g (9.8%)
b)	Fragments inside catcher (79)	=	6.17 g (90.2%)
c)	Mass of original target	=	6.84 g

DISCUSSION:

The results of this test verified that a moderate amount of fragmentation did occur for "Base Case" conditions. It is logical to deduce that a small amount of fragmentation occurred in Tests #1, #2, #4, and #5, although such was not detectable by high-speed photography, due to poor lighting conditions.

CONCLUSION:

The superposition of high-deformation rate and high-strain rate are sufficient to produce a small amount of shattering of a model fuselage when impacted at a velocity of 290 m/s.

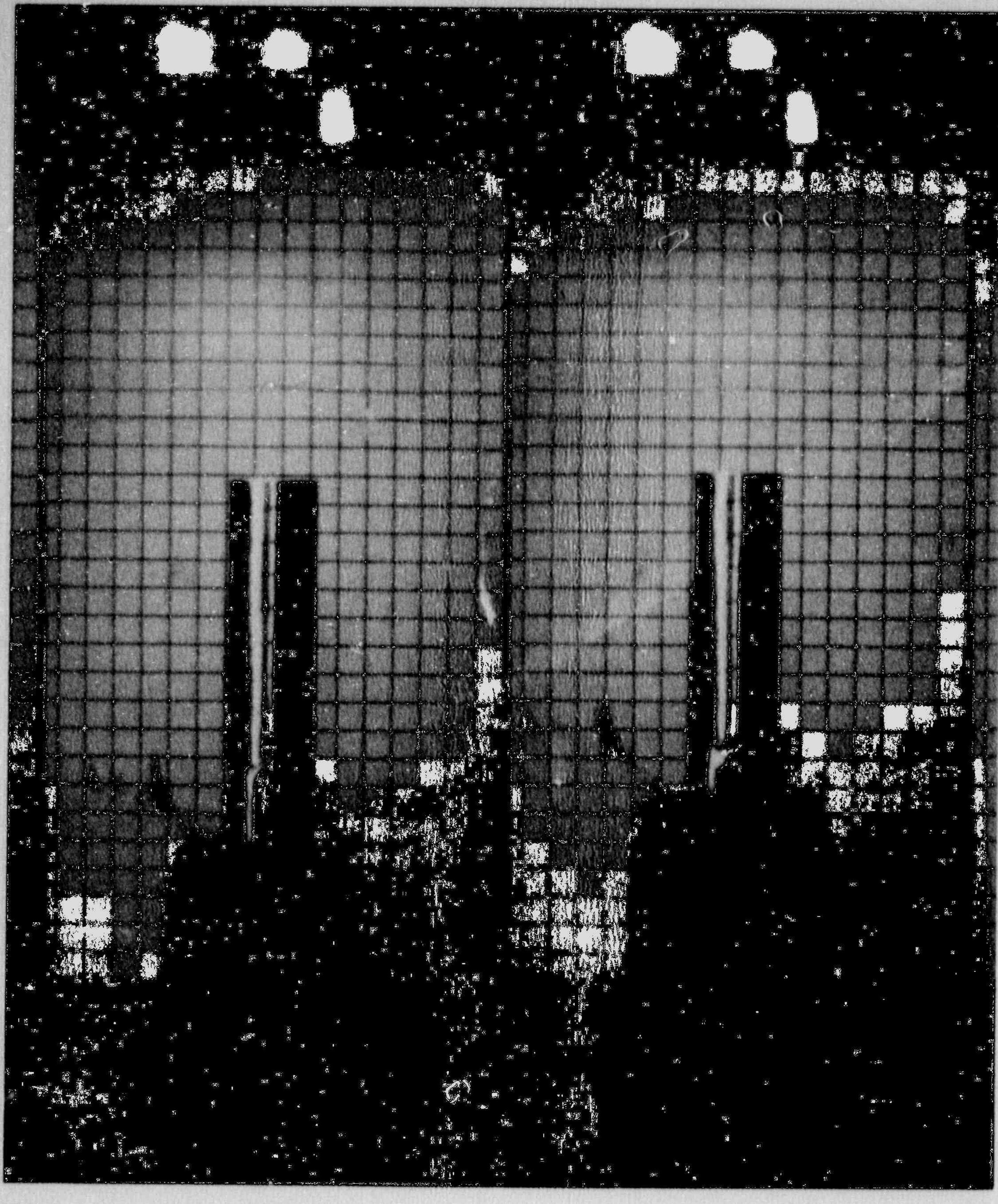

Figure A.10.1. Impact sequence, Base Case w/o 0.005-in. wall.

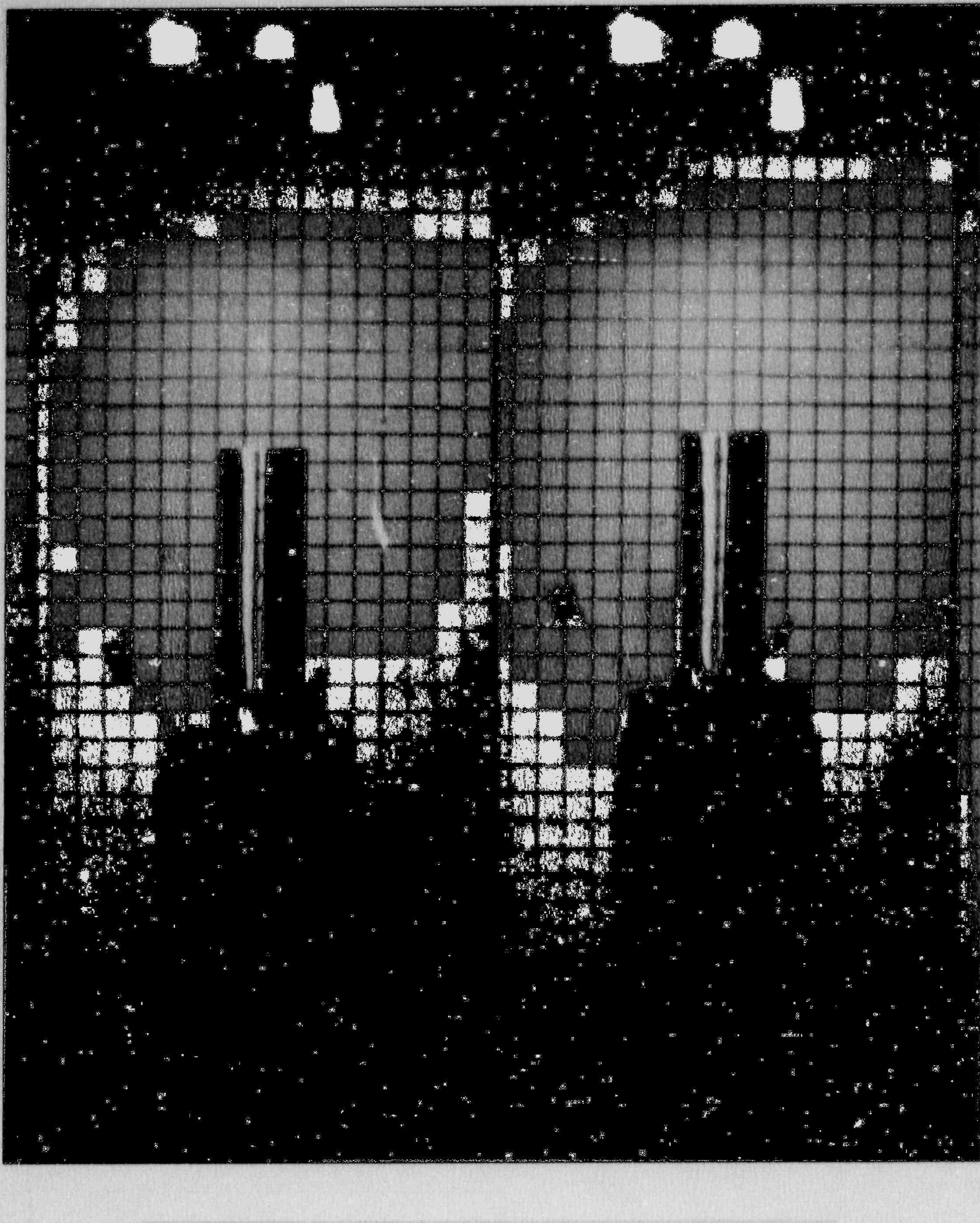

Figure A.10.2. . . . . Base Case w/o 0.005-in. wall.

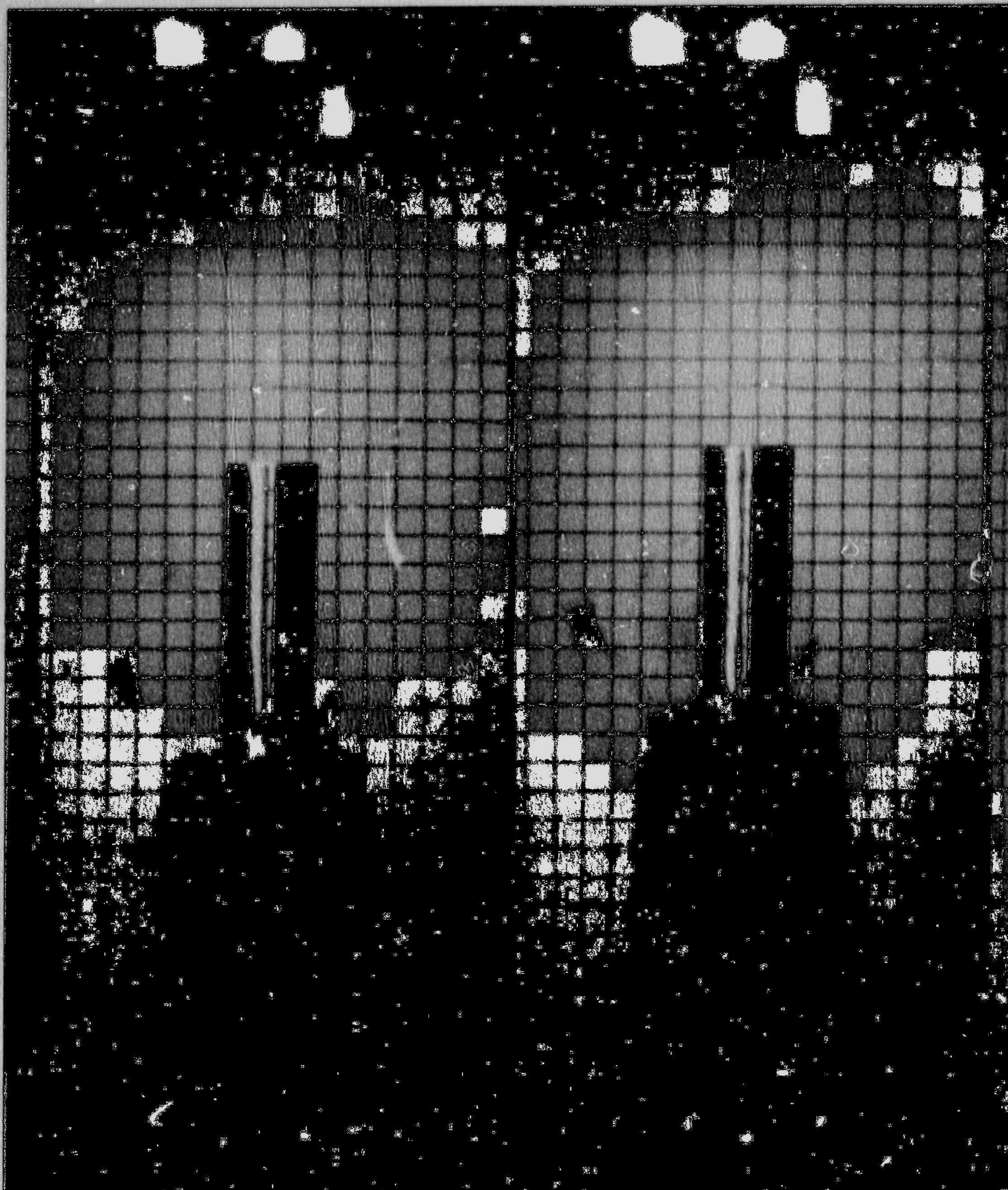

Figure A.10.2. . . . . Base Case w/o 0.005-in. wall.

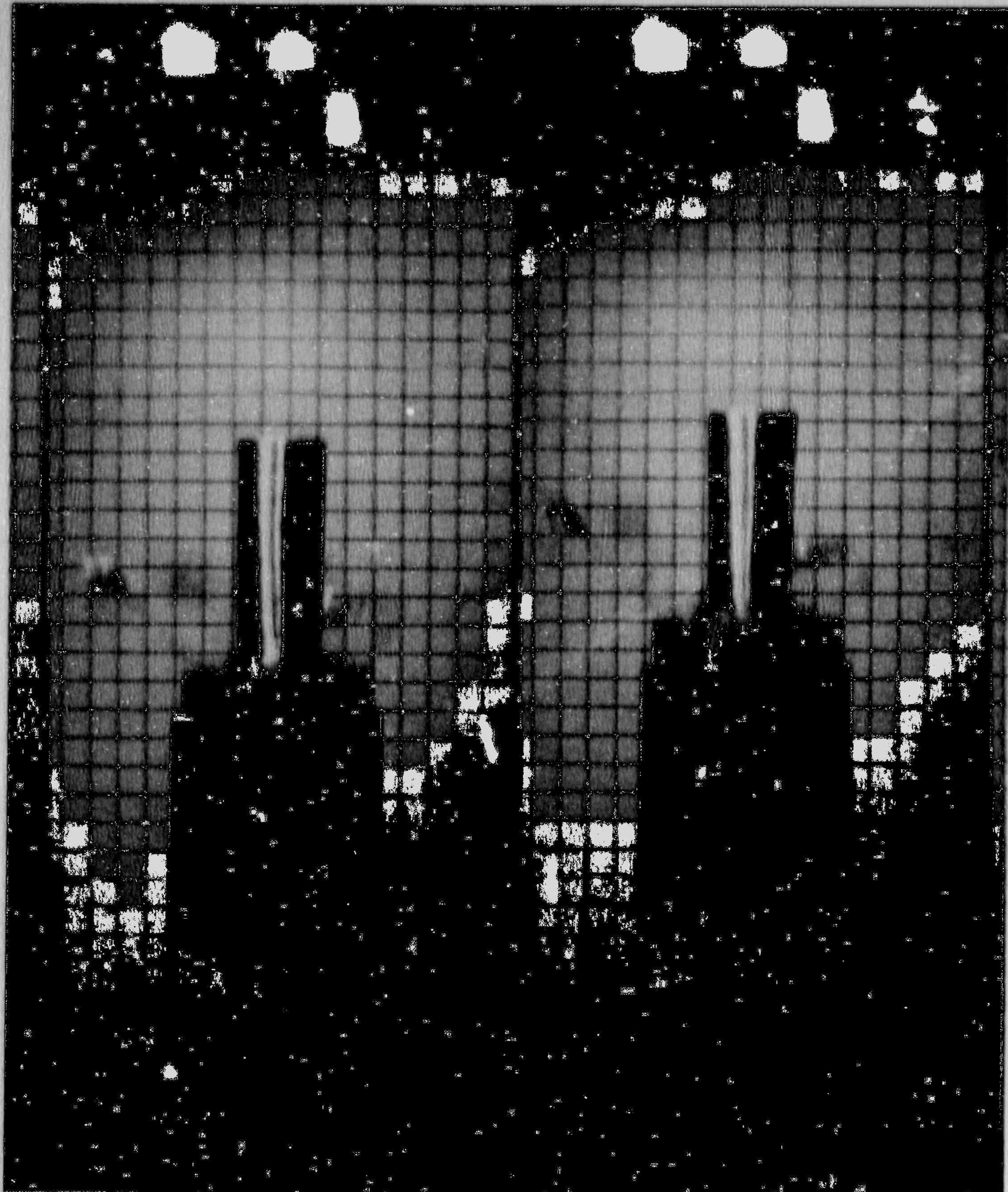

Figure A.10.3. . . . . Base Case w/o 0.005-in. wall.

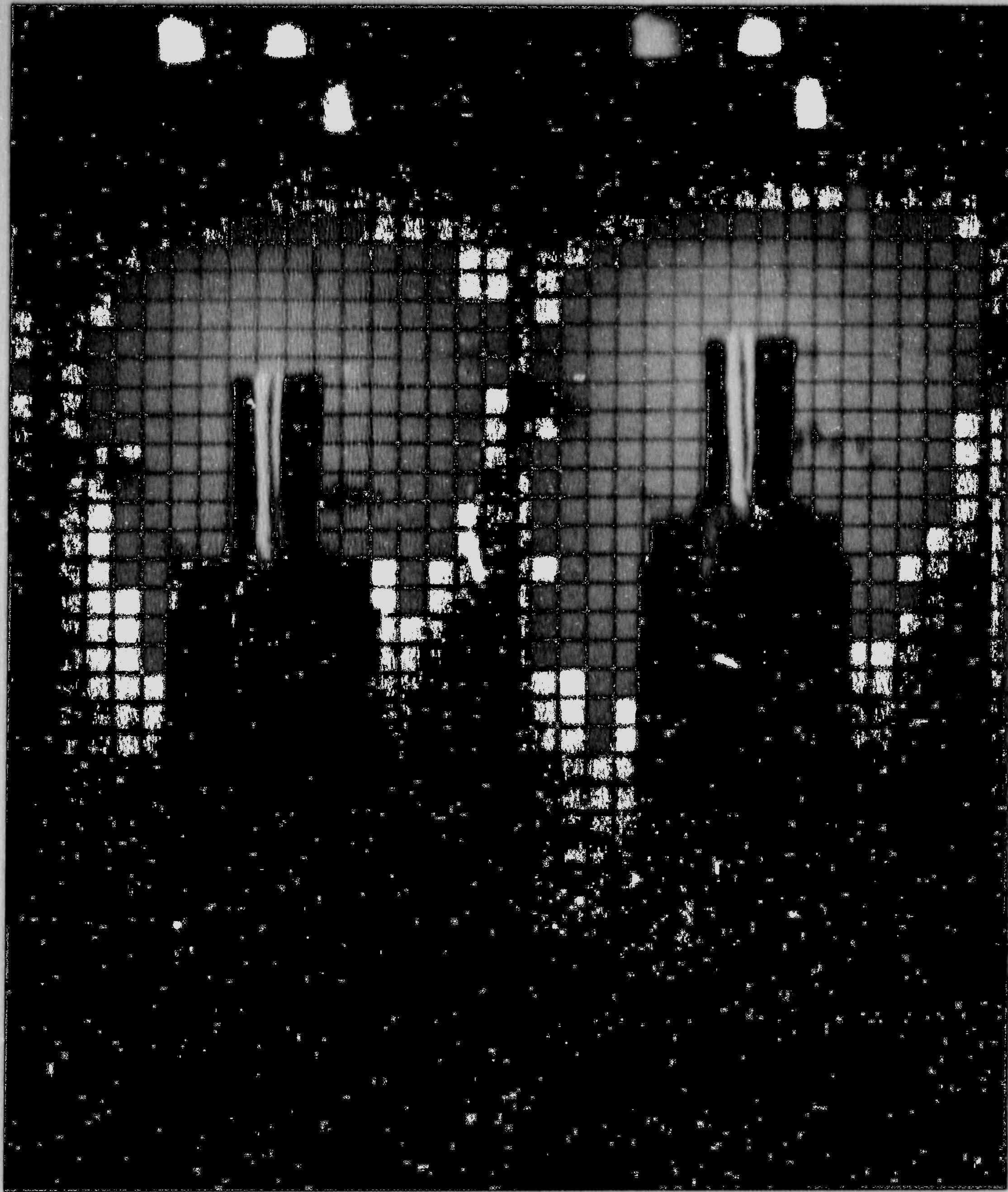

Figure A.10.4. . . . . Base Case w/o 0.005-in. wall.

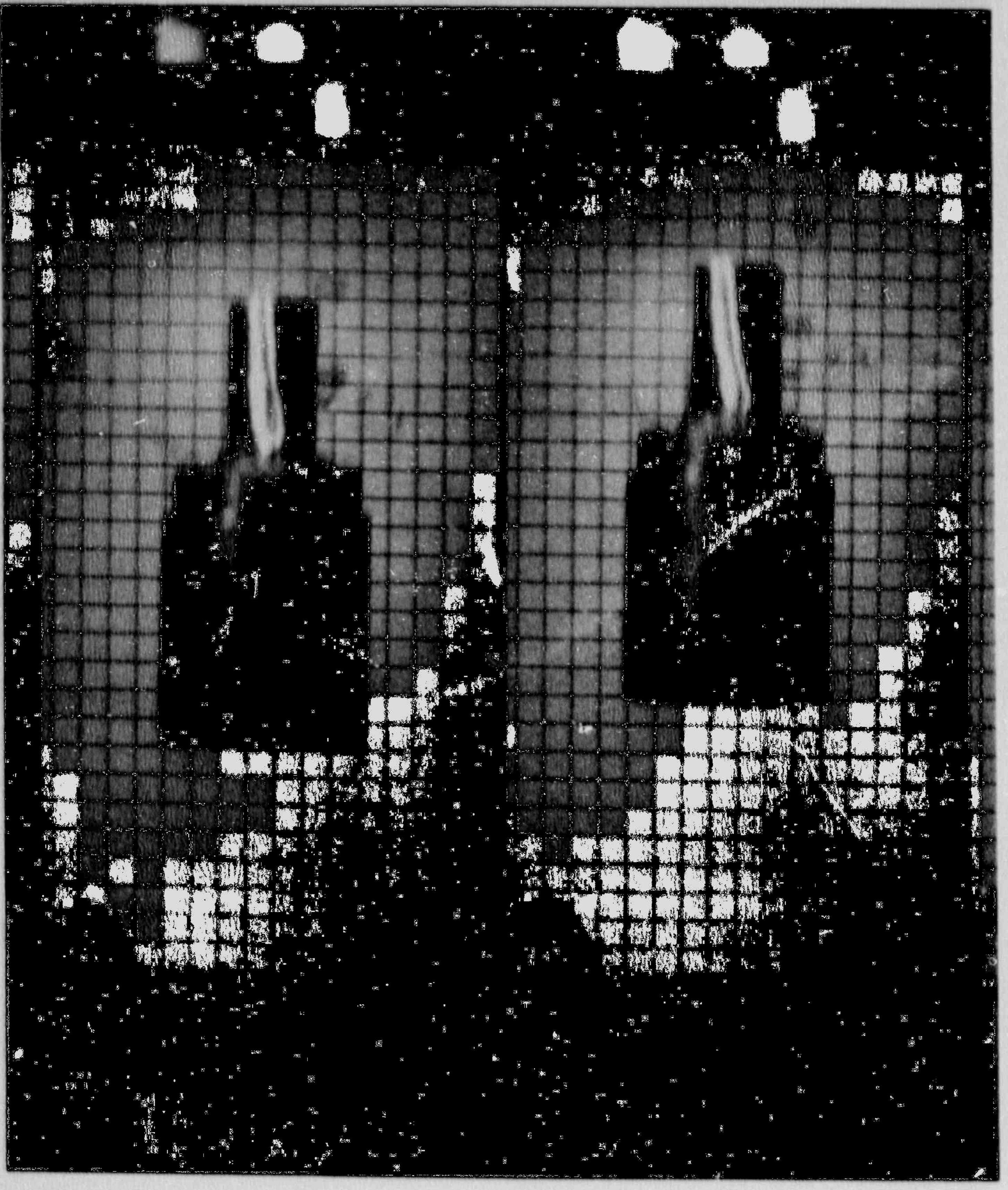

Figure A.10.5. . . . . Base Case w/o 0.005-in. wall.

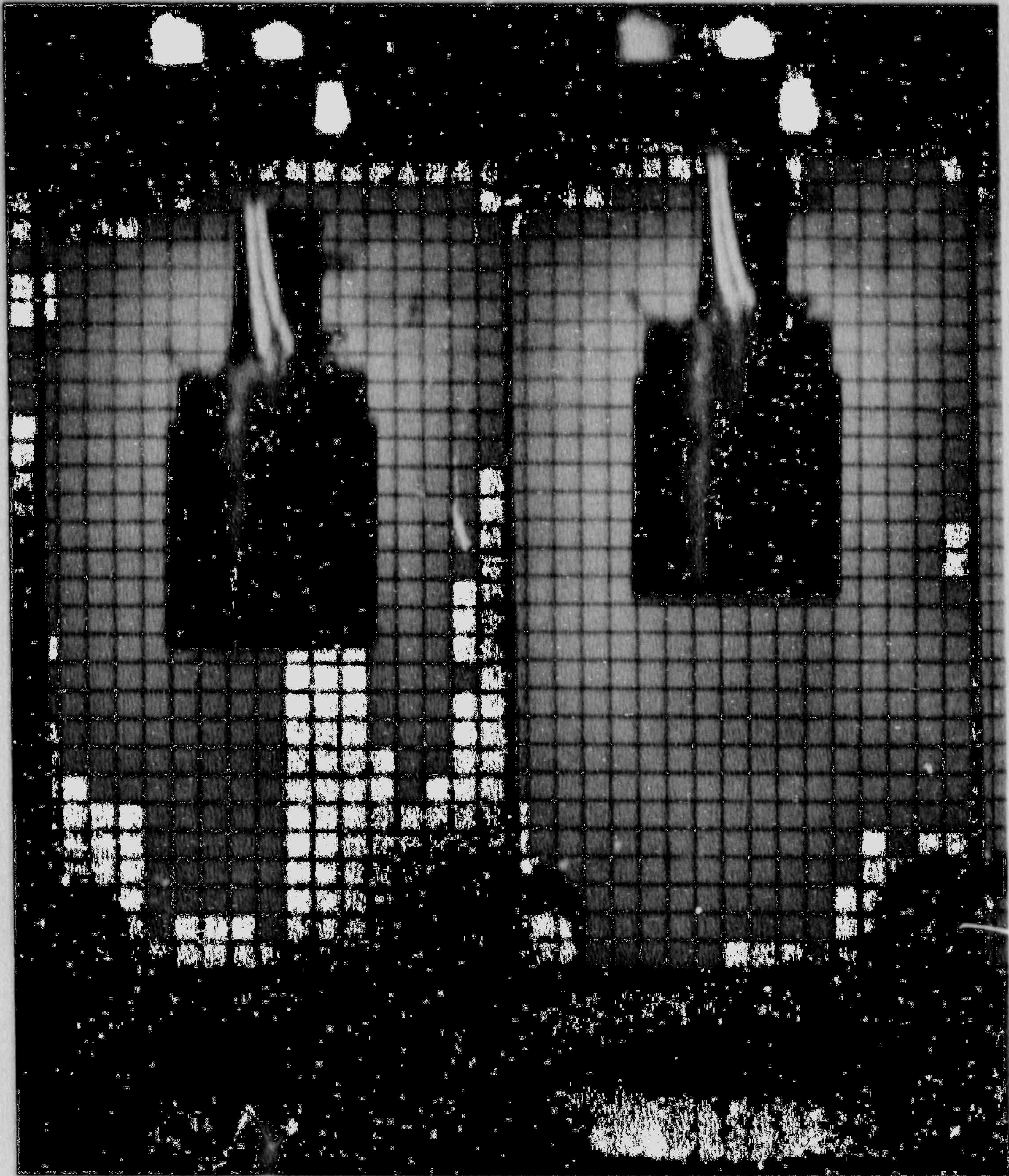

Figure A.10.6. . . . . Base Case w/o 0.005-in. wall.

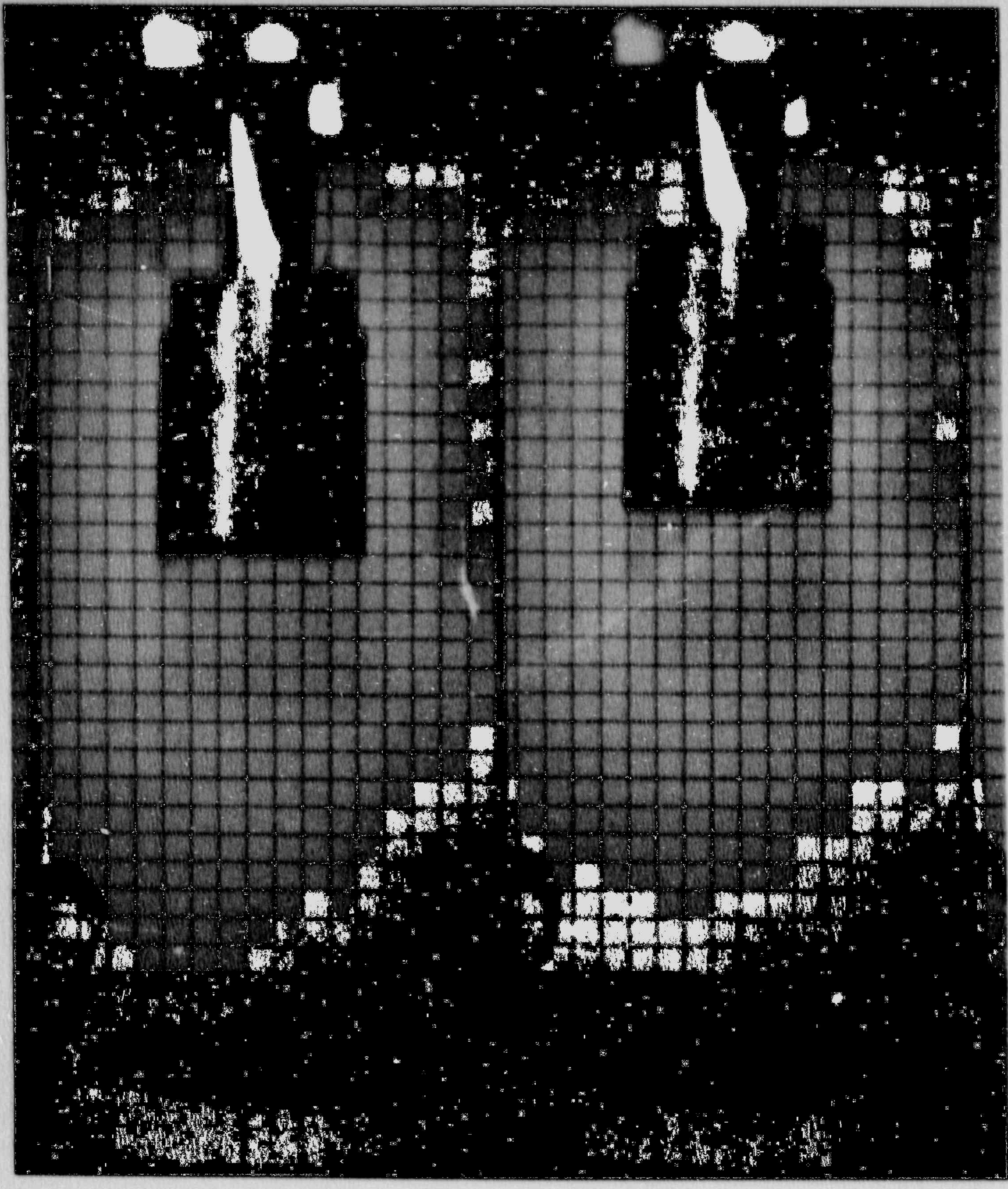

Figure A.10.7. . . . . Base Case w/o 0.005-in. wall.

APPENDIX 11

Kinematic Modeling Fuselage Buckling

The model fuselages buckled and folded in an accordion fashion on impact. The length, L, of fuselage making up one fold is about 2.4 mm (0.0937-in.). A "scoping" study of the accelerations involved in the folding process can be straightforwardly performed by assuming,

- A 2-dimensional model fold.
- The fold is made up of two straight section of the same length, per the sketch below.
- Point-"2" remains stationary during buckling.
- The elasticity of the two members making up the fold do not influence the resulting tangential velocity of point-"1".
- The physical integrity of the fold members is preserved.

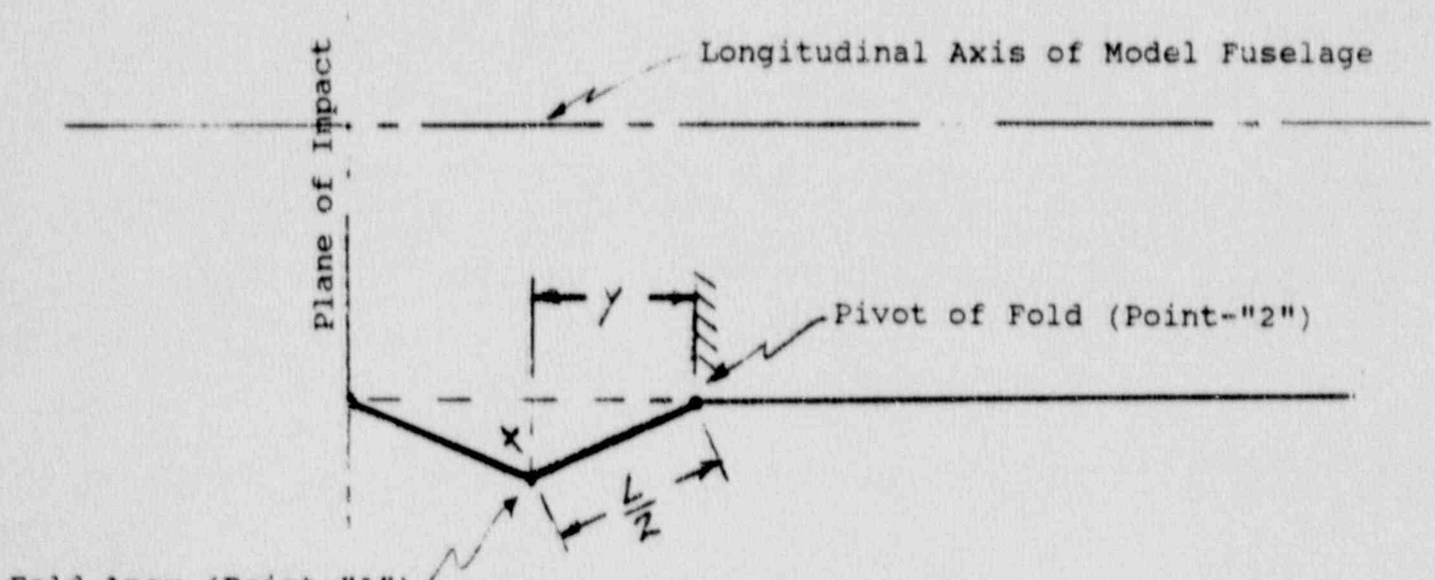

Figure A.11.1. The assumed geometry of a single fold.

From the geometry shown in Figure A.11.1,

$$y^2 + x^2 = (L/2)^2 .$$

By differentiating the expression with respect to time, and solving for the magnitude of "dx/dt",

$$dx/dt = -\left[y/\sqrt{\left((L/2)^2 - y^2\right)}\right] \cdot (dy/dt)$$

where dy/dt is the longitudinal component of the velocity of the apex of the fold (which is one-half the impact velocity for the buckling conditions described). The radial component of velocity of the fold apex is dx/dt. If point-"2" is assumed fixed, then the velocity of the apex is,

$$V = \sqrt{(dx/dt)^2 + (dx/dt)^2}$$

and the normal component of acceleration, A_n, of apex, relative to point-"2", is given by

$$A_n = V^2/(L/2).$$

By prescribing an impact velocity of 290 m/s (950 ft/s) and holding the summed length of members, L, (of the fold) to 2.4 mm (0.0937-in.) one can calculate the displacement, velocity components, and acceleration components as a function of time during buckling and creation of a single fold. The geometric relationships were derived analytically and modeled in the MS-BASIC code listed in Table A.11.1; Table A.11.2 gives the instantaneous properties of the fold geometry, the tangential velocity of the fold apex, (relative to point-"2") and the normal acceleration component.

It is noted that tensile stress due to inertia, for the 2-dimensional buckling model, is independent of wall thickness. A normal component of acceleration of the apex equal to 2.7E07 g's will produce an inertial tensile stress, at the fold pivot, exceeding 309 MPa (45,000 psi). The ultimate tensile strength of 6061-T6 aluminum is 45,000 psi (Ref. 11). Thus, clearly the results from analysis of the 2-dimensional kinematic model suggest the likelihood of deformation rate contributing to fuselage shattering.

Table A.11.1. MS-BASIC model for the kinematics of 2-dimensional buckling.

```
10 KEY OFF
20 REM          THIS CODE MODELS THE LATERAL VELOCITY AND ACCELERATION
30 REM          FOR A COLLAPSING FUSELAGE MODEL. THE PURPOSE IS THAT OF
40 REM          PRODUCING SOME INTERPRETATIONAL DATA FOR USE IN ANALYSIS
50 REM          OF DEFORMATION-RATE FAILURE.
60 REM
70 REM          INPUTS:
80 REM
90 DIM TIME(200),VX1(200),AX(200),X(200),Y(200),VY1(200),A1N(200),V1TAN(200)
100 L=.0937/12:  REM     LENGTH OF A SINGLE "FOLD" (FT.)
110 E=1E+07:     REM     YOUNG'S MODULUS FOR ALUMINUM (PSI)
120 S=30000!:    REM     ESTIMATED STRESS AT TIME BUCKLING IS INITIATED (PSI)
130 DL=(S/E)*L: REM     MAXIMUM COMPRESSION OF A LENGTH OF FOLD (FT.)
140 VY=950:     REM     IMPACT VELOCITY (FPS)
145 VY1=VY/2:   REM     THE LONGITUDINAL VELOCITY COMPONENT OF THE FOLD APEX
150 YMAX=L/2 - DL:      REM     LONGITUDINAL LEG LENGTH FOR FOLD (FT.)
160 YMIN=0:             REM             "             "
170 CLS
180 PRINT TAB(1)"TIME";TAB(15)"X";TAB(30)"Y";TAB(45)"VEL-X";TAB(60)"ACCEL-X"
190 PRINT TAB(1)"(MS)";TAB(15)"(IN.)";TAB(30)"(IN.)";TAB(45)"(FPS)";TAB(60)"(g's
)
200 PRINT
210 REM
220 REM         LET Y VARY FROM YMAX TO YMIN, OBTAIN ACCEL RESPONSE
230 REM
240 YO=L/2
250 FOR Y=YMAX TO YMIN STEP -DL
260 TIME=(YO-Y)/VY1
270 X=((L/2)^2 - Y^2)^.5
280 VX1=(Y/((L/2)^2 - Y^2)^.5)*VY1:      REM      LATERAL VEL. OF FOLD APEX
290 AX=(VX1^2/(((L/2)^2-Y^2)^.5)*(Y^2/((L/2)^2-Y^2) + 1))/32.174
300 N=N+1
310 TIME(N)=TIME:VX1(N)=VX1:AX(N)=AX:X(N)=X:Y(N)=Y: VY1(N)=VY/2
320 V1TAN(N)=(VX1^2 + VY1(N)^2)^.5
330 A1N(N)=((VX1^2 + VY1^2)^.5)^2/(L/2)/32.174:  REM  NORMAL ACCEL. (g's)
340 NEXT Y
350 FOR I=1 TO N STEP 10
360 PRINT TAB(1)TIME(I)*1000;TAB(15)X(I)*12;TAB(30)Y(I)*12;TAB(45)VX1(I);TAB(60)
AX(I)
370 NEXT I
380 PRINT:PRINT:PRINT:INPUT"PRESS <RET>", IY: CLS
390 PRINT TAB(1)"TIME";TAB(15)"X";TAB(30)"Y";TAB(45)"V1TAN";TAB(60)"ACCEL-N"
400 PRINT TAB(1)"(MS)";TAB(15)"(IN.)";TAB(30)"(IN.)";TAB(45)"(FPS)";TAB(60)"(g's
)
410 PRINT
420 FOR I=1 TO N STEP 10
430 PRINT TAB(1)TIME(I)*1000;TAB(15)X(I)*12;TAB(30)Y(I)*12;TAB(45)V1TAN(I);TAB(6
0)A1N(I)
440 NEXT I
450 END
```

Table A.11.II. Instantaneous geometry, tangential velocity of apex, and normal acceleration of the apex relative to the fold pivot point-"2".

TIME (MS)	X (IN.)	Y (IN.)	V1TAN (FPS)	ACCEL-N (g's)
4.931598E-05	5.124477E-03	.0465689	4342.639	1.501323E+08
5.424758E-04	1.673827E-02	4.375789E-02	1329.512	1.407185E+07
1.035636E-03	2.276567E-02	4.094688E-02	977.5136	7606978
1.528796E-03	2.721357E-02	3.813587E-02	817.7446	5323558
2.021955E-03	3.077462E-02	3.532486E-02	723.1198	4162815
2.515115E-03	3.373088E-02	3.251384E-02	659.7441	3465115
3.008275E-03	3.623071E-02	2.970283E-02	614.2231	3003440
3.501435E-03	3.836342E-02	2.689182E-02	580.0773	2678788
3.994594E-03	4.018753E-02	2.408081E-02	553.7476	2441127
4.487753E-03	4.174348E-02	2.126981E-02	533.1073	2262537
4.98091E-03	4.306036E-02	1.845881E-02	516.8037	2126267
5.474068E-03	4.415959E-02	1.564782E-02	503.9393	2021729
5.967225E-03	4.505705E-02	1.283682E-02	493.9017	1941993
6.460382E-03	4.576471E-02	1.002582E-02	486.2648	1882401
6.95354E-03	4.629114E-02	7.214825E-03	480.7346	1839828
7.446697E-03	4.664257E-02	4.403826E-03	477.1125	1812209
7.939855E-03	4.682291E-02	1.592826E-03	475.2749	1798276